

079-14411

NASA TECHNICAL TRANSLATION

NASA TT F-17157

DEFORMATION AND DESTRUCTION OF SOLIDS

S. A. Shesterikov, Editor

Translation of "Deformirovaniye i razrusheniye
tverdykh tel," Moscow, State University, Institute
of Mechanics, Moscow, Scientific Transactions
No. 23, 1973, pp 1-106



NATIONAL AERONAUTICS AND SPACE ADMINISTRATION
WASHINGTON, D.C. 20546 DECEMBER 1978

STANDARD TITLE PAGE

1. Report No. NASA TT F-17157		2. Government Accession No.		3. Recipient's Catalog No.	
4. Title and Subtitle DEFORMATION AND DESTRUCTION OF SOLIDS				5. Report Date December 1978	
				6. Performing Organization Code	
7. Author(s) S. A. Shesterikov				8. Performing Organization Report No.	
				10. Work Unit No.	
9. Performing Organization Name and Address ESDUCK (Franklin) Cairo, Egypt				11. Contract or Grant No. NSF C-724	
				13. Type of Report and Period Covered Translation	
12. Sponsoring Agency Name and Address National Aeronautics and Space Administration and National Science Foundation Washington, D. C.				14. Sponsoring Agency Code	
15. Supplementary Notes Translation of "Deformirovaniye i razrusheniye tverdykh tel," Moscow, State University, Institute of Mechanics, Moscow, Scientific Transactions, No. 23, 1973, pp. 1-106					
16. Abstract					
17. Key Words (Selected by Author(s))			18. Distribution Statement Unclassified - Unlimited		
19. Security Classif. (of this report) Unclassified		20. Security Classif. (of this page) Unclassified		21. No. of Pages 131	
22.					

Moscow State University

Institute of Mechanics

SCIENTIFIC TRANSACTIONS

No. 23

(NauchnyyeTrudy)

No. 23

Deformation and Destruction of Solid Bodies

(Deformirovaniye i razrusheniye tverdykh tel)

Edited by S.A. Shesterikov

Moscow State University Press-1973.

Translated for the National Aeronautics and Space
Administration and National Science Foundation,
Washington, D.C. by ESDUCK (Franklin) Cairo, Egypt, 1978

TABLE OF CONTENTS

	<u>Page</u>
ANNOTATION	
1 - Stability of Cylindrical Shells of General Forms of Fixation. By: V.V. Kashelkin and S.A. Shesterikov.....	1
2 - Method of Calculation on the Destruction of Cylindrical Shells Under the Conditions of Creep. By: A.M. Lokoshchenko and S.A. Shesterikov.....	10
3 - Experimental Investigation of the Destruction Process of Cylindrical Shells and Under the Conditions of Creep. By: S.A. Shesterikov, V.V. Kashelkin, E.A. Myakotin and V.I. Nikolaev...	17
4 - Determination of the Destruction Time of a Cylindrical Shell Under Unsteady Conditions. By: A.M. Lokoshchenko.....	23
5 - Stability of Arch in the Case of Creep. By: V.V. Kashelkin.....	30
6 - The Behaviour of a Highly Corrugated Annular Plate Under Axisymmetrical Loading. By: A.M. Lokoshchenko.....	35
7 - Tension of an Orthotropic Nonlinear Elastic Plate with a Circular Hole. By: M.A. Yumasheva.....	44
8 - Cross Bending of Circular Perforated Plates. By: V.I. Astaf'ev.....	54
9 - Investigation of the Stresses in a Perforated Disk Subjected to Cross Bending, Using an Optical Method. By: L.S. Zlenko, A.M. Lokoshchenko and V.P. Netrebko.....	68
10 - An Approximate Method for the Estimation of the Dynamic Temperature Fields. By: S.A. Shesterikov and M.A. Yumasheva.....	76

	<u>Page</u>
11 - Relaxation and Creep Strength of Pipes Subjected to Complex Stress Strain. By: S.A. Shesterikov, V.D. Kurov, G.P. Mel'nikov, E.A. Myakotin and M.A. Yumasheva.....	84
12 - The Relationship between the Life of Material and the Level of Creep Stresses in the Case of Combined Loading. By: G.A. Tulyakov, G.I. Mel'nikov and Yu. D. Starostin.....	92
13 - About One Method of Estimation of Longevity in the Case of the Combined Action of Creep and Thermal Fatigue. By: G.A. Tulyakov, Yu. D. Starostin and G.P. Mel'nikov.....	95
14 - About the Utilization of San-Venan's Criterion for the Estimation of Life in the Case of Thermal Fatigue Under the Conditions of Complex Loading. By: G.A. Tulyakov and V.A. Metel'kov.....	99
15 - About one Possibility for the Description of the Laws of Creep. By: I.I. Trunin.....	105
16 - The Effect of the Structure of Material on Creep Strength. By: V.D. Kurov, G.P. Mel'nikov and A.A. Sokolov.....	111
17 - The Effect of Hydrostatic Compression of Porous Materials. By: A.M. Lokoshchenko and E.A. Myakotin.....	117

A N N O T A T I O N

This volume includes the works devoted to the individual problems of the strength of elements of constructions operating under conditions of elevated temperatures in the elastic zone. The rheological and plastic properties have been also considered. Particular attention has been paid to the study of the performance of tubular elements and perforated plates, as well as to the problems of the mechanical properties of the material of tubes operating under conditions of cyclic loading.

STABILITY OF CYLINDRICAL SHELLS OF GENERAL FORMS OF FIXATION

By

V.V. Kashelkin and S.A. Shesterikov

This work is devoted to the investigation of the large displacements of the points of a double-layer cylindrical shell subjected to an external hydrostatic load q . The shell of a length $2l$ is formed of two layers each of which having a thickness of h and separated by a distance of 2δ .

Let us assume that the properties of the shell material, subjected to spatial loading, can be described by the following relations [1]:

$$\dot{\epsilon}_\theta = \lambda \sigma_\theta^{n-1} (2\sigma_\theta - \sigma_z), \quad \dot{\epsilon}_z = \lambda \sigma_z^{n-1} (2\sigma_z - \sigma_\theta), \quad \sigma_z^2 = \sigma_\theta^2 - \sigma_\theta \sigma_z + \sigma_\theta^2, \quad (1)$$

where $\dot{\epsilon}_\theta, \dot{\epsilon}_z, \sigma_\theta$ and σ_z are the main deformation rates and the stresses in the circumferential direction and along the generating line.

Assuming an arbitrary fixation of the end cross-sections of the shell, it will be possible to consider that the destruction process takes place such that there are three planes of symmetry: XOY, XOZ and YOZ. The shell cross-sections in the planes of symmetry are shown in Fig. (1). Let us consider that in the CC'AA zone the shell swells, and in the CC'BB zone it contracts. Since the main attention is directed to the study of the destruction process, i.e. the study of large displacements, then it will be possible to consider that the shell behaves as a membrane in the XOZ and YOZ planes.

The equilibrium equations of the BC and CA sections for a mean section of a shell of unit width will have the following form :

$$M_a - T_1(1 - \sin \varphi)R_a - M_c(t_2) = \frac{q}{2}(x_o^2 + y_o^2 - a^2) , \quad (2)$$

$$M_b + T_2(1 - \cos \varphi)R_b + M_c(t_1) = \frac{q}{2}(x_o^2 + y_o^2 - b^2) ,$$

where T_1 and T_2 are the resultant forces $t_1(S)$ and $t_2(S)$, and $M_0(t_1)$ and $M_0(t_2)$ are the moments of the forces $t_1(S)$ and $t_2(S)$ with respect to point O.

The moments $M_{a,b}$ for the double-layer shell can be easily calculated. The remaining notations are shown in Fig.(2).

Let us assume that the generating lines BB' and AA' are described by the following relations :

$$\begin{aligned} y(z) &= \psi \left[\beta_o - \beta(t) \cos \frac{\pi z}{2\ell} \right] + (1 - \psi) \left[\beta_o - \right. \\ &\quad \left. - \frac{1}{2} \beta(t) \left(1 + \cos \frac{\pi z}{\ell} \right) \right] , \\ x(z) &= \psi \left[a_o + \alpha(t) \cos \frac{\pi z}{2\ell} \right] + (1 - \psi) \left[a_o + \right. \\ &\quad \left. + \frac{1}{2} \alpha(t) \left(1 + \cos \frac{\pi z}{\ell} \right) \right] , \end{aligned} \quad (3)$$

where $0 \leq \psi \leq 1$.

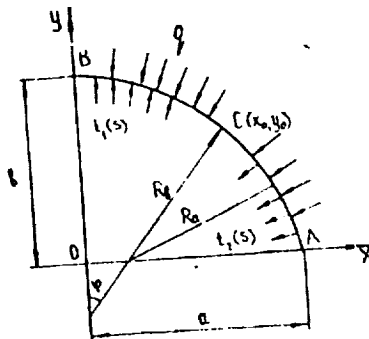


Fig. 2

At $\psi = 0$ we have the case of rigid fixation of the end cross-sections, whereas at $\psi = 1$ we will have the case of hinge supporting of end cross-sections, for other values ψ will correspond to the cases of elastic fixation of the end cross-sections.

The running length of these generating lines will be given by:

$$\ell_1(t) = \int_0^l \sqrt{1 + \beta^2 \left(\frac{x}{2\ell} \right)^2 \left[\psi \sin \frac{\pi z}{2\ell} + (1 - \psi) \sin \frac{\pi z}{\ell} \right]^2} dz$$

$$\ell_2(t) = \int_0^l \sqrt{1 + \alpha^2 \left(\frac{\pi}{2\ell} \right)^2 \left[\psi \sin \frac{\pi z}{2\ell} + (1 - \psi) \sin \frac{\pi z}{\ell} \right]^2} dz$$

This deformation leads to the rise of tensile stresses σ_z in each point of the generating lines BB' and AA' . Since in the XOZ and YOZ planes the shell behaves as a membrane, then σ_z^0 will describe the average stress across the shell thickness and will be directed along the tangent to the generating lines BB' and AA' . Let us assume that σ_z^0 is constant along the shell length. Cutting a strip of a unit width along the generating line BB' (AA'), let us consider a section on this strip; the coordinates of its end projections on the OZ axis will be z and $z + \delta_i$. Projecting the initial forces, acting along the strip, on the OX and OY axes, we get:

$$t_1 = \sigma_z^{01} 2h \frac{d^2 y}{dz^2} \delta_1, \quad t_2 = \sigma_z^{02} 2h \frac{d^2 x}{dz^2} \delta_2$$

there are further on the subscript "1" refers to BB' and the subscript "2" to AA' .

Naturally, t_1 and t_2 depend on the coordinate z . Since we are basically concerned with the destruction process in the middle of the shell, then the value of the second derivative at $z = 0$ will be satisfactory. However, if a certain mean value t_i ($i = 1, 2$) is introduced along the whole length of the shell, then the following expression could be used to represent the forces

$$t_1 = h\beta \frac{\pi}{\ell^2} (2 - \psi) \sigma_z^{01}, \quad t_2 = h\alpha \frac{\pi}{\ell^2} (2 - \psi) \sigma_z^{02}$$

For the rates of deformation in the circumferential direction and along the OZ axis, the following expression is obtained:

$$\begin{aligned} \dot{\epsilon}_\theta &= \dot{\epsilon}_\theta^0 - \gamma \dot{\alpha}_\theta, \\ \dot{\epsilon}_z &= \dot{\epsilon}_z^0, \end{aligned} \quad (4)$$

where $\dot{\kappa}$ is the rate of variation of the curvature.

Taking equations (4) into consideration the following expression is obtained from (1) for σ_θ

$$\sigma_\theta = \sigma_z \frac{\dot{\epsilon}_z^0 + 2(\dot{\epsilon}_\theta^0 - \eta \dot{\kappa}_\theta)}{2\dot{\epsilon}_z^0 + (\dot{\epsilon}_\theta^0 - \eta \dot{\kappa}_\theta)}$$

Taking into consideration that the shell is double-layered, then the moments M_a and M_θ could be calculated :

$$\begin{aligned} M_a &= \frac{-6\dot{\epsilon}_z^0 \dot{\kappa}_a \sigma_z^0 h \delta^2}{[2\dot{\epsilon}_z^0 + (\dot{\epsilon}_\theta^0 - \delta \dot{\kappa}_a)][2\dot{\epsilon}_z^0 + (\dot{\epsilon}_\theta^0 + \delta \dot{\kappa}_a)]} \\ M_\theta &= \frac{-6\dot{\epsilon}_z^0 \dot{\kappa}_\theta \sigma_z^0 h \delta^2}{[2\dot{\epsilon}_z^0 + (\dot{\epsilon}_\theta^0 - \delta \dot{\kappa}_\theta)][2\dot{\epsilon}_z^0 + (\dot{\epsilon}_\theta^0 + \delta \dot{\kappa}_\theta)]} \end{aligned} \quad (5)$$

Let us derive the parameters $T_1, T_2, M_c(t_1)$ and $M_c(t_2)$ for the first stage of the destruction process

$$T_1 = t, S_1 = t, R_\theta \varphi, \quad T_2 = t_2, S_2 = t_2, R_\theta \left(\frac{\pi}{2} - \varphi\right)$$

Here S_1 is the length of the BC arc, and S_2 is the length of the CA arc.

$$M_c(t_1) = \int_0^\varphi dM_c(t_1), \quad M_c(t_2) = \int_0^{\frac{\pi}{2}-\varphi} dM_c(t_2)$$

where

$$dM_c(t_1) = t_1 h_1 dS_1, \quad dM_c(t_2) = t_2 h_2 dS_2$$

and h_1 and h_2 are the arms of the corresponding initial force,

$$M_c(t_1) = t_1 R_\theta^2 (\varphi \sin \varphi + \cos \varphi - 1),$$

$$M_c(t_2) = t_2 R_\theta^2 \left[\left(\frac{\pi}{2} - \varphi\right) \cos \varphi + \sin \varphi - 1 \right]$$

After transformations, the equations of equilibrium can be written in the following form :

$$\begin{aligned}
 & \frac{6\dot{\epsilon}_z^{02} \dot{x}_a \sigma_z^{02} h \delta^2}{[2\dot{\epsilon}_z^{02} + (\dot{\epsilon}_\theta^0 - \delta \dot{x}_a)] [2\dot{\epsilon}_z^{02} + (\dot{\epsilon}_\theta^0 + \delta \dot{x}_a)]} + \gamma_1 \sigma_z^{01} R_a R_\theta \zeta_1 - \\
 & - \gamma_2 \sigma_z^{02} R_a^2 \phi_2 = \frac{q}{2} (a^2 - x_0^2 - y_0^2) , \\
 & \frac{6\dot{\epsilon}_z^{01} \dot{x}_\theta \sigma_z^{01} h \delta^2}{[2\dot{\epsilon}_z^{01} + (\dot{\epsilon}_\theta^0 - \delta \dot{x}_\theta)] [2\dot{\epsilon}_z^{01} + (\dot{\epsilon}_\theta^0 + \delta \dot{x}_\theta)]} + \gamma_2 \sigma_z^{02} R_a R_\theta \zeta_2 - \\
 & - \gamma_1 \sigma_z^{01} R_\theta^2 \phi_1 = \frac{q}{2} (b^2 - x_0^2 - y_0^2) ,
 \end{aligned} \tag{6}$$

where

$$\begin{aligned}
 \gamma_1 &= h \beta \frac{\pi}{\ell^2} (2 - \psi) , \\
 \gamma_2 &= h \alpha \frac{\pi}{\ell^2} (2 - \psi) , \\
 \zeta_1 &= \varphi (1 - \sin \varphi) , \\
 \zeta_2 &= \left(\frac{\pi}{2} - \varphi \right) (1 - \cos \varphi) , \\
 \phi_1 &= \varphi \sin \varphi + \cos \varphi - 1 , \\
 \phi_2 &= \left(\frac{\pi}{2} - \varphi \right) \cos \varphi + \sin \varphi - 1 .
 \end{aligned}$$

Let us introduce some additional notations :

$$\begin{aligned}
 \phi_3 &= \sin \varphi - \varphi \cos \varphi , \\
 \phi_4 &= \left(\frac{\pi}{2} - \varphi \right) \sin \varphi - \cos \varphi , \\
 v_1 &= \cos^2 \varphi - \cos \varphi , \\
 v_2 &= \sin \varphi - \sin^2 \varphi .
 \end{aligned}$$

The functions $\beta(t)$ and $\alpha(t)$ are expressed through $\beta_0(t)$ and $\alpha_0(t)$ as follows :

$$\beta(t) = \beta_0 - \beta(t) ,$$

$$\alpha(t) = \alpha_0 - \alpha(t) .$$

Taking into consideration the geometric relations and introducing the given denotions, we get for $\dot{\beta}$ and $\dot{\alpha}$ the following expressions

$$\dot{\beta} = \dot{R}_\theta \phi_1 + \dot{R}_\alpha \phi_4 ,$$

$$\dot{\alpha} = \dot{R}_\theta \phi_3 - \dot{R}_\alpha \phi_2 .$$

Utilizing the expression for the running length of the generating line $BB'(AA')$, the values of the rates of deformation $\dot{\epsilon}_z^0$ are derived :

$$\dot{\epsilon}_z^{01} = \dot{\beta} \beta \left(\frac{\pi}{2\ell} \right)^2 ,$$

$$\dot{\epsilon}_z^{02} = \dot{\alpha} \alpha \left(\frac{\pi}{2\ell} \right)^2$$

Concerning the rate of deformation of the mean surface in the circumferential direction, we take the value of the rate of deformation of the mean surface of a ring of a radius $R_m = \frac{1}{2}(R_{\alpha_0} + R_{\theta_0})$, subjected to an external hydrostatic load of q ; the thickness of the ring being equal to $2h$. Assuming that $\dot{\epsilon} = B\sigma^m$ for the ring, where $\sigma = q R_m / 2h$, and that $A = B(R_m/h)^m$, we get

$$\dot{\epsilon}_\theta^0 = A \left(\frac{q}{2} \right)^m = f_0$$

According to the assumptions made for the geometry of the shell cross-section

$$\dot{\epsilon}_\theta = \left(\frac{1}{R_\theta} \right) , \quad \dot{\epsilon}_\alpha = \left(\frac{1}{R_\alpha} \right)$$

Let us introduce the dimensionless parameters :

$$\bar{R}_\alpha = \frac{R_\alpha}{L} , \quad \bar{R}_\theta = \frac{R_\theta}{L} , \quad \bar{\beta} = \frac{\beta}{L} , \quad \bar{\alpha} = \frac{\alpha}{L} ,$$

$$\bar{h} = \frac{h}{L} , \quad \bar{\delta} = \frac{\delta}{L} , \quad \bar{\ell} = \frac{\ell}{L}$$

and express the time in the following dimensionless form

$$\tau = \int_0^2 t$$

Further, differentiate with respect to τ and omit the dash of the dimensionless parameters.

After transformations, the system of equations (6) takes the following form :

$$\begin{aligned} a_1 \dot{R}_\theta^2 + a_2 \dot{R}_\alpha \dot{R}_\theta + a_3 \dot{R}_\alpha^2 + a_4 \dot{R}_\theta + a_5 \dot{R}_\alpha &= L_1, \\ b_1 \dot{R}_\theta^2 + b_2 \dot{R}_\alpha \dot{R}_\theta + b_3 \dot{R}_\alpha^2 + b_4 \dot{R}_\theta + b_5 \dot{R}_\alpha &= L_2, \end{aligned} \quad (7)$$

The coefficients of the system of differential equations (7) have the following values :

$$a_1 = 4\alpha^2 \left(\frac{\pi}{2\ell}\right)^4 \phi_3^2 N_1,$$

$$a_2 = -6\alpha \left(\frac{\pi}{2\ell}\right)^2 G_z^{02} h \delta^2 \phi_3 R_\alpha^{-2} - 8\alpha^2 \left(\frac{\pi}{2\ell}\right)^4 \phi_2 \phi_3 N_1,$$

$$a_3 = 6\alpha \left(\frac{\pi}{2\ell}\right)^2 G_z^{02} h \delta^2 \phi_2 R_\alpha^{-2} + [4\alpha^2 \left(\frac{\pi}{2\ell}\right)^4 \phi_2^2 - \delta^2 R_\alpha^{-4}] N_1,$$

$$a_4 = 4\alpha \left(\frac{\pi}{2\ell}\right)^2 \phi_3 N_1,$$

$$a_5 = -4\alpha \left(\frac{\pi}{2\ell}\right)^2 \phi_2 N_1,$$

$$L_1 = -N_1,$$

$$b_1 = -6\beta \left(\frac{\pi}{2\ell}\right)^2 G_z^{01} h \delta^2 \phi_1 R_\theta^{-2} + [4\beta^2 \left(\frac{\pi}{2\ell}\right)^4 \phi_1^2 - \delta^2 R_\theta^{-4}] N_2,$$

$$b_2 = -6\beta \left(\frac{\pi}{2\ell}\right)^2 G_z^{01} h \delta^2 \phi_4 R_\theta^{-2} + 8\beta^2 \left(\frac{\pi}{2\ell}\right)^4 \phi_1 \phi_4 N_2,$$

$$\delta_3 = 4\beta^2 \left(\frac{\pi}{2\ell}\right)^4 \phi_4^2 N_2 ,$$

$$\delta_4 = 4\beta \left(\frac{\pi}{2\ell}\right)^2 \phi_1 N_2 ,$$

$$\delta_5 = 4\beta \left(\frac{\pi}{2\ell}\right)^2 \phi_4 N_2 ,$$

$$L_2 = -N_2 ,$$

$$N_1 = \gamma_1 \epsilon_z^{01} \epsilon_1 R_a R_b - \gamma_2 \epsilon_z^{02} \phi_2 R_a^2 - P \nu_2 R_a (R_b - R_a) ,$$

$$N_2 = \gamma_2 \epsilon_z^{02} \epsilon_2 R_a R_b - \gamma_1 \epsilon_z^{01} \phi_1 R_b^2 - P \nu_1 R_b (R_b - R_a) .$$

The system of equations (7) can be solved on a digital computer by the aid of standard programs.

References

1. Rabotnov, Yu.N. "Polzuchest' elementov Konstruktsii" (Creep of elements of constructions). --- (Moskva), 1966.
2. Kashelkin, V.V. and S.A. Shesterikov, "Splyushchivanie tsilindricheskoi obolochki konechnoi dlini pri polzuchesti" (Destruction of a cylindrical shell of a finite length under creep). --- Vestnik MGU, Mat., Mekh., No. 5 , p. 60 - 64 , 1971 .

METHOD OF CALCULATION ON THE DESTRUCTION OF
CYLINDRICAL SHELLS UNDER THE CONDITIONS OF
CREEP

By

A.M. Lokoshchenko and S.A. Shesterikov

The analysis of the behaviour of a cylindrical shell, subjected to an external evenly distributed pressure under a high temperature, is basically concerned with the determination of time, during which the shell can withstand the applied load. The whole method of calculation of such shells can be divided into four stages: analysis of the geometry of the shell, elaboration of the creep curves of the material, determination of the destruction time of the shell under stationary conditions, and evaluation of the effect of temperature and pressure fluctuations during the destruction time. Such a classification allows the successive determination of the nature of the made assumptions and the magnitude of errors resulting in each stage.

Let us consider a long cylindrical shell whose cross-section has a small ovality. The service time of such a shell under the action of an external evenly-distributed pressure q , depends on two geometric factors, viz. the ratio of the thickness H to the mean radius R_0 and the coefficient of initial ovality Δ_{00} :

$$H/R_0 = 2H/(a_{10} + a_{20}) \quad , \quad \Delta_{00} = (a_{10} - a_{20})/(a_{10} + a_{20}) \ll 1 \quad , \quad (1)$$

where $2a_{10}$ and $2a_{20}$ are the maximum and minimum diameters of the shell cross-section before the application of the pressure. The case, where the shell has an excessively large length in comparison with the cross-sections to the extent that the effect of end fixation can be neglected, will be considered below. In this case, the destruction of an oval ring of a unit width under the action of a hydrostatic pressure will be considered.

Under stationary conditions the hypothesis of a steady creep with an exponential function of $\dot{\rho}$ for the rate of creep in the stress σ [1] is the simplest hypothesis, which sufficiently describes the time characteristics of the material in an integral form :

$$\dot{\rho} = B\sigma^n \quad (2)$$

where ρ is the creep deformation; the dot denotes differentiation with respect to time. The coefficient B and the exponent n , which are derived from the creep experiments, denote that the material depends only on the temperature T .

In the investigation of the behaviour of oval rings most of the authors (as for example [2]) have considered that the deviation of the mean line from the circle is proportional to the cosine of the double polar angle. In [3], the pure moment stress condition of a noncircular ring has been considered. The form of this ring at any given time is approximated by the conjunction of two arcs of circles with radii R_1 and R_2 . The examination of this form of the ring (see Fig. 1) allows to investigate the deformation of the ring close to the moment of destruction.

Let us consider the destruction of such a ring in the case of a non-linear creep [2] taking into consideration the deformation ε_0 of the mean line. Three geometric hypotheses will be adopted: 1) the form of the mean line is approximated to the connected arcs of two circles (see Fig. 1); 2) the change of length of the mean line due to creep deformation can be neglected

$$(\pi/2 - \varphi)R_1 + \varphi R_2 = (\pi/2)R_0 \quad (3)$$

and 3) the hypothesis of plane sections for the total deformations

$$\varepsilon = \varepsilon_0 - \kappa \bar{z} \quad (4)$$

(κ is the variation of curvature and \bar{z} is the coordinate along the normal to the mean line). The geometry of the mean line is determined by means of the following three parameters: R_1 , R_2 and φ . For the determination of these parameters let us derive the equilibrium equations of the elements $A_1 A_2$ considering that the moment is equal to zero at the conjunction point $A_0(x_0, y_0)$:

$$\begin{aligned} q a_i &= [B^T (\gamma+1) \dot{x}_i]^{-1} [(\dot{\varepsilon}_{0i} + 0,5 \dot{x}_i H)^{T+1} - (\dot{\varepsilon}_{0i} - 0,5 \dot{x}_i H)^{T+1}] , \\ 0,5 q (a_i^2 - x_0^2 - y_0^2) &= [(\gamma+1)(\gamma+2)B^T \dot{x}_i^2]^{-1} \{ 0,5(\gamma+2)H \dot{x}_i [(\dot{\varepsilon}_{0i} - \\ &- 0,5 H \dot{x}_i)^{T+1} + (\dot{\varepsilon}_{0i} + 0,5 H \dot{x}_i)^{T+1}] + (\dot{\varepsilon}_{0i} - 0,5 H \dot{x}_i)^{T+2} - (\dot{\varepsilon}_{0i} + 0,5 H \dot{x}_i)^{T+2} \} , \\ i &= 1, 2, \quad \gamma^n = 1. \end{aligned} \quad (5)$$

These relations are obtained under the assumption that in the analysis of the process of shell destruction it is possible to neglect the

instantaneous deformations as compared with the creep deformations. The subscript i indicates the point of the ring (A_1 or A_2) to which the corresponding value is related. The coordinates a_1 , a_2 , x_0 and y_0 can be easily expressed through the main geometric parameters :

$$\begin{aligned} a_1 &= R_1 + (R_2 - R_1) \sin \varphi, \quad a_2 = R_2 - (R_2 - R_1) \cos \varphi, \\ x_0 &= R_2 \sin \varphi, \quad y_0 = R_1 \cos \varphi. \end{aligned} \quad (6)$$

The system of equations (3) and (5), in addition to substitution in (6), consists of five equations for the determination of R_1 , R_2 , φ , $\dot{\epsilon}_{01}$, and $\dot{\epsilon}_{02}$. The general form of this nonlinear system can be solved only numerically. However, in the case of a very small initial ovality of the ring Δ_{00} the destruction time of the ring can be simply evaluated in terms of the other parameters. Let us introduce the property of ring bending $\Delta(t)$

$$a_1 = R_0(1 + \Delta), \quad a_2 = R_0(1 - \Delta).$$

If we linearize (5) by Δ and make the necessary transformations, it will be possible to get for Δ the following differential equation :

$$\dot{\Delta}(t) = 5Bnq^n (R_0/H)^{n+2} \Delta \quad (7)$$

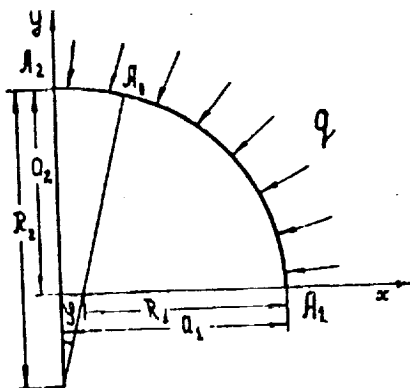


Fig. 1

It is clear that the destruction process is terminated when the condition $\Delta(t^*) = 1$ is fulfilled. Substituting this equation in the solution of equation (7), the following expression for the destruction time could be obtained :

$$t^* = (5Bnq^n)^{-1} (H/R_0)^{n+2} \ln(1/\Delta_0). \quad (8)$$

The parameter Δ_0 , characterizing the ovality of the ring as a result of application of pressure, - is related in the case of elastic loading to the parameter of ovality of the loaded shell Δ_{00} by the following relationship :

$$\Delta_0 = \Delta_{00} / (1 - q/q_0) , \quad q_0 = EH^3 / (4R_0^3) \quad (9)$$

Equation (7) is obtained from system (5) when the first orders of Δ are only preserved. In the corresponding system of reference [4], the terms with Δ^2 were preserved and an expression was obtained for the destruction time, which could lead, in certain cases, to incorrect values (for example, at $n > 8$). Such a drawback is not noticed in equation (8). In addition to the indicated work, some relationships were derived for the destruction time by several authors in the solution of a similar problem by other methods. Let us compare the results of calculation using these relationships for the case of $n = 3$.

Introduce the dimensionless parameter of the destruction time

$$\tau^* = B q^n (R_0/H)^{n+2} t^* \quad (10)$$

Therefore, equation (8) can be written in the following form :

$$\tau^* = 0,067 \ell n (t/\Delta_0) . \quad (11)$$

According to Hoff and others [5], the expression of τ^* , taking into consideration the equation of transition from the model shell to the real case, will have the following form :

$$\tau^* = 0,035 \ell n [1 + 0,315 H^2 / (R_0 \Delta_0)^2] \quad (12)$$

Yu. M. Volohkov and Yu. V. Nemirovskii [6] have obtained the following expression for τ^* :

$$\tau^* = 0,0175 H^2 / (R_0 \Delta_0)^2 . \quad (13)$$

The times τ^* , calculated according to equations (11)-(13), are given in table 1 at $H/R_0 = 0,01$, and in Table 2 at $H/R_0 = 0,1$.

Let us now represent equation (8) in a more general form. From Fig.(2) it follows that the following condition should be fulfilled, i.e. for the given

$$q R_0 = H G_0 , \quad (14)$$

pressure q it is possible to introduce the average compression characterized by the stress σ_0 . Using the replacement (14) we get from (8)

$$B\sigma_0^n t^* = (0,2/n)(H/R_0)^2 \ln(1/\Delta_0). \quad (15)$$

The left part of (15) can be represented by the aid of (2) in the following form

$$\rho^* = B\sigma_0^n t^*$$

where ρ^* is the creep deformation in the case of pure tension, accumulated under the action of the mean stress σ_0 for the destruction time of the shell. Finally, a relationship in the following form is obtained:

$$\rho^* = (0,2/n)(H/R_0)^2 \ln(1/\Delta_0). \quad (16)$$

Equation (16) expresses the following condition: the process of ring destruction is determined in the case of creep when for the given shell parameters (H , R_0 and Δ_{00}) a creep deformation (given by equation (16)) is accumulated.

Table 1

$$H/R_0 = 0.01$$

Δ_0	10^{-3}	10^{-2}	10^{-1}
(11)	0.460	0.310	0.154
(12)	0.122	0.010	0.0001
(13)	1.75	0.0175	0.0002

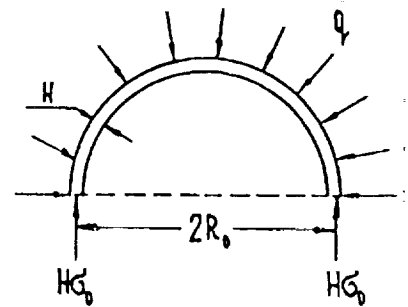


Fig. 2

Table 2

$$H/R_0 = 0.1$$

Δ_0	10^{-3}	10^{-2}	10^{-1}
(11)	0.460	0.310	0.154
(12)	0.282	0.122	0.010
(13)	175	1.75	0.017

In the application of equation (16) the calculation of the shell in the stationary conditions is conducted as follows. The geometric parameters of the shell (H , R_0 and Δ_{00}) are first determined. A series of tests on creep are then conducted for the determination of the value of n . From the series of creep curves, the curve corresponding to the mean stress σ_0 is chosen according to (14). On the selected curve the value of p^* , obtained from (16), is marked and the time t^* is subsequently determined.

The described method has the merit that only the creep parameter (the index n) should be calculated, whereas the original creep curves are used instead of the coefficient B .

The investigation of the shell destruction can be extended to the nonstationary conditions (unsteady creep, as well as variable stress and temperature). Since the available experimental data on creep under nonstationary conditions are very limited, it could be assumed, as a first approximation, that expression (16) remains valid under these conditions. The only property of material (the value of n), included in (16), can be considered as independent of the temperature T . Therefore, the problem is reduced to the determination of p^* from the given conditions of $T(t)$ and $\sigma(t)$ (the stress is related to pressure through (9)). The following method is more valid: stationary tests on creep are conducted under the given laws of variation of $T(t)$ and $\sigma(t)$, and the destruction time t^* is determined graphically from the obtained curve $p(t)$ according to the value of p^* calculated from (16). If the curves of creep, for the given range of stresses and temperatures, admit an analytical interpretation in the form

$$\dot{p} = f_1(p) f_2(T) \sigma_0^n \quad (17)$$

then, by integration of (17), for the given laws of variation of $T(t)$ and $\sigma(t)$, a relationship for $p(t)$ could be obtained from which the destruction time is determined using again (16).

References

1. Rabotnov, Yu.N. "Polzuchest' elementov konstruktsii" (Creep of elements of construction). --- Moskva, 1966.
2. Timoshenko, S.P. "Ustoichivost' uprugikh sistem" (Stability of elastic systems). --- Moskva, 1946.
3. Van'ko, V.I. and G.A. Shesterikov, "Splyushchivanie kol'tsa v usloviyakh polzuchesti" (Destruction of a ring under the conditions of creep). --- Izv. AN SSSR, "Mekh. tverd. tela", No. 5 : 127 - 130, 1966.
4. Van'ko, V.I. and S.A. Shesterikov, "Nelineino vyazkie tsilindricheskie obolochki pod vneshnim davleniem" (Nonlinear viscous cylindrical shells subjected to an external pressure). --- Izv. AN SSSR, "Mekh. tverd. tela", No.1 : 110-114, 1971.

5. Hoff N.J., W.E.Jahsman and W. Nachbar . A study of creep collapse of a long circular cylindrical shell under uniform external pressure. "J. Aero/Space sci.", 1959, 26, N 10, 633-669.
6. Volohkov, Yu.M. and Yu.V. Nemirovskii, "Nesimmetrichnoe vypuchivanie tsilindricheskikh obolochek v usloviyakh polzuchesti" (Asymmetrical swelling of cylindrical shells under the conditions of creep). --- Izv. AN SSSR, "Mekh. Tverd. tela", No. 4 , p. 136-138 , 1967 .

EXPERIMENTAL INVESTIGATION OF THE DESTRUCTION
PROCESS OF CYLINDRICAL SHELLS AND UNDER THE
CONDITIONS OF CREEP

By

S.A. Shesterikov, V.V. Kashelkin, E.A. Myakotin
and V.I. Nikolaev

Very few experimental works have been published on the process of creep buckling of metallic shells. This is related to the tremendous difficulties encountered with on setting up the experiments, and the long duration of the tests.

One of the first works devoted to this subject is that of Hoff [1]. This work includes experimental data on tests of 43 aluminium cylindrical shells. The shells were tested on bending under a steady moment at 260°. After a short period of creep, when the rate of creep was slowed down, the end section of the cylinder was continuously turned with a constant speed during a long period of time before the buckling of the cylinder. It was found that buckling took place in the zone of maximum pressure at one end of the cylinder or in its middle. The comparison of the experimental data with the theoretical values [1,2] gave satisfactory results.

The basic section of the work of Gerard and Gilbert [3] was devoted to the experimental investigation of creep buckling of thick-walled aluminium cylinders subjected to compressive and torsional loads. Two series of tests (each using 18 specimens) were conducted on compression and torsion at a temperature of 340°. In conclusion, it was stated that the method of critical deformation [4] was somewhat successful in predicting the critical time of cylinders under compression and torsion. The conception of Gerard was subject to criticism by Hoff [5], who noted that the experiments [3] conducted on thick and short cylinders are not satisfactory.

In [6], the results of the experiment carried out on long cylindrical tubes are given. The displacement of the extreme points of the smallest diameters of these tubes was measured. Loading was held when the rate of displacement began to increase intensively. This time was considered critical and was compared with the theoretical values. The authors considered that the comparison of the theoretical values with the experimental results is not reliable, due to the impossibility of measuring accurately the initial defects, the large scatter of the data on creep, ... etc.

The work of N.M. Matchenko [7] represents the experimental data obtained on the stability of cylindrical shells, compressed from both ends under creep conditions. Two series of tests were conducted on lead specimens at room temperature. In the case of loss of shell stability, solid

annular swellings appeared and the effect of bangs was not observed. The critical time was taken as the moment at which buckling appeared, which was determined according to the change of the character of axial deformation. The obtained time was high in comparison with that given by equations. These equations lead to the replacement of the secant and tangential modules for the calculation of the critical load [8] by new time dependant generalized modules.

In the work of A.S. Wol'mir and N.G. Zykin [9] experimental data are given on the stability of compressed rectangular (in a plane) cylindrical panels of duraluminium under the conditions of creep. The tests were conducted on ten panels at a temperature of 250°. The properties of the material were described in accordance with the ageing theory. The bending-time curves were plotted for panels with different values of initial bending and at different compressive stresses. For shells with a given value of initial camber, the critical time fell abruptly with the increase of the compressive stress. For loads constituting 90-95% of the critical elastic load, the critical time amounted in several cases to few seconds. The experimental data are in good agreement with the calculated values as far as the criterion of initial inconsistencies is obeyed.

The paper of A.P. Kuznetsov and N.M. Yungerman [10] represents the results of the experimental investigations carried out on the stability of duraluminium thin-walled cylindrical shells under the conditions of creep on compression and pure bending. The specimens were tested at a temperature of 255° before the moment of their actual destruction, which instantaneously occurred "as a bang". The following parameters were measured: the rotation of the end face cross section, the displacement of this section in the plane of action of the moment and the shell destruction in the mean section, and the longitudinal compressive deformation. The compression tests were conducted on 38 shells, and the bending tests were performed on 34 shells. In the compression tests the loss of stability took place with the formation of 6-9 half-waves along the circumference and 2-3 rows of half-waves along the length. The shells, which have lost stability, had the same shape as those after the instantaneous loss of stability. In the bending tests the waves were formed in the compression zone. The form and dimensions of these waves were close to the waves formed in axial compression. The creep characteristics of the material were determined by specimens made of tubes. The loss of the shell stability in the case of creep took place under loads above or below the lower critical load. The large scatter of the results is due to the fact that all the shells have different initial defects and the creep characteristics, themselves, have a considerable scatter. The general deformation, at which loss of stability takes place in the case of creep, is less than the elastic deformation corresponding to the upper critical stress. However, this general

deformation is higher than the elastic deformation corresponding to the lower critical stress. The scatter of the experimental data increases with the decrease of stresses, i.e. with the increase of the creep deformation. The same conclusion about the values of the critical shell deformations in the case of compression under creep conditions was theoretically obtained in [11] on the basis of the nonlinear equations of the shell, where the ageing hypothesis was assumed for the creep of the material. On the basis of the experimental results, it was concluded that the value of the critical time of loss of stability of shells under creep conditions, obtained according to the value of the elastic deformation corresponding to the lower critical compressive stress of shells with high significant initial defects, renders a guaranteed lower limit for the critical times of compression and bending.

In the works of Samuelson [12,13], the results of the experimental investigation of the buckling process of shells subjected to a steady axial load and to bending are given. He used shells made of aluminium alloy, and the test temperature was 225°. In the experiments, it was observed that the form of the shell is asymmetric. On all the curves of axial deformation vs. time it was noted that there is a section of accelerated creep before the loss of stability. The results were processed according to the ageing theory.

An investigation similar to that of the stability of aluminium cylinders, subjected to axial compression, was conducted in [14].

The large volume of published theoretical works devoted to different aspects of analysis of the processes of destruction and loss of stability of thin-walled elements under creep, i.e. evidently insufficiently confirmed by experimental investigations. These investigations would have, at least, qualitatively confirmed the hypotheses postulated in the investigation. This gap significantly influences the choice of further trends in the investigations, since few of the simple schemes used in engineering methods of calculation require experimental confirmation. For the study of these problems it was decided to conduct a series of experiments on cylindrical shells, subjected to an evenly-distributed external pressure. The results of tests have allowed to derive the relationships, suggested for the description of the destruction process of the shells.

On the basis of the analysis of the destruction process of the shells, a simple relationship of the following form was previously obtained:

$$t^* = \frac{1}{3n\lambda} \left(\frac{h}{R_0} \right)^{n+2} \left(\frac{2}{q} \right)^n \ell^n \frac{1}{\Delta_{10}}, \quad (1)$$

where t^* is the time of the destruction process, in hours;
 $2h$ is the thickness of the shell wall, in mm;
 R_0 is the average radius of the shell, in mm;
 Δ_{10} is a dimensionless parameter characterizing the initial defect of the shell;
 q is the pressure, in kg/mm^2 ;
 n and λ are the characteristic parameters of creep.

The parameters n and λ are determined on the basis of the experimental creep curves for the corresponding test temperature. It is assumed that the rate of creep $\dot{\epsilon}$ is related to the applied stress σ according to the following relationship:

$$\dot{\epsilon} = \lambda \sigma^n \quad (2)$$

In the high temperature testing laboratory of the Institute of Mechanics of Moscow State University, the creep of tubular specimens made of steel KH18N10T was tested on IMEKH-5 stands under stresses of 1, 2, 3, 4, 5, 6 and 8 kg/mm^2 at a temperature of 850°.

The description of the test rig, the procedure of testing the creep of tubular specimens, as well as the obtained creep curves are represented in the NII reports No. 1006 and 1120 of the Institute of Mechanics of Moscow State University.

As a result of treatment of the creep curves, the values of the creep parameters were obtained from the condition of the minimum values of the mean deviations for the indicated stresses and temperature:

$$n = 3.28, \quad \lambda = 8.32 \cdot 10^{-5} \left(\frac{\text{kg}}{\text{mm}^2} \right)^{-3.28} \frac{1}{\tau_{\text{hour}}}$$

By substantiation of the method of calculation of shells in the case of creep stability, and checking the previously obtained relationships, a series of tests were carried out on two rigs allowing the examination of cylindrical shells under external pressures and at temperatures of up to 1000°.

The obtained results indicate that the destruction times, measured in the experiments and determined from equation (1), have the same order of magnitude, assuming that the initial inaccuracy is of the order of 0.01-0.001. The conducted measurements of the shells before testing have shown that the initial inaccuracy amounts to ~ 0.002 . The results of the tests and the calculated data are demonstrated in Table 1.

Table 1

① № № п/п	② Диаметр образца	③ Толщина стенки	④ Темпе- ратура	Давле- ние ⑤ p кг/см ²	Время в ⑥ часах эк- сперимен- тально	Время в ча- сах теорети- ческое при ⑦ t = 0,01
1	60	1	850	1,0	84	190
2	45	2,5	850	11,0	135	55
3	45	1,5	850	9,0	3,5	5,6
4	45	0,5	850	1,0	29	21,5
5	45	0,5	850	1,3	11,3	9,1
6	45	0,5	850	1,4	8	7
7	45	0,5	850	1,8	4	3,12
8	36	0,5	850	1,0	112	85
9	36	0,5	850	1,2	51	46,5
10	36	0,5	850	1,4	23	27,8
11	22	0,5	850	5	8	5,1

Key: 1- No. of specimens; 2- Specimen diameter; 3- Wall thickness;
4- Temperature; 5- Pressure p, kg/cm²; 6- Experimental time, in hours;
7- Theoretical time, in hours.

References

1. Hoff N.J. Buckling at high temperature. "J. Roy. Aeronaut. Soc." 61(563), 1957.
2. Hoff N.J. Creep bending and buckling of thin circular cylindrical shells. "PJRAL Report No. 355", July, 1956.
3. Gerard G., A.C. Gilbert. "A critical strain approach to creep buckling of ...^{*)}
4. Gerard G. A creep buckling hypothesis. "J. Astronaut. Sci." 23(9), 1956.

^{*)} Translator's note: This reference is incomplete in the original text.

5. Hoff N.J. On a critical strain approach to creep buckling of plates and shells. "J. Astronaut. Sci.", 26(2) , 1959 .
6. Wah T., R.K. Gregory. Creep collapse of long cylindrical shells under high temperature and external pressure. "J.S. Astronaut. Sci.", 28(3) , 1961 .
7. Matchenko, N.M. "Ustoichivost' tsilindricheskikh obolochek pri polzuchesti" (Stability of cylindrical shells under creep). --- Zh prikl. mekh. i tekhn. fiz., No. 4, 1966.
8. Vol'mir, A.S. "Ustoichivost' deformiruemyykh sistem" (Stability of deformed systems). --- Fizmatgiz, Moskva , 1967.
9. Vol'mir, A.S. and P.G. Zykin, "Ustoichivost' obolochek v "bal'shom" pri polzuchesti" (Stability of shells under creep). --- Sb. "Teplovye napryazheniya v elementakh turbomashin", Kiev, No. 2 , 1962.
10. Kuznetsov, A.P. and N.M. Yungerman, "Eksperimental'noe issledovanie ustoichivosti obolochek v usloviyakh polzuchesti" (Experimental investigation of the stability of shells under creep). --- Zh. prikl. mekh. i tekhn. fiz., No. 4 , 1965.
11. Kuznetsov, A.P. and L.M. Kurshin, "K raschetu na ustoichivost' obolochek v usloviyakh polzuchesti po teorii stareniya" (Calculation of the stability of shells under creep conditions according to the ageing theory). --- Sb. "Problemy ustoichivosti v stroitel'noi mekhanike". Moskva , Stroiizdat, 1965.
12. Samuelson Lars Ake. An experimental investigation of creep buckling of circular cylindrical shells subject to axial compression. "Medd. Flygtekn. försöks inst", No. 98 , 1964 .
13. Samuelson Lars Ake. Experimental investigation of creep buckling of circular cylindrical shells under axial compression and bending. "Trans. ASME", 90(4) , 1968 .
14. Papirno R., E. Goldman. Experimental creep buckling of aluminium cylinders in axial compression, "Exp. Mech.", 9(8) , 1969 .
15. Kashelkin V.V. and S.A. Shesterikov, "Splyushchivanie dlinnoi tsilindricheskoi obolochki s prodol'nymi rebrami" (Destruction of a long cylindrical shell with longitudinal ribs). --- Izv. AN SSSR, Mekh. tverd. tela, No. 2 , 1971.

DETERMINATION OF THE DESTRUCTION TIME OF A CYLINDRICAL SHELL UNDER UNSTEADY CONDITIONS

By
A.M. Lokoshenko

The process of destruction of a ring under creep conditions, subjected to an external evenly-distributed pressure of q , will be approximately considered. It is assumed that the form of the ring of thickness $2h$ and of unit width is insignificantly different from the circular shape. In deriving the solution, the deformation of the mean line is taken into consideration. It is also assumed, as in [1], that during the whole process the ring has two axes of symmetry, and that the maximum and minimum diameters ($2a_1$ and $2a_2$) of the ring are the basic parameters. The destruction is defined as the condition when the minimum diameter of the ring tends to zero.

Apart from the generally adopted hypothesis of plane sections, we consider, as in [1], that at any moment of time the ring can be approximated by the conjunction of two circles with radii R_1 and R_2 (in Fig. 1, the first quarter is only shown).

Let us investigate the unsteady behaviour of the ring, where the properties of its material can be described by the relationship between the stress σ , creep deformation p and the rate of deformation \dot{p} in the form of the theory of strength;

$$\dot{p} = B p^{-\alpha} \sigma^n, \quad (1)$$

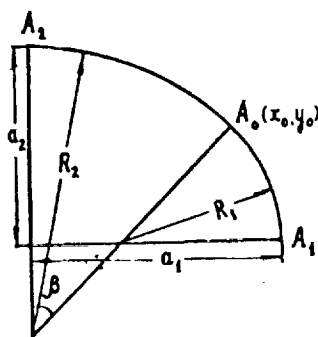


Fig. 1

where B , α and n are constants for the given material. For simplicity, n is represented in the form of the ratio of two integer odd numbers,

whereas α is given in the form of the ratio of an even number to an odd one. The parameter z will be defined as the distance between an arbitrary point of the ring and the mean line dividing the width to two equal halves. Therefore, on the basis of (1) and the hypothesis of plane sections we will have :

$$\sigma = (\dot{\rho} \rho^\alpha / B)^T = [(\dot{\epsilon}_0 - \dot{\alpha} h z) (\epsilon_0 - \alpha h z)^\alpha / B]^T, \quad T^{n+1} \quad (2)$$

where ϵ_0 and α are the deformation and the variation of the curvature of the mean line; the dot denotes that differentiation is carried out with respect to time t . If equation (2) is used and the equilibrium equation is written in a general form, a system of nonlinear differential equations is obtained, which can only be used for numerical calculation. Therefore, an approximate method for the solution of the problem will be only given. For simplicity, it is assumed that the deformation of the mean line and curvature in each point vary with time according to the same relationship, i.e. it is assumed that a time function $S(t)$ is operating (varying from one point to another), which makes it possible to determine the deformation and curvature in each point of the mean line from their rates :

$$\epsilon_0 = \dot{\epsilon}_0 S(t), \quad \alpha = \dot{\alpha} S(t),$$

In both relationships, the function $S(t)$ is the same.

The behaviour of the ring is investigated as in the analysis of buckling of a viscoplastic rod [2]. (y will be taken as the ratio $\dot{\epsilon}_0 / (h \dot{\alpha})$). From (2) we then get :

$$\sigma = B^{-T} \dot{\epsilon}_0^\alpha (\dot{\alpha} h z)^{\alpha-1} (y-z)^{\kappa-1}, \quad \kappa = (\alpha+1)T^{+1}$$

Now the resultant force and bending moment in an arbitrary cross section are calculated :

$$Q = h \int_{-1}^1 \sigma dz = B^{-T} \dot{\epsilon}_0^\alpha \dot{\alpha}^{(\kappa-1)} h^\kappa \kappa^{-1} \varphi,$$

$$M = h^2 \int_{-1}^1 \sigma z dz = B^{-T} \dot{\epsilon}_0^\alpha \dot{\alpha}^{(\kappa-1)} h^{(\kappa+1)} \kappa^{-1} (\kappa+1)^{-1} (y\varphi - \kappa\psi)$$

In the last expression the functions φ and ψ were introduced for the sake of accuracy. These functions are determined as follows :

$$\varphi = (y+1)^\kappa - (y-1)^\kappa, \quad \psi = (y+1)^\kappa + (y-1)^\kappa. \quad (3)$$

The equation of equilibrium of a ring of unit width will be satisfied in points A_1 and A_2 (see Fig. 1), (it should be also taken into consideration that the bending moment in the point of connection of the two circles A_0 is equal to zero). Let the coordinates of point A_0 be denoted by x_0, y_0 . The equations of equilibrium in points A_1 and A_2 will have the following form :

$$\begin{aligned} q a_i &= B^{-T} h^{\kappa} S_i^{\alpha T} \kappa^{-1} \dot{x}_i^{(\kappa-1)} \varphi_i, \\ 0,5 q (a_i^2 - x_0^2 - y_0^2) &= \frac{h^{(\kappa+1)} S_i^{\alpha T} \dot{x}_i^{(\kappa-1)}}{\kappa(\kappa+1) B^T} (\kappa \psi_i - y_i \varphi_i). \end{aligned} \quad (4)$$

Here and hereafter, the subscript i and the acquired values 1 and 2, indicate that the corresponding function is taken in point A_1 or A_2 . The system of equations (4) can be reduced to the following form :

$$\dot{x}_i = \left(\frac{a_i q \kappa B^T}{h^{\kappa} S_i^{\alpha T} \varphi_i} \right)^{\frac{1}{\kappa-1}}, \quad \frac{(\kappa+1)(a_i^2 - x_0^2 - y_0^2)}{2 h a_i} = \kappa \frac{\psi_i}{\varphi_i} - y_i. \quad (5)$$

Let us investigate in details the right hand side of the second equation in (5). Referring to (3), it is possible to show that at $y_i \gg 1$ this part of the equation can be approximated to the following form with an accuracy of up to y_i^{-2}

$$\kappa \frac{\psi_i}{\varphi_i} - y_i \approx \frac{(K^2 - 1)}{3 y_i} \quad (6)$$

Even at $y_i = 1$ the divergence is extremely insignificant : $(K^2 - 1)/3$ as compared to the accurate value $(K-1)$; moreover, K varies in the range of 1 to 2 (see [3]). Consequently, the relationship (6) can be practically applied up to $y_i = 1$. On the other hand, at $y_i \ll 1$, we have :

$$(\kappa \psi_i / \varphi_i) - y_i \approx 1/y_i \quad (7)$$

Expressions (6) and (7) are very simple, and the functions φ_1 and φ_2 can be expressed through them. Substituting in (5), we get a system of two nonlinear differential equations solved with respect to their derivatives. In this case the system has a very simple form and can be integrated by means of a digital computer using standard programs.

Let us now find an approximate value for the destruction time of the ring (t_*) in the case of a small initial ovality. From [1] it follows that such a ring maintains a small ovality during a time of $\sim 0.9 t_*$. The small ovality of the ring corresponds to the case $y_i \gg 1$. Then, from

(5) and (6) we have :

$$1/y_i \approx 3(a_i^2 - x_o^2 - y_o^2)/(2(\kappa-1)ha_i)$$

For the function φ_i the following approximation is obtained :

$$\varphi_i \approx 2\kappa y_i^{(\kappa-1)} \approx 2\kappa \left[\frac{2(\kappa-1)ha_i}{3(a_i^2 - x_o^2 - y_o^2)} \right]^{\kappa-1} \quad (8)$$

Substituting (8) in (5) we finally get :

$$\ddot{x}_i = \left(\frac{1}{R_i} \right)' = \frac{3(a_i^2 - x_o^2 - y_o^2)}{2(\kappa-1)ha_i} \left(\frac{qB^r a_i}{2h^{\kappa} S_i^{\alpha r}} \right)^{\frac{1}{\kappa-1}} \quad (9)$$

From Fig. 1 it is clear that :

$$a_1 = R_1 + (R_2 - R_1)\sin\beta, \quad a_2 = R_2 - (R_2 - R_1)\cos\beta, \quad x_o = R_2 \sin\beta, \quad y_o = R_1 \cos\beta. \quad (10)$$

Let us take the condition $\beta = \frac{\pi}{4}$. Introducing the mean radius R_o we get :

$$R_1 + R_2 = 2R_o, \quad x_o = R_2/\sqrt{2}, \quad y_o = R_1/\sqrt{2} \quad (11)$$

Let us now introduce the ovality parameter Δ as follows :

$$a_1 = R_o(1+\Delta), \quad a_2 = R_o(1-\Delta) \quad (12)$$

The ovality parameter Δ_o of the elastic ring is related to the parameter Δ_{oo} of the unloaded ring by the following relationship

$$\Delta_o = \Delta_{oo} q_e / (q_e - q), \quad q_e = 2Eh^3/R_o^3 \quad (13)$$

where q_e is the critical pressure according to Euler [4] and E is young modulus.

From (10) - (12) we will get :

$$R_1 = R_o(1-\Delta_1), \quad R_2 = R_o(1+\Delta_1), \quad \Delta_1 = (1+\sqrt{2})\Delta \quad (14)$$

The relationship (9) acquires the following form :

$$\dot{\Delta}_1 = \frac{3R_0 \Delta}{(\kappa-1)h(1+\Delta)} \left[\frac{qB^T R_0 (1+\Delta)}{2h^\kappa S_1^{\alpha T}} \right]^{\frac{1}{\kappa-1}}, \quad \dot{\Delta}_2 = \frac{-3R_0 \Delta}{(\kappa-1)h(1-\Delta)} \left[\frac{qB^T R_0 (1-\Delta)}{2h^\kappa S_2^{\alpha T}} \right]^{\frac{1}{\kappa-1}}$$

From this equation it is possible to get the approximate value of variation of Δ with respect to time :

$$\frac{3R_0 \Delta}{(\kappa-1)h} \left(\frac{qB^T R_0}{2h^\kappa} \right)^{\frac{1}{\kappa-1}} = \frac{\dot{\Delta}_1 \left(\frac{1}{\alpha+1} \right)}{R_0},$$

$$\frac{\dot{\Delta}}{\Delta^{\alpha+1}} = D, \quad D = (\sqrt{2} - 1) B \left(\frac{qR_0}{2h} \right)^n \left(\frac{R_0}{h} \right)^{2\alpha+2} \left(\frac{3n}{\alpha+1} \right)^{\alpha+1}$$

By integration we get :

$$\Delta(t) = [\Delta_0^{-\alpha} - \alpha D t]^{-\frac{1}{\alpha}} \quad (15)$$

As an estimate for the destruction time t_* let us accept the condition $\Delta(t_*) = 1$. Moreover, let us take into consideration the condition $\Delta_0^{-\alpha} \gg 1$ and the relationship (15). Therefore, the final equation relating the destruction time of the shell with the material characteristics, the shell parameters and the magnitude of the approximate pressure, will acquire a very simple form :

$$t_* = (\alpha D \Delta_0^\alpha)^{-1} \quad (16)$$

It is easy to note that in the case of an unsteady creep ($\alpha = 0$), formula (16) coincides in transition with the corresponding expression obtained from (5).

Similarly [5] it is possible to introduce a mean value for the compressive stress arising in the ring due to the action of pressure q , which can be expressed in the following simple relationship :

$$\sigma = \frac{qR_0}{2h}$$

If the creep curve for this stress σ is derived, we will have a relationship of the following form :

$$\dot{\rho} = B \rho^{-\alpha} \sigma^n$$

Considering σ as constant, it will be easy to get the following relationship :

$$B \left(\frac{q R_0}{2h} \right)^n = \frac{p^{\alpha+1}}{(\alpha+1)t} \quad (17)$$

Combining (15) and (17) for any $\alpha \neq 0$ we get :

$$\Delta^{-\alpha}(t) = \Delta_0^{-\alpha} - \frac{(\sqrt{2}-1)\alpha}{(\alpha-1)} \left(\frac{3n}{\alpha+1} \right)^{\alpha+1} \left(\frac{R_0}{h} \right)^{2(\alpha+1)} p^{(\alpha+1)}$$

Resorting to the same method followed in the derivation of equation (16), we will have a deformation p^* corresponding to the moment of destruction :

$$p^* = \frac{(\alpha+1)}{3n} \left[\frac{(\alpha+1)(1+\sqrt{2})}{\alpha} \right]^{\left(\frac{1}{\alpha+1}\right)} \cdot \left(\frac{h}{R_0} \right)^2 \cdot \left(\frac{1}{\Delta_0} \right)^{\left(\frac{\alpha}{\alpha+1}\right)} \quad (18)$$

By the aid of (18) it will be possible to determine the destruction time t_* on the creep curve, by the value corresponding to the pressure σ or the time during which the deformation p^* is accumulated. In equation (18) the parameters n and α of the material are included, whereas the original creep curves are utilized instead of the coefficient B .

References

1. Van'ko, V.I. and S.A. Shesterikov, "Splyushchivanie kol'tsa v usloviyakh polzuchesti" (Ring destruction under the conditions of creep). --- Izv. AN SSSR "Mekh. tverd. tela", No. 5: 127-130, 1966.
2. Lokoshchenko, A.M. and S.A. Shesterikov, "Relaksatsiya trub i vypuchivanie sterzhnei iz vyazko-plasticheskogo materiala" (Relaxation of tubes and buckling of rods of a visco-plastic material). --- Zhurnal prikl. mekh. i tekhn. fiz., No. 4: 154-159, 1966.
3. Shesterikov, S.A. "Ob. odnom uslovii dlya zakonov polzuchesti" (About one condition for the laws of creep). --- Izv. AN SSSR OTN "Mekhanika i Mashinostroenie", No. 1, 1959.
4. Timoshenko, S.P. "Ustoichivost' uprugikh sistem" (Stability of elastic systems). --- Moskva, 1946.

5. Lokoshchenko, A.M. and S.A. Shesterikov, "Metodika rascheta na splyushchivanie tsilindricheskikh obolochek v usloviyakh polzuchesti" (Method of calculation of cylindrical shells on their destruction under the conditions of creep). --- Look the present collection.

STABILITY OF ARCH IN THE CASE OF CREEP

By
V.V. Kashelkin

Let us consider the problem of stability of a sloping arch, subjected to an evenly distributed pressure q . In similar constructions, a loss of stability in the form of a "clap" is observed. This loss of stability can be discovered only on the consideration of the geometric nonlinearity. The arch is deformed in the case of creep, and the properties of its material can be described according to the theory of workhardening [1] by the following relationship :

$$\dot{p} = p^{-\alpha} \sigma^n \quad (1)$$

where p is the creep deformation
 σ is the stress
 n is the creep index
 α is the workhardening index.

Fig.(1) shows an arch of a length ℓ and height C_0 , and which is hinge supported from both ends. It is assumed that the arch axis represents an arc of a sinusoid

$$w_0 = C_0 \sin \frac{\pi x}{\ell}$$

The arch has a rectangular cross section of a height $2h$ and width b .

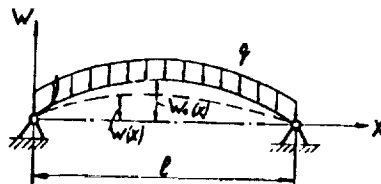


Fig. 1

For the solution of this problem let us adopt the combined variational principle, postulated in the work of Sanders, McComb and Schlechte [2]. This principle is based on the simultaneous variation of the field of creep rate and the field of stress rate, as shown in Pian's work [3].

For nonlinear problems, the function is expressed as follows :

$$\begin{aligned} K = & \int_V [\dot{\epsilon}_{ij} \dot{\epsilon}_{ij} + \frac{1}{2} \dot{\epsilon}_{ij} \dot{u}_{\alpha,i} \dot{u}_{\alpha,j} - \frac{1}{2} (\dot{\epsilon}_{ij}^N + 2\dot{p}_{ij}) \dot{\epsilon}_{ij}] dV - \\ & - \int_{\Sigma_u} \dot{T}_i (\dot{u}_i - \dot{u}_i^e) d\Sigma - \int_{\Sigma_T} \dot{T}_i^e \dot{u}_i d\Sigma \end{aligned} \quad (2)$$

where σ_{ij} is the stress tensor;
 e_{ij} is the tensor of total deformation;
 e_{ij}^M is the tensor of instantaneous deformation;
 P_{ij} is the tensor of creep deformation;
 u_i is the displacement;
 Σ_u is the section of the surface in which the deformations u_i^e are given;
 Σ_T is the section of the surface in which the forces T_i^e are given.

The dots denote differentiation with respect to time.

In this case it is necessary to get an exact expression for the component of deformation, namely :

$$e_{ij} = \frac{1}{2} (u_{ij} + u_{j,i} + u_{k,i} u_{k,j})$$

Denoting by y the distance from some point to the arch axis, we have according to the law of plane cross sections :

$$e = u_x + \frac{1}{2} (w_x^2 - w_{0,x}^2) - y (w_{xx} - w_{0,xx})$$

Now the function (2) can be reduced to the following form :

$$K = \theta \int_{-h}^h \int_0^l \left[\dot{\sigma} (\dot{u}_{,x} + w_{,x} \dot{w}_{,x} - y \dot{w}_{,xx}) + \frac{1}{2} \sigma \dot{w}_{,x}^2 - \frac{\dot{\sigma}^2}{2E} - \dot{\sigma} P^{-\alpha} \dot{\sigma}^n \right] dy dx \quad (3)$$

Here, it is assumed that the instantaneous deformation is elastic. According to [3], it is also assumed that the arch axis preserves its sinusoidal form, and that the moment is distributed along the arch according to the sinusoidal law. Therefore :

$$\begin{aligned} w &= c \sin \frac{\pi x}{\ell} = \eta c_0 \sin \frac{\pi x}{\ell} , \\ u &= 0 , \\ \sigma &= \sigma_e \left(\sigma_0 + \sigma_1 \frac{y}{2h} \sin \frac{\pi x}{\ell} \right) . \end{aligned} \quad (4)$$

Here $\sigma_e = \frac{\pi^2 h^2 E}{3 \ell^2}$ is the critical Eulerian stress for a beam of length ℓ ; η , σ_0 and σ_1 are dimensionless parameters.

Substituting (4) in (3) and varying K with respect to η , σ_0 and σ_1 , we get a system of three equations.

As a first approximation, let us assume that the creep deformation is equal to :

$$P = \left(\frac{\pi c_0}{2 \ell} \right)^2 (\eta^2 - 1)$$

Introduce the dimensionless time parameter τ as follows :

$$\tau = \left(\frac{\pi C_0}{2\ell} \right)^{-2\alpha} \sigma_e^{n-1} E t \quad (5)$$

Omitting the transformations, the final form of the system of equations is obtained, in which differentiation is carried out with respect to the dimensionless parameter of time:

$$\begin{aligned} \left(\frac{C_0}{2h} \right) \dot{\sigma}_0 \eta + \frac{1}{3} \dot{\sigma}_1 + \left(\frac{C_0}{2h} \right) \sigma_0 \dot{\eta} &= 0, \\ 6 \left(\frac{C_0}{2h} \right)^2 \dot{\eta} \eta - \dot{\sigma}_0 - (\eta^2 - 1)^{-\alpha} K_0 &= 0, \\ \left(\frac{C_0}{2h} \right) \dot{\eta} - \frac{1}{12} \dot{\sigma}_1 - (\eta^2 - 1)^{-\alpha} K_1 &= 0. \end{aligned} \quad (6)$$

Here K_0 and K_1 have the following values :

$$\begin{aligned} K_0 &= \frac{1}{2} \left[2\sigma_0^n + \sum_{m=1}^{\left[\frac{n}{2} \right]} \psi_m \sigma_0^{n-2m} \sigma_1^{2m} \right] \\ 4K_1 &= \sum_{m=1}^{\left[\frac{n+1}{2} \right]} \xi_m \sigma_0^{n-(2m-1)} \sigma_1^{2m-1}, \end{aligned}$$

where

$$\begin{aligned} \psi_m &= \frac{n(n-1)\dots[n-(2m-1)]}{(2m)!} \cdot \frac{1 \cdot 3 \cdot 5 \dots (2m-1)}{2 \cdot 4 \cdot 6 \dots 2m} \cdot \left(\frac{1}{2} \right)^{2m-1} \\ \xi_m &= \frac{n(n-1)\dots[n-(2m-2)]}{(2m-1)!} \cdot \frac{1 \cdot 3 \cdot 5 \dots (2m-1)}{2 \cdot 4 \cdot 6 \dots 2m} \cdot \left(\frac{1}{2} \right)^{2m-1} \end{aligned}$$

The initial conditions of equations (6) can be written as follows [1] :

$$\eta(0) = \eta_i, \quad \sigma_0(0) = \sigma_{0i}, \quad \sigma_1(0) = \sigma_{1i}.$$

The parameters η_i , σ_{0i} and σ_{1i} represent the values of the corresponding parameters obtained immediately after the application of the load. If we consider that the instantaneous deformation is elastic it will be convenient to utilize the variational principle of Reissner, assuming the same distribution of stresses and displacements as in the case of creep.

In this case, Reissner's function acquires the following form :

$$K = \delta \int_{-h}^h \int_0^\ell \left\{ \sigma \left[\frac{1}{2} (w_{,x}^2 - w_{0,x}^2) - y(w_{,xx} - w_{0,xx}) \right] - \frac{\sigma^2}{2E} \right\} dy dx + \int_0^\ell q w dx$$

Calculating this function and varying it with respect to η_i , σ_{oi} and $\sigma_{\eta i}$, we get the following system [1]:

$$\sigma_{\eta i} = 12 \left(\frac{c_o}{2h} \right) (\eta_i - 1), \quad \sigma_{oi} = 3 \left(\frac{c_o}{2h} \right)^2 (\eta_i^2 - 1),$$

$$\sigma_{oi} \left(\frac{c_o}{2h} \right) \eta_i + \frac{1}{12} \sigma_{\eta i} + \frac{q \ell^4}{EJ} \cdot \frac{1}{2\pi^5} \cdot \frac{1}{2h} = 0$$

where J is the moment of inertia of the arch cross section. Excluding σ_{oi} and $\sigma_{\eta i}$, we get the following algebraic equation for η_i :

$$3 \left(\frac{c_o}{2h} \right)^2 (\eta_i^3 - \eta_i) + (\eta_i - 1) + \tilde{\alpha} = 0$$

where

$$\tilde{\alpha} = \frac{1}{2\pi^5} \frac{q \ell^4}{EJ} \frac{1}{c_o}. \quad (7)$$

From (7) it follows that $\tilde{\alpha}$ as a function of η_i attains its extreme value at

$$\eta_i = \eta_{icr} = \pm \frac{\sqrt{3 \left(\frac{c_o}{2h} \right)^2 - 1}}{3 \left(\frac{c_o}{2h} \right)}, \quad (8)$$

If $\left(\frac{c_o}{2h} \right)^2 < \frac{1}{3}$, the deflection will proportionally increase with the loads, if $\left(\frac{c_o}{2h} \right)^2 > \frac{1}{3}$: when the critical value of the load parameter $\tilde{\alpha}_{cr}$ is attained a clap is produced and the deflection will instantaneously vary according to a definite value. The critical load can be derived from equation (7) if the value of η_{icr} , given in (8), is substituted in it.

Calculations were conducted for the arch, for which

$$\left(\frac{c_o}{2h} \right)^2 = \frac{2}{3} \quad \text{at } n=3 \quad \text{and } \alpha = 0, 1, 2$$

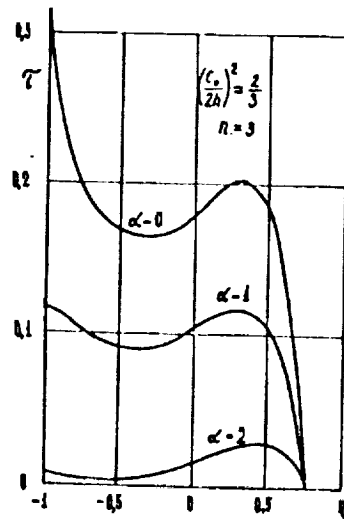


Fig. 2

The results are shown in Fig.(2) where the strong dependence of the process of arch deformation on the value of α characteristic of workhardening is clear.

References

1. Rabotnov, Yu.N. "Polzuchest' elementov konstruktssii" (Creep of elements of construction). --- Nauka, Moskva, 1966.
2. Sanders J.L., H.G. McComb and F.R. Schlechte. A variational theorem for creep with applications to plates and columns. "NACA Rept. No.1342", 1957.
3. Pian T.H.H. Creep buckling of curved beam under lateral loading. "Proc. 3rd U.S. Nat. Congr. Appl. Mech. N.Y. 1958".

THE BEHAVIOUR OF A HIGHLY CORRUGATED ANNULAR PLATE
UNDER AXISYMMETRICAL LOADING

By
A.M. Lokoshchenko

Let us consider a highly corrugated annular plate (shell of revolution) subjected to an axisymmetrically distributed pressure q and a centrally located concentrated force P (see Fig. 1). A is the internal radius of the plate, R its external radius, and $h \ll R$ its thickness. The external contour of the plate is fixed, whereas the central rigid circular disc of the radius A can move along the axis of symmetry. Moreover, the boundary conditions of the plate correspond to fixation along both contours. The plate is made of an elastic material with Young modulus E and Poisson's coefficient ν .

The first investigations on corrugated plates were confined to deflections of the order of the plate thickness. The longitudinal deformations, as well as the square of the tilt angle ψ , compared to unity, were neglected. D.Yu. Panov [1] considered finely corrugated plates by the application of Lyav's theory of thin-walled shells and solved the problem in series analysing the produced functions into powers of the parameters of loading and corrugation. V.I. Feodos'ev [2,3] extended

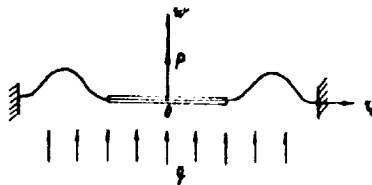


Fig. 1

Meissner's equation to the case of deflections of the order of thickness and used Bubnov-Galerkin's method for the investigation of the stability of inclined corrugated plates. L.E. Andreeva [4] replaced the corrugated plate by a flat one and considered the influence of corrugation by introducing the coefficients of anisotropy in the radial and circumferential directions. L.E. Andreeva [5] has investigated the behaviour of such a plate by the aid of V.I. Feodos'v's equations [2]. E.L. Aksel'rad [6,7] has derived the equations of noninclined shells of revolution in the case of existence of large deflections (see also [8]). However it is suitable to use them only at $\psi^2 \ll 1$. In [9], the nonlinear problem has been

reduced to a succession of linear problems by the analysis of Meisser's functions into trigonometric series. P.I. Begun [10] has investigated the behaviour of a corrugated plate using the linear approximation of equation (6) and adopting Bubnov-Galerkin's method.

Let us consider the deformation of a highly corrugated thin annular plate whose deflections may be of the same order of magnitude as its height. The plate is deformed basically due to the bending of the corrugation. Therefore, no limits are set to the tilt angles ψ . In the calculation it is assumed that the elongation of the meridian arc compared to unity is insignificant.

Since this is an axisymmetrical problem, then let us consider the cross section of the plate (see Fig. 1). Using Lagrange variables, the characteristics of the stress-deformation state in the plate will be determined as functions of z_0 , where z_0 is the distance between the considered point in the undeformed condition and the axis of symmetry. The distances from the considered point on the plate after the application of the load, to the z_0 axis and the axis of symmetry will be denoted by $w(z_0)$ and $v(z_0)$, respectively. The lower o signs indicate the values of the functions in the case of a zero load, whereas the upper ones indicate the values of the functions on the middle surface.

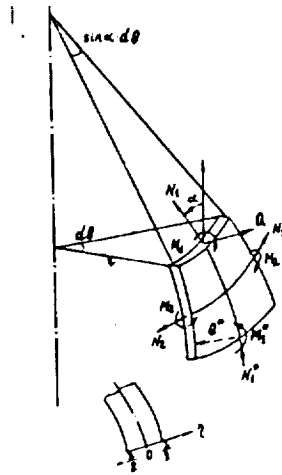


Fig. 2

Fig. (2) illustrates an element of the surface, cut by two meridian sections as well as two sections simultaneously perpendicular to the non-sectorial plane and the middle surface in the adjacent points. Let us denote the radius of curvature of the meridian arc by R , the element of the meridian arc directed to the external contour by ds the angle between the tangent to ds and the axis of symmetry by (α) , the variation in the angle in the process of deformation ($\psi = \alpha_0 - \alpha$) and elongation deformations in the meridian and

circumferential directions by ε_1 and ε_2 , and the corresponding variations in the curvature by \mathcal{K}_1 and \mathcal{K}_2 . The edges of the shell element are subjected to normal forces of N_1 and N_2 per unit length, as well as to a shear force of Q and bending moments of M_1 and M_2 .

Let us introduce the following dimensionless variables :

$$\begin{aligned} a &= A/R, \quad \bar{r}_0 = r_0/R, \quad \bar{r} = r/R, \quad \bar{R}_1 = R_1/R, \quad \bar{w} = w/R, \quad \lambda = h/R, \\ \bar{x} &= x/R, \quad \bar{q} = \frac{(1-\nu^2)R}{2Eh} q, \quad \bar{P} = \frac{(1-\nu^2)}{2\pi ERh} P, \quad \bar{N} = \frac{(1-\nu^2)}{Eh} N, \\ \bar{Q} &= \frac{(1-\nu^2)}{Eh} Q, \quad \bar{M} = \frac{12(1-\nu^2)R}{Eh^3} M \end{aligned} \quad (1)$$

The dashes should be omitted everywhere.

Let us consider the conditions of equilibrium of the shell element. Equating the sum of the forces projections in the direction tangential to the meridial curve with zero, we get according to (1) (as, for example, in [11]) the following :

$$d(N_1 z) ds - N_2 \sin \alpha - Q z / R_1 = 0 \quad (2)$$

The equation of the moments relative to the tangent to the circle will have the following form :

$$d(M_1 z) / ds - M_2 \sin \alpha + 12 Q z / \lambda^2 = 0 \quad (3)$$

If the central axisymmetrical section of the shell is cut, and all the forces acting on it are projected on the axis of rotation, then we will get :

$$N_1 \cos \alpha + Q \sin \alpha = (2/z) \int_0^z q \tau d\tau + P/z \quad (4)$$

Moreover, we will confine ourselves with the case $q = \text{const.}$ From geometrical considerations it is clear that (see Fig. 2) :

$$dw/ds = -\cos \alpha; \quad dz/ds = \sin \alpha; \quad dz_0/ds_0 = \sin \alpha_0; \quad (5)$$

$$\frac{d(\cdot)}{dz_0} = \frac{d(\cdot)}{ds} \cdot \frac{ds}{ds_0} \cdot \frac{ds_0}{dz_0} = \frac{(1+\varepsilon_1^0)}{\sin \alpha_0} \cdot \frac{d(\cdot)}{ds}$$

Further on, the derivatives of all the functions in \mathcal{Z}_0 will be denoted by a dash. According to the definition of R_1 we will have :

$$\frac{1}{R_1} = - \frac{d\alpha}{ds} = \frac{(\psi' - \alpha_0') \sin \alpha_0}{(1 + \varepsilon_1^0)} \quad (6)$$

The circumferential deformation ε_2 of any point on the plate will be given by :

$$\varepsilon_2 = (\mathcal{Z} + \eta \cos \alpha) / (\mathcal{Z}_0 + \eta \cos \alpha_0) - 1$$

Let us analyse this expression in a series according to the parameter η (see Fig. 2) of the distance from the considered point to the middle surface. Noting the small thickness ($\lambda \ll 1$) of the considered plate we shall confine ourselves in this expansion with the linear part

$$\varepsilon_2 = (\mathcal{Z}/\mathcal{Z}_0 - 1) + ((\mathcal{Z} \cos \alpha - \mathcal{Z} \cos \alpha_0)/\mathcal{Z}_0^2) \eta$$

Therefore, the deformation of the plate will be determined according to the hypothesis of plane cross sections (see Fig. 2) :

$$\begin{aligned} \varepsilon_{1,2} &= \varepsilon_{1,2}^0 + \alpha_{1,2} \eta ; \quad \varepsilon_2^0 = \frac{\mathcal{Z}}{\mathcal{Z}_0} - 1 ; \quad \alpha_1 = \frac{1}{R_1} - \frac{1}{R_{10}} = \\ &= \frac{(\psi' + \varepsilon_1^0 \alpha_0')}{(1 + \varepsilon_1^0)} \sin \alpha_0 ; \quad \alpha_2 = \frac{(\mathcal{Z}_0 \cos \alpha - \mathcal{Z} \cos \alpha_0)}{\mathcal{Z}_0^2} . \end{aligned} \quad (7)$$

Assuming an elastic relationship for the stresses $\sigma_{1,2}$ and deformations $\varepsilon_{1,2}$, we get :

$$N_{1,2} = \int_{-0,5\lambda}^{0,5\lambda} \sigma_{1,2} d\eta = \varepsilon_{1,2}^0 + \eta \varepsilon_{2,1}^0 ; \quad M_{1,2} = \int_{-0,5\lambda}^{0,5\lambda} \sigma_{1,2} \eta d\eta = \alpha_{1,2} + \eta \alpha_{2,1} . \quad (8)$$

The system of equations (2) - (8) defines the stress-deformation state in a thin-walled elastic shell. This system would be significantly simplified if it is assumed that $\varepsilon_1^0 \ll 1$. This assumption is quite justified, since the large displacements in the corrugated plate occur mainly due to bending and not due to the elongation of the meridian arc. In this case, equations (2) - (8) can be reduced to a system of five differential equations with

respect to z_0 at $\alpha \leq z_0 \leq 1$:

$$z' = \frac{\sin \alpha}{\sin \alpha_0} ;$$

$$\psi' = \frac{(M_1 - \nu x_2)}{\sin \alpha_0} - \alpha_0' (N_1 - \nu \epsilon_2^0) ;$$

$$N_1' = Q(\psi' - \alpha_0') - \frac{(1-\nu)[N_1 - (1+\nu)\epsilon_2^0] \sin \alpha}{z \sin \alpha_0} ; \quad (9)$$

$$M_1' = \frac{(1-\nu)[(1+\nu)x_2 - M_1] \sin \alpha - 12\lambda^{-2} z Q}{z \sin \alpha_0} ;$$

$$w' = - \frac{\cos \alpha}{\sin \alpha_0}$$

Here

$$\alpha = \alpha_0 - \psi, \epsilon_2^0 = \frac{z}{z_0} - 1, x_2 = \frac{z_0 \cos \alpha - z \cos \alpha_0}{z_0^2}, Q = \frac{P + q z^2}{z_0 \sin \alpha} - N_1 \epsilon \tan \alpha$$

The relationship $\alpha_0(z_0)$ and $\alpha_0'(z_0)$ are determined according to the initial form of corrugation. System (9) is solved under the following boundary conditions :

$$z(\alpha) = \alpha, z(1) = 1, \psi(\alpha) = \psi(1) = 0, w(1) = 0. \quad (10)$$

After the solution of the differential equations (9) the variables N_2 and M_2 are determined in terms of the obtained functions by the aid of algebraic relation

$$N_2 = \nu N_1 + (1 - \nu^2) \epsilon_2^0 ; M_2 = \nu M_1 + (1 - \nu^2) x_2$$

System (9) allows, in the case of a very high corrugation, to investigate the deflections of a plate, of the same order of magnitude as the dimensions of the corrugation. This is clear from the fact that in comparing the equations with their solutions no limitations are set on the parameter ψ .

The boundary problem (9) - (10) can be solved by the successive comparison and solution of the corresponding Coche problems. Taking the value of the argument $\tau_0 = a$ as an initial value, we choose three pairs for the initial values of the functions $N_1(a)$ and $M_1(a)$, under which the Coche problem is solved, and get three pairs for the values $\tau(1)$ and $\psi(1)$. In the three dimensional space $\{N_1(a), M_1(a), \tau(1)\}$, a plane is drawn through the three obtained points. Then the intersection of this plane with the $\tau(1) = 1$ plane is found according to (10). Finally, the linear relationship between $N_1(a)$ and $M_1(a)$ is determined. Similarly, by the investigation of the three-dimensional space $\{N_1(a), M_1(a), \psi(1)\}$ we get a second linear equation relating $N_1(a)$ with $M_1(a)$. Solving these two linear algebraic equations simultaneously in three arbitrary pairs of initial values we get the new combination of $N_1(a)$ and $M_1(a)$. By the repetition of the shown process of determination of the initial values, it will be possible to solve with a sufficient accuracy system (9) under the boundary conditions defined by (10).

The initial form of the corrugation is widely described by an expression comprising the three free parameters C , m and n :

$$w_0(\tau_0) = C \cos^n \left\{ \frac{\pi}{2} \left[\frac{2}{(1-a)} \left(\tau_0 - \frac{a+1}{2} \right) \right]^m \right\} \quad (11)$$

Therefore, the functions $\alpha_0(\tau_0) = 0.5\pi + \arctg w'_0$ and $\alpha'_0(\tau_0)$, could be determined. These functions are used in system (9) which was solved on a digital computer.

The relationships between the functions $N_1(a)$ and $M_1(a)$ and the value of the uniformly distributed pressure q are shown by continuous lines in Figs(3 and 4) for the following values of the parameters :

$$\begin{aligned} a &= 0.6 ; & c &= 0.12 ; & m &= 6 ; & n &= 8 ; \\ \lambda &= 0.01 ; & \nu &= 0.5 ; & P &= 0 . \end{aligned}$$

In Fig. 5, curve 1 characterizes the relationship between the deflection of the rigid centre $w(a)$ and the pressure q .

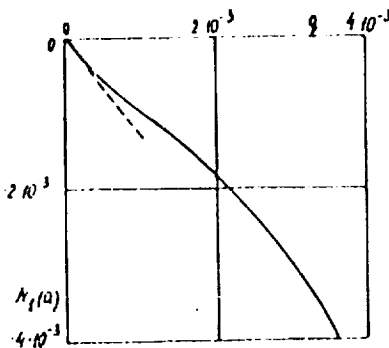


Fig. 3

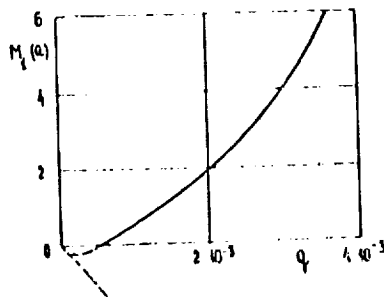


Fig. 4

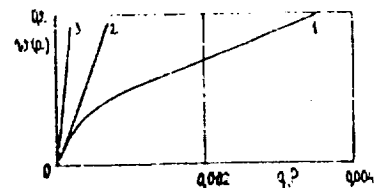


Fig. 5

In the case of small loads P and q , the investigated functions are expanded in series in terms of the small parameter sustaining only the first term.

$$\begin{aligned} r &= r_0 + (P+q)\rho; \quad \psi = (P+q)\varphi; \\ N_1 &= (P+q)N_3; \quad M_1 = (P+q)M_3; \\ w &= w_0 + (P+q)v \end{aligned}$$

Equation (9) is then reduced to a linear system of differential equations

$$\begin{aligned} \rho' &= -\varphi \operatorname{ctg} \alpha_0; \quad \varphi' = M_3 \operatorname{cosec} \alpha_0 - \beta/\tau_0^2 - \alpha_0' (N_3 - \beta/\tau_0); \\ N_3' &= \alpha_0' N_3 \operatorname{ctg} \alpha_0 - (\delta \alpha_0' / \tau_0) \operatorname{cosec} \alpha_0 - (1-\nu) [N_3 - (1+\nu)\beta/\tau_0] / \tau_0; \\ M_3' &= [(1-\nu^2)\beta/\tau_0^3] \operatorname{cosec} \alpha_0 - (1-\nu)M_3/\tau_0 - 12(\delta - \\ &\quad - N_3 \tau_0 \cos \alpha_0) / (\lambda^2 \tau_0 \sin^2 \alpha_0); \\ v' &= -\varphi; \quad a \leq \tau_0 \leq 1; \quad \rho(a) = \rho(1) = 0; \quad \varphi(a) = \varphi(1) = 0, \quad v(1) = 0, \end{aligned} \quad (12)$$

where β denotes $(\tau_0 \varphi - \rho \operatorname{ctg} \alpha_0)$, and $\delta = (P + q \tau_0^2) / (P + q)$

The dotted lines in Figs.(3-4) represent the solution of system (12). In the "load deflection" plane this solution represents the straight line tangential to the characteristics of the plate at the origin of coordinates. In Fig.(5) the straight line 2 represents the plate under the action of an evenly distributed pressure, whereas the straight line 3 represents a plate subjected only to a concentrated load P acting in the centre (using (12)).

In Fig.(6) the profile of a deformed shell is shown for different values of an evenly distributed pressure q . The results of the numerical calculation (9)-(10) show that the shell meridian is mainly deformed due to bending in the peripheries of its edges. The part of the meridian adjacent to the external fixed contour suffers a particularly high bending. The displacement of the highly extended middle part of the meridian with the increase of pressure q consists basically in its rotation with respect to the external end of the meridian.

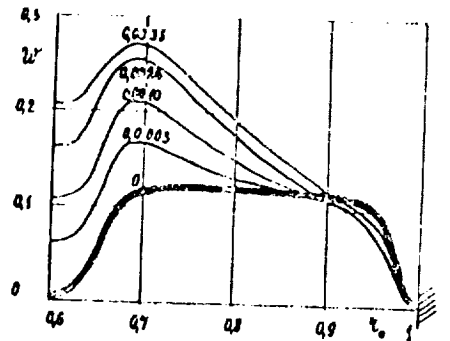


Fig. 6

In conclusion it is observed that the system of equations (9)-(10) allows to investigate the behaviour of plates with one or many corrugations (they don't need to be equal).

It is possible to take into consideration corrugations of different forms (including circular), enlarged boundary corrugation, angle of fixation of the external contour ... etc. The number of corrugations and their parameters are taken into consideration in discussing the initial form $w_0(\zeta_0)$.

References

1. Panov, D.Yu. "O bol'shikh progibakh Kruglykh membran so slabym gorform" (About large deflections of round membranes with a weak corrugation). --- "Prikl. mat. i mekh.", 5(2): 303-318, 1941.
2. Feodos'ev, V.I. "O bol'shikh progibakh i ustoychivosti krugloi membrany s melkoi gofrirovkoi" (About large deflections and stability of round membranes with a small corrugation). --- "Prikl. mat. i mekh.", 9(5): 389-412, 1945.
3. Feodos'ev, V.I. "Ob odnom sposobe resheniya nelineynykh zadach ustoychivosti deformiruemyykh sistem" (A method for the solution of the nonlinear problems of stability of deformed systems). --- "Prikl. mat. i mekh.", 27(2): 265-274, 1963.

4. Andreeva, L.E. "Raschet gofrirovannykh membran kak anizotropnykh plastinok" (Calculation of corrugated membranes as anisotropic plates) .— "Inzhenernyi, Sb." vol.21 : 128 - 141 , 1955 .
5. Andreeva, L.E. "Chislennoe reshenie zadachi o bol'shikh progibakh gofrirovannoi membrany" (Numerical solution of the problem of large deflections of a corrugated membrane). — "Izv. AN SSSR, Mekh. Tverd. tela.", No. 3: 83 -89, 1967 .
6. Aksel'rad, E.L. "Uraveniya deformatsii obolochek vrashcheniya i izgiba tonkostennykh sterzhnei pri bol'shikh uprugikh peremesocheni-nyakh" (The equations of deformation of shells of revolution and bending of thin walled rods under the conditions of large elastic displacements). — "Izv. AN SSSR, Otd. tekhn. n., Mekhan. i mashinostr.", No. 4: 84 - 92 , 1960 .
7. Aksel'rad, E.L., "Raschet gofrirovannoi membrany kak nepologoi obolochki" (Calculation of corrugated membranes as nonsloping shells). — "Izv. AN SSSR, Otd. tekhn. n., Mekhan. i mashinostr.", No. 5 : 67 - 76 , 1963 .
8. Reissner E. On axisymmetrical deformations of thin shells of revolution. "Proc. Sympos. Appl. Math.", No. 3 : 27 - 52 , 1950 .
9. Aksel'rad, E.L. "Periodicheskie resheniya osesimmetrichnoi zadachi teorii obolochek" (Periodical solution of the axisymmetrical problem of the theory of shells). — "Izv. AN SSSR, Mekh. tverd. tela.", No. 2 : 77-83, 1966.
10. Begun, P.I. "Raschet gofrirovannykh membran nekotorykh datchikov sistem avtomaticheskogo upravleniya" (Calculation of the corrugated membranes of some transducers of automatic control systems). — Sb.: "Tekhn. ekspluatatsiya morskogo flota", vol.123 , Tr. TsNIIMF ,125 - 135 .
11. Birger, I.A. "Kruglye plastinki i obolochki vrashcheniya" (Round plates and shells of revolution). — Moskva , 1961.

TENSION OF AN ORTHOTROPIC NONLINEAR ELASTIC
PLATE WITH A CIRCULAR HOLE

By

M.A. Yumasheva

In the available literature, the problem of stress concentration near a hole was solved either for an anisotropic but linearly elastic medium, or for a physically nonlinear but isotropic body. The concentration of stresses near the holes of orthotropic elastic plates was discussed in the books of G.I. Savin [1] and S.G. Lekhnitskii [2]. The orthotropic strips with holes, subjected to tension and bending, were investigated in few works [3,4]. The influence of the nonlinearity of the relationship between stresses and deformations on stress concentration near holes was also studied in [1] for isotropic materials. The plastic distribution of stresses around holes of circular or other forms, was considered in the book published by V.V. Sokolovskii [5].

Numerous researches (for example, [6,7]) were devoted to the approximate methods used for the solution of the problem of determination of the coefficient of stress concentration in the plastic zone of an infinite isotropic plate with a circular hole existing under tension.

It is highly significant to analyse the concentration of stresses and to determine their distribution around a circular hole of an orthotropic plate existing under axial tension, whose material follows the nonlinear relationships between stresses and deformations, taking into consideration at the same time its anisotropic and physically nonlinear properties.

Let us consider an infinite "orthotropic" plate with a circular hole of a radius a existing under the conditions of an evenly distributed axial tension p extending to infinity (see Fig. 1). Let us locate the origin of the coordinates in the centre of the hole and take the major anisotropy directions of the mechanical properties (it is assumed that the direction of the tensile force coincides with one of the major axes of anisotropy) as the direction of the x and y axes.

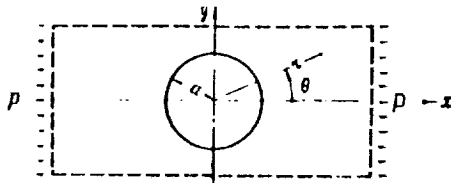


Fig. 1

Assume that the relationship between the deformations ϵ_{ik} and stresses σ_{lm} could be expressed in the following form [8]

$$\epsilon_{ik} = S_{iklm} \sigma_{lm} + \psi(f) q_{iklm} \sigma_{lm}, \quad (1)$$

$$\psi(f) = \frac{b_n}{2n-1} f^{n-1}, \quad f = \frac{1}{2} q_{iklm} \sigma_{ik} \sigma_{lm},$$

where S_{iklm} is the tensor of elastic constants; q_{iklm} is the tensor of material constants taking into consideration the anisotropy of nonlinear properties; b and n are constants describing the nonlinearity of the material.

For a plane stress state of an orthotropic body, expressed in functions of stresses, the equations of equilibrium will be automatically satisfied. From the conditions of compatibility, a nonlinear differential equation is derived for the stress function $\mathcal{F}(x, y)$

$$a_{11} \frac{\partial^4 \mathcal{F}}{\partial y^4} + (2a_{12} + a_{66}) \frac{\partial^4 \mathcal{F}}{\partial x^2 \partial y^2} + a_{22} \frac{\partial^4 \mathcal{F}}{\partial x^4} = R(\psi), \quad (2)$$

$$R(\psi) = -\psi \left[q_{11} \frac{\partial^4 \mathcal{F}}{\partial y^4} + (2q_{12} + q_{66}) \frac{\partial^4 \mathcal{F}}{\partial x^2 \partial y^2} + q_{22} \frac{\partial^4 \mathcal{F}}{\partial x^4} \right] - 2 \frac{\partial \psi}{\partial y} \left[q_{11} \frac{\partial^3 \mathcal{F}}{\partial y^3} + \right. \\ \left. + (q_{12} + \frac{1}{2} q_{66}) \frac{\partial^3 \mathcal{F}}{\partial y \partial x^2} \right] - 2 \frac{\partial \psi}{\partial x} \left[(q_{12} + \frac{1}{2} q_{66}) \frac{\partial^3 \mathcal{F}}{\partial y^2 \partial x} + q_{22} \frac{\partial^3 \mathcal{F}}{\partial x^3} \right] - \\ - \frac{\partial^2 \psi}{\partial y^2} \left(q_{11} \frac{\partial^2 \mathcal{F}}{\partial y^2} + q_{12} \frac{\partial^2 \mathcal{F}}{\partial x^2} \right) - \frac{\partial^2 \psi}{\partial x^2} \left(q_{12} \frac{\partial^2 \mathcal{F}}{\partial y^2} + q_{22} \frac{\partial^2 \mathcal{F}}{\partial x^2} \right) - q_{66} \frac{\partial^2 \psi}{\partial x \partial y} \frac{\partial^2 \mathcal{F}}{\partial x \partial y}$$

where the following notations were introduced :

$$S_{1111} = a_{11}, \quad S_{2222} = a_{22}, \quad S_{1122} = a_{12}, \quad 4S_{1212} = a_{66}, \\ q_{1111} = q_{11}, \quad q_{2222} = q_{22}, \quad q_{1122} = q_{12}, \quad 4q_{1212} = q_{66}$$

Let us consider in details the case of a weakly anisotropic material. In this case the perturbation method can be used. According to this method, the quantities characterizing the deviation of the properties of an anisotropic medium from the corresponding isotropic material are taken

as small parameters, and the problems of the isotropic theory of plasticity (nonlinear elasticity) are obtained in each approximation. However, if the perturbation method is used, with complex parameters characterizing the deviation of the anisotropic properties from the corresponding isotropic and linear properties of the material, we will get the problems of isotropic linear elasticity in each approximation.

Assuming $q_{11} = 2$, we denote

$$a_{11} = \frac{1}{E}, \quad a_{12} = -\frac{\nu}{E} \quad (4)$$

The parameters $\alpha_1, \dots, \alpha_6$ are then introduced in the following relationships

$$\begin{aligned} a_{22} &= \frac{1}{E} (1 + \alpha_2), \quad a_{66} = \frac{2(1+\nu)}{E} (1 + \alpha_1), \quad q_{22} = 2 + \alpha_3, \\ q_{66} &= 4 \left(\frac{3}{2} + \alpha_5 \right), \quad \psi = \alpha_6 (f_0 + \alpha f_1), \quad q_{12} = -1 + \alpha_4 \end{aligned} \quad (5)$$

where

$$f_0 = \sigma_{11}^2 + \sigma_{22}^2 - \sigma_{11}\sigma_{22} + 3\tau_{12}^2, \quad \alpha f_1 = \frac{\alpha_3}{2} \sigma_{22}^2 + \alpha_4 \sigma_{11}\sigma_{22} + 2\alpha_5 \tau_{12}^2$$

there $\alpha_1, \dots, \alpha_5$ are small parameters characterizing the anisotropy of the material, and α_6 is a small parameter characterizing the non-linearity of the properties of material.

Using the conditions (4) and (5), equation (2) can be rewritten in the following form :

$$\begin{aligned} & \frac{1}{E} \nabla^4 \mathcal{F} + \frac{\alpha_2}{E} \frac{\partial^4 \mathcal{F}}{\partial x^4} + \frac{2(1+\nu)}{E} \alpha_1 \frac{\partial^4 \mathcal{F}}{\partial x^2 \partial y^2} + \alpha_6 \left[2f_0 \nabla^4 \mathcal{F} + \right. \\ & + 4 \frac{\partial f_0}{\partial y} \left(\frac{\partial^3 \mathcal{F}}{\partial y^3} + \frac{\partial^3 \mathcal{F}}{\partial x^2 \partial y} \right) + 4 \frac{\partial f_0}{\partial x} \left(\frac{\partial^3 \mathcal{F}}{\partial x^3} + \frac{\partial^3 \mathcal{F}}{\partial x \partial y^2} \right) + \\ & + \frac{\partial^2 f_0}{\partial y^2} \left(2 \frac{\partial^2 \mathcal{F}}{\partial y^2} - \frac{\partial^2 \mathcal{F}}{\partial x^2} \right) + \frac{\partial^2 f_0}{\partial x^2} \left(-\frac{\partial^2 \mathcal{F}}{\partial y^2} + 2 \frac{\partial^2 \mathcal{F}}{\partial x^2} \right) + 6 \frac{\partial^2 \mathcal{F}}{\partial x \partial y} \frac{\partial^2 f_0}{\partial x \partial y} \left. \right] + \\ & + \left[\alpha_4 \left(f_0 \frac{\partial^4 \mathcal{F}}{\partial x^2 \partial y^2} + 2 \frac{\partial f_0}{\partial x} \frac{\partial^3 \mathcal{F}}{\partial x \partial y^2} + \frac{\partial^2 f_0}{\partial x^2} \frac{\partial^2 \mathcal{F}}{\partial y^2} + \alpha_3 \left(f_0 \frac{\partial^4 \mathcal{F}}{\partial x^4} + \right. \right. \right. \end{aligned}$$

$$+ 2 \frac{\partial f_0}{\partial x} \frac{\partial^3 \mathcal{F}}{\partial x^3} + \frac{\partial^2 f_0}{\partial x^2} \frac{\partial^2 \mathcal{F}}{\partial x^2} \Big) + 4 \alpha_5 \left(f_0 \frac{\partial^4 \mathcal{F}}{\partial x^2 \partial y^2} + \frac{\partial f_0}{\partial x} \frac{\partial^3 \mathcal{F}}{\partial x \partial y^2} + \right.$$

$$\left. + \frac{\partial f_0}{\partial y} \frac{\partial^3 \mathcal{F}}{\partial y \partial x^2} + \frac{\partial^2 f_0}{\partial x \partial y} \frac{\partial^2 \mathcal{F}}{\partial x \partial y} \right) + 2 \alpha f_1 \nabla^4 \mathcal{F} + 4 \alpha \frac{\partial f_1}{\partial y} \left(\frac{\partial^3 \mathcal{F}}{\partial y^3} + \frac{\partial^3 \mathcal{F}}{\partial x^2 \partial y} \right) +$$

$$+ 4 \alpha \frac{\partial f_1}{\partial x} \left(\frac{\partial^3 \mathcal{F}}{\partial x^3} + \frac{\partial^3 \mathcal{F}}{\partial x \partial y^2} \right) + \alpha \frac{\partial^2 f_1}{\partial y^2} \left(2 \frac{\partial^2 \mathcal{F}}{\partial y^2} - \frac{\partial^2 \mathcal{F}}{\partial x^2} \right) + \alpha \frac{\partial^2 f_1}{\partial x^2} \left(- \frac{\partial^2 \mathcal{F}}{\partial y^2} + \right.$$

$$\left. + 2 \frac{\partial^2 \mathcal{F}}{\partial x^2} \right) + 6 \alpha \frac{\partial^2 f_1}{\partial x \partial y} \frac{\partial^2 \mathcal{F}}{\partial x \partial y} \Big] + \alpha \left[\alpha_4 \left(f_1 \frac{\partial^4 \mathcal{F}}{\partial y^2 \partial x^2} + \right. \right.$$

$$\left. + 2 \frac{\partial f_1}{\partial y} \frac{\partial^3 \mathcal{F}}{\partial y \partial x^2} + \frac{\partial^2 f_1}{\partial y^2} \frac{\partial^2 \mathcal{F}}{\partial x^2} \right) + \alpha_4 \left(f_1 \frac{\partial^4 \mathcal{F}}{\partial x^2 \partial y^2} + \right.$$

(6)

$$+ 2 \frac{\partial f_1}{\partial x} \frac{\partial^3 \mathcal{F}}{\partial y^2 \partial x} + \frac{\partial^2 f_1}{\partial x^2} \frac{\partial^2 \mathcal{F}}{\partial y^2} \Big) + \alpha_3 \left(f_1 \frac{\partial^4 \mathcal{F}}{\partial x^4} + 2 \frac{\partial f_1}{\partial x} \frac{\partial^3 \mathcal{F}}{\partial x^3} + \right.$$

$$\left. + \frac{\partial^2 f_1}{\partial x^2} \frac{\partial^2 \mathcal{F}}{\partial x^2} \right) + 4 \alpha_5 \left(f_1 \frac{\partial^4 \mathcal{F}}{\partial x^2 \partial y^2} + \frac{\partial f_1}{\partial x} \frac{\partial^3 \mathcal{F}}{\partial x \partial y^2} + \right.$$

$$\left. \left. + \frac{\partial f_1}{\partial y} \frac{\partial^3 \mathcal{F}}{\partial y \partial x^2} + \frac{\partial^2 f_1}{\partial x \partial y} \frac{\partial^2 \mathcal{F}}{\partial x \partial y} \right) \right] \Bigg\} = 0 .$$

The solution $\mathcal{F}(x, y)$ of the differential equation (6) is a function of the small parameters introduced in this equation. This function, which can be denoted by $\mathcal{F}(x, y, \alpha_i)$, can be expanded in series in terms of powers of α_i .

$$\begin{aligned} \mathcal{F}(x, y, \alpha_i) = & \mathcal{F}_0(x, y) + \mathcal{F}_1 \alpha_1 + \mathcal{F}_2 \alpha_2 + \mathcal{F}_3 \alpha_3 + \mathcal{F}_4 \alpha_4 + \mathcal{F}_5 \alpha_5 + \mathcal{F}_6 \alpha_6 + \\ & + \mathcal{F}_7 \alpha_1^2 + \mathcal{F}_8 \alpha_2^2 + \mathcal{F}_9 \alpha_3^2 + \mathcal{F}_{10} \alpha_4^2 + \mathcal{F}_{11} \alpha_5^2 + \mathcal{F}_{12} \alpha_6^2 + \mathcal{F}_{13} \alpha_1 \alpha_2 + \mathcal{F}_{14} \alpha_1 \alpha_3 + \\ & + \mathcal{F}_{15} \alpha_1 \alpha_4 + \mathcal{F}_{16} \alpha_1 \alpha_5 + \mathcal{F}_{17} \alpha_1 \alpha_6 + \mathcal{F}_{18} \alpha_2 \alpha_3 + \mathcal{F}_{19} \alpha_2 \alpha_4 + \mathcal{F}_{20} \alpha_2 \alpha_5 + \\ & + \mathcal{F}_{21} \alpha_2 \alpha_6 + \mathcal{F}_{22} \alpha_3 \alpha_4 + \mathcal{F}_{23} \alpha_3 \alpha_5 + \mathcal{F}_{24} \alpha_3 \alpha_6 + \mathcal{F}_{25} \alpha_4 \alpha_5 + \mathcal{F}_{26} \alpha_4 \alpha_6 + \mathcal{F}_{27} \alpha_5 \alpha_6 + \dots \end{aligned} \quad (7)$$

Substituting the series of $\mathcal{F}(x, y)$ in the differential equation (6), and expanding the terms in powers of α_i , the coefficients of all the terms should be equated to zero so that equation (6) is satisfied for all the values of α_i . This requirement leads to an endless system of biharmonic equations for the determination of the functions $\mathcal{F}_0, \mathcal{F}_1, \dots$. The first of these equations can be written in the following form :

$$\nabla^4 \mathcal{F}_0 = 0 \quad (8)$$

The differential equations, obtained after equating the coefficients of α_i , α_i^2 and $\alpha_i \alpha_k$ to zero, will have the following form :

$$\nabla^4 \mathcal{F} + A_j = 0 \quad , \quad j = 1, 2, \dots, \quad (9)$$

Moreover, A_j represents expressions composed of the functions $\mathcal{F}_0, \mathcal{F}_1, \dots, \mathcal{F}_{j-1}$ and their derivatives; consequently, it represents the already known solutions of previous differential equations. Although the expressions A_j are determined without any main difficulty, yet they are quickly complicated with the increase of j . It is noted that the function \mathcal{F}_0 will satisfy the boundary conditions :

$$\left. \begin{aligned} \sigma_z = 0 \quad , \quad \tau_{z\theta} = 0 \quad & \text{at} \quad z = a \quad , \\ \sigma_r = \frac{P}{2} (1 + \cos 2\theta) \quad , \quad \sigma_\theta = \frac{P}{2} (1 - \cos 2\theta) \\ \tau_{r\theta} = -\frac{P}{2} \sin 2\theta \end{aligned} \right\} \quad z = \infty \quad (10)$$

This necessitates that the function $\mathcal{F}_j (j \neq 0)$ should satisfy the zero boundary conditions.

The equations of \mathcal{F}_j are obtained as follows :

$$\begin{aligned} \nabla^4 \mathcal{F}_1 &= -2(1+\nu) \frac{\partial^4 \mathcal{F}_0}{\partial x^2 \partial y^2}, \\ \nabla^4 \mathcal{F}_2 &= -\frac{\partial^4 \mathcal{F}_0}{\partial x^4}, \\ \nabla^4 \mathcal{F}_6 &= -\epsilon \left[2f_0 \nabla^4 \mathcal{F}_0 + 4 \frac{\partial f_0}{\partial y} \left(\frac{\partial^3 \mathcal{F}_0}{\partial y^3} + \frac{\partial^3 \mathcal{F}_0}{\partial x^2 \partial y} \right) + 4 \frac{\partial f_0}{\partial x} \left(\frac{\partial^3 \mathcal{F}_0}{\partial x^3} + \frac{\partial^3 \mathcal{F}_0}{\partial x \partial y^2} \right) + \right. \\ &\quad \left. + \frac{\partial^2 f_0}{\partial y^2} \left(2 \frac{\partial^2 \mathcal{F}_0}{\partial y^2} - \frac{\partial^2 \mathcal{F}_0}{\partial x^2} \right) + \frac{\partial^2 f_0}{\partial x^2} \left(-\frac{\partial^2 \mathcal{F}_0}{\partial y^2} + 2 \frac{\partial^2 \mathcal{F}_0}{\partial x^2} \right) + 6 \frac{\partial^2 f_0}{\partial x \partial y} \frac{\partial^2 \mathcal{F}_0}{\partial x \partial y} \right]. \end{aligned} \quad (11)$$

etc.

Having the expansion (7), it will be possible also to find expressions for the components of stresses and, consequently, for the deformations and displacements, in the form of exponential series in terms of α_i .

The solution of equation (8) under the boundary conditions (10) is a function of the stresses \mathcal{F}_0 [6], and takes the form :

$$\mathcal{F}_0 = \frac{P}{4} \left[r^2 - 2a^2 \ln \frac{r}{a} - \frac{(r^2 - a^2)^2}{r^2} \cos 2\theta \right]. \quad (12)$$

Taking into consideration that

$$\begin{aligned} x &= r \cos \theta, \quad \frac{\partial}{\partial x} = \cos \theta \frac{\partial}{\partial r} - \frac{1}{r} \sin \theta \frac{\partial}{\partial \theta}, \\ y &= r \sin \theta, \quad \frac{\partial}{\partial y} = \sin \theta \frac{\partial}{\partial r} + \frac{1}{r} \cos \theta \frac{\partial}{\partial \theta} \end{aligned}$$

and using equation (12), the right hand sides of the equations of $\mathcal{F}_1, \mathcal{F}_2$ and \mathcal{F}_6 of system (11) are calculated. Therefore, the following nonuniform differential equations are obtained :

$$\nabla^4 \mathcal{F}_1 = -2 \frac{(1+\nu) 3P}{a^2} \left[-\rho^4 \cos 4\theta + (-4\rho^4 + 10\rho^6) \cos 6\theta \right],$$

$$\nabla^4 \mathcal{F}_2 = \frac{3P}{a^2} \left[3\rho^4 \cos 4\theta + (-4\rho^4 + 10\rho^6) \cos 6\theta \right],$$

$$\begin{aligned} \nabla^4 \mathcal{F}_6 = & -\frac{3P^3 E}{a^2} \left[2\rho^6 + 87\rho^8 - 312\rho^{10} + 540\rho^{12} + (-90\rho^6 + 424\rho^8 - \right. \\ & - 876\rho^{10} + 756\rho^{12} - 810\rho^{14}) \cos 2\theta + (21\rho^4 - 72\rho^6 + 180\rho^8 + 81\rho^{12}) \cos 4\theta + \\ & \left. + (36\rho^4 - 122\rho^6) \cos 6\theta \right], \end{aligned} \quad (13)$$

where $\rho = \frac{a}{r}$

Solving these equations under zero boundary conditions, the stress functions \mathcal{F}_1 and \mathcal{F}_2 are derived:

$$\mathcal{F}_1 = -6(1+\nu)Pa^2 \left[-\omega_4^4 \cos 4\theta + (-4\omega_4^6 + 10\omega_6^6) \cos 6\theta \right],$$

$$\mathcal{F}_2 = 3Pa^2 \left[3\omega_4^4 \cos 4\theta + (-4\omega_4^6 + 10\omega_6^6) \cos 6\theta \right], \quad (14)$$

where

$$\omega_4^4 = \frac{1}{192} (1 + \rho^4 - 2\rho^2), \quad \omega_4^6 = \frac{1}{1152} (1 + 2\rho^6 - 3\rho^4), \quad \omega_6^6 = \frac{1}{640} (\rho^2 + \rho^6 - 2\rho^4)$$

Similarly, the function \mathcal{F}_6 is derived.

Moreover, knowing the value of the functions \mathcal{F}_0 , \mathcal{F}_1 , \mathcal{F}_2 and \mathcal{F}_6 , the right hand sides of the equations of \mathcal{F}_7 , \mathcal{F}_8 , \mathcal{F}_{13} , \mathcal{F}_{17} , \mathcal{F}_{21} , \mathcal{F}_{24} , \mathcal{F}_{26} and \mathcal{F}_{27} are calculated, and a new value is found for the functions of stresses and the stresses themselves by solving the equations. The final equations are not introduced here due to their bulkiness.

Now all the relationships are transformed to the dimensionless form:

$$\bar{\sigma}_\theta = \frac{\sigma_\theta}{\sigma_s}, \quad \alpha_6 = \kappa \sigma_s^3, \quad \bar{\rho} = \frac{\rho}{\rho_s}, \quad \bar{E} = \frac{E}{E_s},$$

where $\sigma_s = \sqrt{f_s}$, $P_s = \frac{\sigma_s}{2\sqrt{2}}$ and f_s = the value of the function f at which considerable nonlinear deformations appear; P_s is obtained from $f_s(\sigma_\theta^0, \sigma_z^0, \tau_{z\theta}^0)$ (5) at $\theta = \frac{\pi}{2}$, $P = \frac{a}{r} = 1$.

The expression of the stress $\bar{\sigma}_\theta$ at $P = 1$ can be rewritten in the following form :

$$\bar{\sigma}_\theta = \frac{\bar{P}}{2\sqrt{2}} \left\{ \varphi_0(\theta) + \varphi_1(\alpha_1, \alpha_2, \theta) + \varphi_2(\alpha_1^2, \alpha_2^2, \alpha_1, \alpha_2, \theta) - \right. \\ \left. - \frac{\bar{P}^2 E \alpha_6}{8} [\varphi_3(\theta) + \varphi_4(\alpha_1, \alpha_2, \alpha_3, \alpha_4, \alpha_5, \theta)] \right\}, \quad (15)$$

where φ_0 , φ_1 , φ_2 , φ_3 and φ_4 are functions which can be easily expressed through f_i . Using this equation, the variation of the stress $\bar{\sigma}_\theta$ along the contour of the hole at $r = a (P=1)$ was calculated. Moreover, the material constants introduced in the expression of $\bar{\sigma}_\theta$, were experimentally determined for a plastic reinforced by fibre glass, made on the basis of polyester resin PN-1 with fibre glass T-1 as a filler. The coefficient $k = bn/2n-1$ (1) the Young modulus E , the Poisson's coefficient ν , and the parameter f_s were taken as follows :

$$K = 0.035 \cdot 10^{-11} (\text{cm}^2/\text{kg})^2, \quad E = 1.5 \cdot 10^5 \text{ kg/cm}^2, \quad n = 2,$$

$$\nu = 0.12, \quad f_s = 0.36 \cdot 10^6 (\text{kg/cm}^2)^2.$$

The results of the calculation are given in Fig. 2-4, where the dotted lines denote the curves representing the isotropy of material, whereas the solid lines denote its anisotropy.

Fig. 2 shows the distribution of σ_θ along the edge of the hole at $P=1$ and $\alpha_6 = 0$ (elastic solution). The sign (x) denotes the values of the stresses obtained by taking into consideration in (15) the terms up to $\alpha_i^2 (i=1,2)$, including the case when $\alpha_1 = \alpha_2 = 0, 2$. Curve 1 represents the zero approximation ($\alpha_1 = \alpha_2 = 0$).

The calculation has shown that the difference between the first approximation (considering the terms up to α_i , including the last one) and the zero one does not exceed 10%, whereas the difference between the second and first approximation (considering the terms up to α_i^2 , including the last one) does not exceed 2.5%.

For comparison, the distribution of $\bar{\sigma}_\theta$ (curve 2) as calculated by the following equation :

$$\bar{\sigma}_\theta = \frac{P}{2\sqrt{2} E_1 N} \left[-\sqrt{\frac{E_1}{E_2}} \cos^2 \theta + (1 + n) \sin^2 \theta \right]$$

is shown in Fig. 2.
where

$$n = \sqrt{2\left(\frac{E_1}{E_2} - \nu_1\right) + \frac{E_1}{G}}; N = \frac{\sin^4 \theta}{E_1} + \left(\frac{1}{G} - \frac{2\nu_1}{E_1}\right) \sin^2 \theta \cos^2 \theta + \frac{\cos^4 \theta}{E_2}$$

is determined by the exact solution of the linearly elastic anisotropic problem [2]. Curve 2 is calculated for $\alpha_1 = \alpha_2 = 0.2$ at

$$\frac{1}{E_2} = \frac{1}{E} (1 + \alpha_2); \frac{1}{G_{12}} = \frac{2(1 + \nu)}{E} (1 + \alpha_1)$$

The deviation of this curve from the exact solution of the second approximation does not exceed 2.5%.

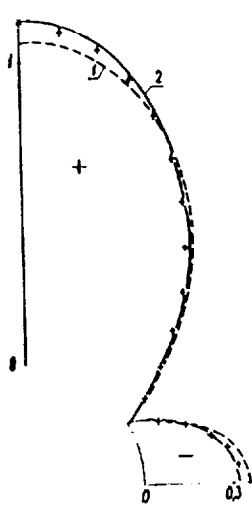


Fig. 2

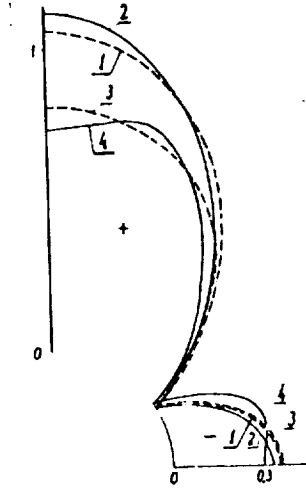


Fig. 3

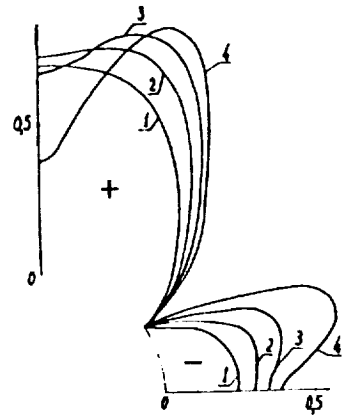


Fig. 4

In Fig. 3, the distribution of $\bar{\sigma}_\theta$ at $\alpha_1 = \alpha_2 = \alpha_3 = \alpha_4 = \alpha_5 = 0.2$, $\alpha_6 = 0.756 \cdot 10^{-4}$ and $\bar{P} = 1$ is given. This distribution varies with the number of terms taken into consideration in equation (15). Curve 1 corresponds to the case when the first term of the equation was considered, curve 2 - when the first, second and third terms were considered, curve 3 - when the first and fourth terms were considered, whereas curve 4 corresponds to the

complete utilization of equation(15). As clear from the graph, the nonlinearity of the material has a more significant influence on the variation of stress than anisotropy. It should be noted that if the anisotropy of the mechanical properties of the material was not taken into consideration $\alpha_i = 0 (i=1,2,3,4,5)$, then the given solution would have coincided with the solution obtained by Kauderer [6]. The variation of $\bar{\sigma}_\theta$ with the increase of load (the curves 1, 2, 3 and 4 correspond to loads $\bar{P} = 0.8; 1; 1.2; 1.5$ for an anisotropic material) for the same values of the parameters α_i , is shown in Fig. 4.

As seen from the graphs, the maximum stress σ_θ decreases as a result of nonlinearity and anisotropy of the material; with the increase of the load, the maximum stress $\bar{\sigma}_\theta$ will be displaced.

References

1. Savin G.N. "Raspredelenie napryazhenii okolo otverstii" (Stress distribution near holes). --- Kiev, "Nauk., Dumka", 1968.
2. Lekhnitskii S.G., "Anizotropnye plastinki" (Anisotropic plates). --- Moskva, OGIZ, 1947.
3. Nagibin L.N. "O napryazhennom sostoyanii anizotropnoi plastinki s dvumya krugovymi otverstiyami" (About the stress state of an anisotropic plate with two circular holes). --- Sb.: "Nekotorye zadachi teorii uprugosti o kontsentratsii napryazhenii i deformatsii uprugikh tel" Saratov, Sarstovskii Univerzitet, vol. 3 : 32 - 44, 1967.
4. Hayaschi T. On the tension of an orthogonally anisotropic strip with two circular holes. "Proc. Jap. Nat. Congr. Appl. Mech.", vol. 8 : 115-118, 1958.
5. Sokolovskii V.V. "Teoriya plastichnosti" (Theory of plasticity). --- Moskva-Leningrad, Izd. 2-e AN SSSR, 1950.
6. Kauderer G. "Nelineinaya mekhanika" (Nonlinear mechanics). --- Moskva, Izdatelstvo In. lit., 1961.
7. Tsurpal I.A. "Fizicheski nelineinnye uprygie plastiny, oslablennye proizvod'nym otverstiem" (Physically nonlinear elastic plates, weakened by an arbitrary hole). --- Sb.: "Kontsentratsiya napryazhenii" Kiev, "Nauk Domka", vol. 1 : 305-311, 1965.
8. Yumasheva M.A. "Izhib konsoli iz nelineino deformirovannogo ortotropnogo materiala" (Bending of a cantilever from a nonlinearly deformed orthotropic material). --- "Mekhanika polimerov", No. 5 : 773-778, 1966.

CROSS BENDING OF CIRCULAR PERFORATED PLATES

By
V.I. Astaf'ev

Let us consider the case of bending due to a side pressure of $q(x,y)$, moments of $m(s)$ and $h(s)$ and shearing forces of $P(s)$, applied on the contour of a thin homogeneous isotropic plate of thickness (see Fig. 1). The plate is multilinked and is limited by a composite contour of $L = L_0 + L_1 + \dots + L_n$. It is assumed that the plate is linearly elastic and obeys the conventional hypotheses of the theory of bending of plates. The stress and strain states of the plate can be then determined by the bending of the middle surface $w(x,y)$ (see, for example, references [1] and [2] . Thus , we have :

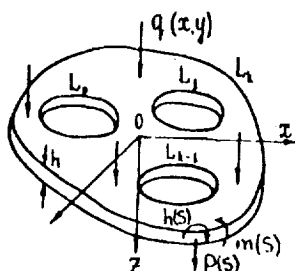


Fig. 1

$$\left. \begin{aligned} M_x &= -D \left(\frac{\partial^2 w}{\partial x^2} + \nu \frac{\partial^2 w}{\partial y^2} \right) , \\ M_y &= -D \left(\nu \frac{\partial^2 w}{\partial x^2} + \frac{\partial^2 w}{\partial y^2} \right) , \\ H_{xy} &= -D (1 - \nu) \frac{\partial^2 w}{\partial x \partial y} , \\ N_x &= -D \frac{\partial}{\partial x} \Delta w , \\ N_y &= -D \frac{\partial}{\partial y} \Delta w . \end{aligned} \right\} \quad (1)$$

where M_x , M_y and H_{xy} are the specific bending and torsional moments; N_x and N_y are the specific shearing forces; $D = Eh^3/12(1-\nu^2)$ is the cylindrical stiffness of the plate; E and ν are the modulus of elasticity and Poisson coefficient; $\Delta = \partial^2/\partial x^2 + \partial^2/\partial y^2$ is the Laplace operator.

The equation of bending $w(x, y)$ has the following form :

$$\Delta \Delta w = q/D \quad (2)$$

In polar coordinates (r, φ) , expressions (1) and the Laplace operator Δ are written as follows :

$$\left. \begin{aligned} M_r &= -D \left(\frac{\partial^2 w}{\partial r^2} + \frac{1}{r} \frac{\partial w}{\partial r} + \frac{1}{r^2} \frac{\partial^2 w}{\partial \varphi^2} \right), \\ M_\varphi &= -D \left(\frac{1}{r} \frac{\partial^2 w}{\partial r^2} + \frac{1}{r} \frac{\partial w}{\partial r} + \frac{1}{r^2} \frac{\partial^2 w}{\partial \varphi^2} \right), \\ H_{r\varphi} &= -D (1 - \nu) \left(\frac{1}{r} \frac{\partial^2 w}{\partial r \partial \varphi} - \frac{1}{r^2} \frac{\partial w}{\partial \varphi} \right), \\ N_r &= -D \frac{\partial}{\partial r} \Delta w, \\ N_\varphi &= -D \frac{1}{r} \frac{\partial}{\partial \varphi} \Delta w, \\ \Delta &= \frac{\partial^2}{\partial r^2} + \frac{1}{r} \frac{\partial}{\partial r} + \frac{1}{r^2} \frac{\partial^2}{\partial \varphi^2} \end{aligned} \right\} \quad (3)$$

The general solution of equation (2) can be written as the summation $w = w_0 + w_1$, where w_0 is a certain particular solution of equation (2), whereas w_1 is a biharmonic function; the general solution of the biharmonic equation is given by $\Delta \Delta w = 0$. According to the method of N.I. Muskhelishvili[3] the biharmonic function $w(x, y)$ can be represented in terms of the two functions $\varphi_1(z)$ and $\chi_1(z)$ of the complex variable :

$$w_1 = \frac{2q}{D} \operatorname{Re} \{ \bar{z} \varphi_1(z) + \chi_1(z) \} \quad (4)$$

These functions are analytical in the zone occupied by the plate. Let us take for w_0 the function of bending of a unlinked plate subjected to a side load of q . In polar coordinates, w_0 can be written in the form [1] :

$$w_0 = \frac{q r^4}{64 D} + \frac{2q}{D} \left(C_0 r^2 + D_0 + \sum_{n=1}^{\infty} (C_n r^2 + D_n) r^n \cos n\varphi \right) \quad (5)$$

or

$$w_0 = \frac{q z^2 \bar{z}^2}{64 D} + \frac{2q}{D} \operatorname{Re} \left\{ \bar{z} \varphi_0(z) + \chi_0(z) \right\}, \quad (6)$$

where

$$\varphi_0(z) = z \sum_{n=0}^{\infty} c_n z^n, \quad \chi_0(z) = \sum_{n=0}^{\infty} d_n z^n, \quad z = x + iy, \quad \bar{z} = x - iy.$$

Therefore, the general solution of equation (2) acquires the following form :

$$w = \frac{q z^2 \bar{z}^2}{64 D} + \frac{2q}{D} \operatorname{Re} \left\{ \bar{z} \varphi(z) + \chi(z) \right\}, \quad (7)$$

where

$$(z)' \chi + (z)'' \chi = (z) \chi', \quad (z)' \phi + (z)'' \phi = (z) \phi'$$

The moments and shearing forces can be expressed in terms of $\varphi(z)$ and $\chi(z)$ as follows :

$$\left. \begin{aligned} M_x + M_y = M_r + M_\varphi &= -4q(1+\nu)(\varphi'(z) + \overline{\varphi'(z)}) - \\ &- \frac{q(1+\nu)}{4} z \bar{z}, \\ M_y - M_x + 2i H_{xy} &= (M_\varphi - M_r + 2i H_{z\varphi}) e^{-2i\varphi} = \\ &= 4q(1-\nu)(\bar{z} \varphi''(z) + \chi''(z)) + \frac{q(1-\nu)}{8} \bar{z}^2, \\ N_r + i N_y &= (N_r - i N_\varphi) e^{-i\varphi} = -8q \varphi''(z) \cdot \frac{q}{2} \bar{z}. \end{aligned} \right\} \quad (8)$$

In [2] it is shown that in the general case of a definite multilinked zone, occupied by the plate, the functions $\varphi_i(z)$ and $\chi_i(z)$ can be represented in the following form :

$$\left. \begin{aligned} \varphi_i(z) &= \sum_{p=0}^{K-1} (A_p z + a_p) \ell_n(z - z_p) + \varphi_n(z) \\ \chi_i(z) &= \sum_{p=0}^{K-1} (\bar{a}_p z + \alpha_p) \ell_n(z - z_p) + \chi_n(z) \end{aligned} \right\} \quad (9)$$

where A_p and α_p are substantial constants, α_p is a complex constant, $\varphi_*(z)$ and $\chi_*(z)$ are regular functions in the zone occupied by the plate, and z_p is the internal point of the L_p ($p = 0, 1, \dots, k-1$) contour.

If L_p ($p = 0, 1, \dots, k-1$) represents circles, then according to [4], the functions $\varphi_*(z)$ and $\chi_*(z)$, which are regular outside these circular holes, can be written in the form of Appel's representation :

$$\left. \begin{aligned} \varphi_*(z) &= \sum_{p=0}^{k-1} \sum_{n=1}^{\infty} \frac{E_{np}}{(z - z_p)^n} \\ \chi_*(z) &= \sum_{p=0}^{k-1} \sum_{n=1}^{\infty} \frac{F_{np}}{(z - z_p)^n} \end{aligned} \right\} \quad (10)$$

where z_p is the centre of the L_p ($p = 0, 1, \dots, k-1$) circle.

The boundary conditions on the external corner L_k will be :

$$w = 0, \quad \frac{\partial w}{\partial n} = 0 \quad \text{on} \quad L_k \quad (11)$$

in the case of a firmly supported external contour, or :

$$w = 0, \quad M_n = 0 \quad \text{on} \quad L_k \quad (12)$$

in the case of a freely supported external contour, where n is the external line normal to the L_k contour.

If on the composite $L' = L_0 + L_1 + \dots + L_{k-1}$ contour the force flux $p(S)$ as well as the moments $m(S)$ are given (the first basic problem of the theory of bending of plates), then the following boundary problem will be obtained for the analytical functions $\varphi(z)$ and $\chi(z)$:

$$-x\varphi(z) + z\overline{\varphi'(z)} + \overline{\chi'(z)} = f_1 + if_2 + iC_0 z + C_1, \quad \text{on} \quad L' \quad (13)$$

where $x = \frac{3+\nu}{1+\nu}$; C_0 is the substantial constant; C_1 is the complex constant and θ is the angle between the line normal to the L' contour

$$\begin{aligned} f_1 + if_2 &= \frac{1}{2q(1-\nu)} \left[\int_0^s (m + if)(dx + idy) - \int_0^s (m_0 + if_0)(dx + idy) \right]; \\ f(s) &= \int_0^s p(s) ds ; \quad f_0(s) = \int_0^s p_0(s) ds ; \\ m_0(s) &= -\frac{q}{64} \left[8(1+\nu)z\bar{z} + 2(1-\nu)(z^2 e^{2i\theta} + \bar{z}^2 e^{2i\theta}) \right] \end{aligned} \quad (14)$$

$$f_0(s) = -\frac{q}{64} [2i(1-\nu)(z^2 e^{2i\theta} - \bar{z}^2 e^{-2i\theta}) - 16i \int_0^s (\bar{z} dz - z d\bar{z})], \quad z \in L' \quad (14)$$

and the axis x . The boundary condition (13) can be represented in the following more convenient form [4]:

$$-x \overline{\varphi'(z)} + \varphi'(z) + (\bar{z} \varphi''(z) + \chi''(z)) e^{2i\theta} = f_1^* + i f_2^* + i c_0 \quad \text{on } L' \quad (15)$$

where

$$f_1^* + i f_2^* = \frac{1}{2q(1-\nu)} [(m - if) - (m_0 - i f_0)]$$

In the case of the second basic problem (on the L' contour the deflections and tilt angles, i.e. the dw/dn ratio, are given), the boundary conditions can be written in accordance to (13) or (15) at

$$x = -1; \quad f_1 + i f_2 = \frac{D}{2q} \left(\frac{\partial w}{\partial n} + i \frac{\partial w}{\partial s} \right) e^{i\theta} - \frac{1}{3q} z^2 \bar{z}, \quad z \in L';$$

$$f_1^* + i f_2^* = \frac{D}{2q} e^{i\theta} \frac{d}{ds} \left(\frac{\partial w}{\partial y} + i \frac{\partial w}{\partial x} \right) - \frac{1}{3q} (2z\bar{z} - \bar{z}^2 e^{2i\theta}), \quad z \in L'$$

Let us consider in details the bending of a circular plate of a radius a , perforated with k uniformly distributed circular holes of radius λ , whose centres lie on a circle of a radius b at the points (see Fig. 2)

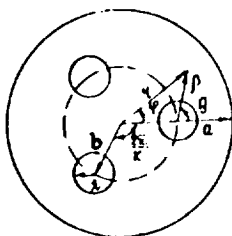
$$z_p = b \exp(2\rho i \pi / k), \quad (\rho = 0, 1, \dots, k-1),$$


Fig. 2

i.e. L_k is a circle of a radius a , whose centre lies in the origin of the coordinates ($L' = L_0 + L_1 + \dots + L_{k-1}$), and L_p is a circle of a radius λ , whose centre lies in z_p ($p = 0, 1, \dots, k-1$). Let us introduce the following two systems of coordinates: (z, φ) , which is related to the plate centre, and (ρ, θ) , which is related to the hole centre L_0 . $z = b + \zeta = b + \rho e^{i\theta}$. It will be considered that the contours of the holes are free from external loads on L' , i.e. $m(s) = p(s) = 0$. If q has the property of cyclic symmetry, i.e. it is equal and invariant in the case of rotation of the system of coordinates (z, φ) by an angle multiple of $2\pi/k$, then the deflection w , the bending moments M_z , M_φ and $H_{z\varphi}$, and the shearing forces N_z and N_φ , will have the property of cyclic symmetry. From the condition of cyclic symmetry it follows that $\varphi_0(z)$ and $\chi_0(z)$ will have the following form:

$$\varphi_0(z) = z \sum_{n=0}^{\infty} C_n z^{nk}; \quad \chi_0(z) = \sum_{n=0}^{\infty} D_n z^{nk}; \quad (16)$$

whereas the coefficients A_p , α_p , a_p , E_d and F_d ($p = 0, 1, \dots, k-1$) in the expressions of $\varphi_1(z)$ and $\chi_1(z)$ will have the form:

$$\left. \begin{aligned} A_0 &= A_1 = \dots = A_{k-1} = A; \quad \alpha_0 = \alpha_1 = \dots = \alpha_{k-1} = \alpha; \\ a_p &= b e_p; \quad E_d = E_n e_p^{n+1}; \quad F_d = F_n e_p^n \end{aligned} \right\} \quad (17)$$

where

$$e_p = \exp(2\pi i p/k); \quad p = 0, 1, \dots, k-1$$

From (16) and (17), the expressions of $\varphi(z)$ and $\chi(z)$ can be rewritten as:

$$\left. \begin{aligned} \varphi(z) &= z \sum_{n=0}^{\infty} C_n z^{nk} + \sum_{p=0}^{k-1} \left[(A z + B e_p) \ln(z - z_p) + \right. \\ &\quad \left. + \sum_{n=1}^{\infty} \frac{E_n e_p^{n+1}}{(z - z_p)^n} \right] \\ \chi(z) &= \sum_{n=0}^{\infty} D_n z^{nk} + \sum_{p=0}^{k-1} \left[(B \bar{e}_p z + \alpha) \ln(z - z_p) + \right. \\ &\quad \left. + \sum_{n=1}^{\infty} \frac{F_n e_p^n}{(z - z_p)^n} \right] \end{aligned} \right\} \quad (18)$$

Then, the deflection w can be written in the following form :

$$w = \frac{q z^2 \bar{z}^2}{64 D} + \frac{2q}{D} \operatorname{Re} \left\{ \sum_{n=0}^{\infty} (C_n z \bar{z} + D_n) z^{nk} + \right. \\ \left. + \sum_{p=0}^{k-1} \left[(A z \bar{z} + B e_p \bar{z} + B \bar{e}_p z + \alpha) \ell_n(z - z_p) + \right. \right. \\ \left. \left. + \sum_{n=1}^{\infty} \left(E_n e_p \bar{z} + F_n \right) \frac{e_p^n}{(z - z_p)^n} \right] \right\} \quad (19)$$

For a freely supported plate, the boundary conditions (12) take the form :

$$w = 0, \quad \frac{\partial^2 w}{\partial z^2} + \frac{1}{z} \frac{\partial w}{\partial z} = 0 \quad \text{at } z = a \quad (20)$$

To fulfill the boundary conditions (20), w is expanded in series in terms of z , and the real part of these series is taken

$$w = \frac{q z^4}{64 D} + \frac{2q}{D} \left\{ C_0 z^2 + D_0 + k A z^2 \rho_n z + k \alpha \ell_n z - \right. \\ \left. - k B b + \sum_{n=1}^{\infty} (C_n z^2 + D_n) z^{nk} \cos nk \varphi + \right. \\ \left. + \sum_{n=1}^{\infty} (P_{1n} z^2 + P_{2n}) \left(\frac{b}{z} \right)^{nk} \cos nk \varphi \right\}; \quad (z > b), \quad (21)$$

where

$$P_{1n} = k \sum_{m=1}^{\infty} E_m b^{m-1} \binom{nk-2}{m-1} - \frac{1}{n} \left(A + \frac{B}{b} \frac{nk}{nk-1} \right);$$

$$P_{2n} = k \sum_{m=1}^{\infty} F_m b^{-m} \binom{nk-1}{m-1} - \frac{1}{n} \left(\alpha + B b \frac{nk}{nk+1} \right);$$

$\binom{m}{n} = C_m^n$ - binomial coefficients.

Craus [5], solving the problem by an another method (by constructing a biharmonic function having the property of cyclic symmetry with the aid of Hawland's representation [6]), he was able to derive a similar expression for w . However, an erroneous solution was derived when the obtained expression was expanded in terms of z . In the expression of P_{1n} and P_{2n}

the corresponding terms $\frac{1}{n}(A + \frac{B}{b} \frac{nk}{nk-1})$ and $\frac{1}{n}(\alpha + Bb \frac{nk}{nk+1})$ are absent.

Substituting (21) in the boundary conditions (20), the coefficients C_0 , D_0 , C_n and D_n ($n \geq 1$) can be expressed in terms of A , B , α , E_n and F_n ($n \geq 1$):

$$\left. \begin{aligned} C_0 &= -\frac{1}{64} \frac{3+\nu}{1+\nu} a^2 - k A \ell n a - \frac{1}{2} \frac{3+\nu}{1+\nu} k A + \frac{1}{2} \frac{1-\nu}{1+\nu} k \alpha a^{-2}; \\ D_0 &= \frac{1}{128} \frac{5+\nu}{1+\nu} a^4 + \frac{1}{2} \frac{3+\nu}{1+\nu} k A a^2 + k B b - \\ &\quad - k \alpha \ell n a - \frac{1}{2} \frac{1-\nu}{1+\nu} k \alpha; \\ C_n &= (c_{1n} P_{1n} + c_{2n} P_{2n}) \left(\frac{b}{a}\right)^{nk} \cdot \frac{1}{a^{nk}}; \\ D_n &= (c_{3n} P_{1n} + c_{4n} P_{2n}) \left(\frac{b}{a}\right)^{nk} \cdot \frac{1}{a^{nk}} \end{aligned} \right\} \quad (22)$$

where

$$\begin{aligned} c_{1n} &= \frac{(1+\nu)(nk-1)}{2nk+\nu+1}; & c_{2n} &= -\frac{(1-\nu) \cdot nk}{2nk+\nu+1} a^{-2} \\ c_{3n} &= -\frac{(3+\nu)nk}{2nk+\nu+1} a^2; & c_{4n} &= -\frac{(1+\nu)(nk+1)}{2nk+\nu+1} \end{aligned}$$

According to the property of cyclic symmetry, the curved problem (15) for $\varphi(z)$ and $\chi(z)$ will have the same form on each of the L_p , $p = 0, 1, \dots, k-1$. contours. Therefore, this problem can be considered only on the L_0 contour. Writing the expressions (18) in the system of (ρ, θ) coordinates (where $z = b + \zeta$), and expanding them in series in powers of ζ , the following results are obtained for A , B , E_n , α and F_n :

$$A = -\lambda^2/16; \quad B = -Ab; \quad (23)$$

$$\alpha = v_0 + \sum_{n=1}^{\infty} (M_{on} E_n + N_{on} F_n); \quad (24)$$

$$\left. \begin{aligned} E_m &= q_m + \sum_{n=1}^{\infty} (I_{mn} E_n + J_{mn} F_n) \\ F_m &= v_m + \sum_{n=1}^{\infty} (M_{mn} E_n + N_{mn} F_n) \end{aligned} \right\} (m = 1, 2, \dots) ; \quad (25)$$

Where

$$\left. \begin{aligned} v_0 &= \left\{ A \left[b^2 + \lambda^2 \left(1 - k + 2 \frac{1+\nu}{1-\nu} \ell n k \frac{\lambda}{b} \left(\frac{b}{a} \right)^k \right) \right] + \right. \\ &\quad \left. + \frac{1}{32} \frac{3+\nu}{1-\nu} \lambda^2 (\lambda^2 - a^2) + \frac{1}{16} \frac{1+\nu}{1-\nu} \lambda^2 b^2 - \right. \\ &\quad \left. - 2 \frac{1+\nu}{1-\nu} \lambda^2 \sum_{s=1}^{\infty} \frac{1+sk}{s} \left(\frac{b}{a} \right)^{2sk} \left[C_{1s} \left(A + \frac{B}{b} \frac{sk}{sk-1} \right) + C_{2s} B b \frac{sk}{sk+1} \right] \right\} / u_1; \\ M_{on} &= 2 \frac{1+\nu}{1-\nu} \lambda^2 \left\{ -n^0 A_{n+1} + k b^{-n-1} \sum_{s=1}^{\infty} C_{1s} (1+sk) \left(\frac{b}{a} \right)^{2sk} \binom{sk-2}{n-1} \right\} / u_1; \\ N_{on} &= 2 \frac{1+\nu}{1-\nu} \lambda^2 \left\{ k b^{-n} \sum_{s=1}^{\infty} C_{2s} (1+sk) \left(\frac{b}{a} \right)^{2sk} \binom{sk-1}{n-1} \right\} / u_1; \\ u_1 &= 1 - k \left(\frac{\lambda}{a} \right)^2 + 2 \frac{1+\nu}{1-\nu} \lambda^2 \sum_{s=1}^{\infty} \frac{C_{2s}}{s} (1+sk) \left(\frac{b}{a} \right)^{2sk}; \end{aligned} \right\} \quad (26)$$

$$\left. \begin{aligned} q_m &= \frac{\lambda^{2m}}{2} \left\{ \frac{1}{32} b^2 \delta_{1,m} - A \left[{}^{m+1}A_0 \lambda^2 + {}^m A_0 b + (m+1) ({}^m B_0 b + \right. \right. \\ &\quad \left. \left. + {}^{m+1} B_0 b^2) \right] - q_{1,m} v_0 - \sum_{s=1}^{\infty} \frac{1}{s} \left[R_{1sm} \left(A + \frac{B}{b} \frac{sk}{sk-1} \right) + R_{2sm} B b \frac{sk}{sk+1} \right] \right\}; \\ I_{mn} &= \frac{\lambda^{2m}}{2} \left\{ -n \left[{}^{m+1}A_{n+1} \lambda^2 + {}^m A_{n+1} b \right] - q_{1,m} M_{on} + k b^{-n-1} \sum_{s=1}^{\infty} R_{1sm} \binom{sk-2}{n-1} \right\}; \\ J_{mn} &= \frac{\lambda^{2m}}{2} \left\{ (m+1) {}^{m+1}A_n - q_{1,m} N_{on} + k b^{-n} \sum_{s=1}^{\infty} R_{2sm} \binom{sk-1}{n-1} \right\}; \end{aligned} \right\} \quad (27)$$

$$Q_{1m} = \sum_{s=1}^{\infty} \frac{1}{s} R_{2sm} + (m+1)^{m+1} A_0 ;$$

$$R_{1sm} = b^{-m-1} \left(\frac{b}{a} \right)^{2sk} \left[C_{1s} (1+sk) \left(\binom{sk}{m+1} \lambda^2 + \binom{sk}{m} b^2 \right) + \right. \\ \left. + C_{3s} sk \binom{sk-1}{m} \right] ;$$

$$R_{2sm} = b^{-m-1} \left(\frac{b}{a} \right)^{2sk} \left[C_{2s} (1+sk) \left(\binom{sk}{m+1} \lambda^2 + \binom{sk}{m} b^2 \right) + \right. \\ \left. + C_{4s} sk \binom{sk-1}{m} \right] ;$$

$$\mathcal{Y}_m = -b \mathcal{Q}_m - \frac{m-1}{m} \lambda^2 \mathcal{Q}_{m-1} + \frac{\mathfrak{A} \lambda^{2m+2}}{m(m+1)} \left\{ -\frac{1}{16} b \delta_{1m} + A^m A_0 + \right. \\ \left. + Q_{2m} \mathcal{Y}_0 + \sum_{s=1}^{\infty} \frac{1}{s} \left[R_{3sm} \left(A + \frac{B}{b} \frac{sk}{sk-1} \right) + R_{4sm} B b \frac{sk}{sk+1} \right] \right\} ;$$

$$M_{mn} = -b J_{mn} - \frac{m-1}{m} \lambda^2 J_{m-1,n} + \frac{\mathfrak{A} \lambda^{2m+2}}{m(m+1)} \left\{ n^m A_{n+1} + \right. \\ \left. + Q_{2m} M_{0n} - k b^{-n-1} \sum_{s=1}^{\infty} R_{3sm} \binom{sk-2}{n-1} \right\} ;$$

$$N_{mn} = -b J_{mn} - \frac{m-1}{m} \lambda^2 J_{m-1,n} + \frac{\mathfrak{A} \lambda^{2m+2}}{m(m+1)} \left\{ Q_{2m} N_{0n} - \right. \\ \left. - k b^{-n} \sum_{s=1}^{\infty} R_{4sm} \binom{sk-1}{n-1} \right\} ;$$

$$Q_{2m} = \sum_{s=1}^{\infty} \frac{1}{s} R_{4sm} ;$$

$$R_{3sm} = b^{-m} \left(\frac{b}{a} \right)^{2sk} C_{1s} (1+sk) \binom{sk}{m} ;$$

(28)

$$R_{4sm} = b^{-m} \left(\frac{b}{a} \right)^{2sk} C_{2s} (1 + sk) \binom{sk}{m};$$

$${}^m A_n = (-1)^m \binom{m+n-1}{m} \sum_{p=1}^{k-1} \frac{\bar{e}_p^n}{(b-z_p)^{m+n}};$$

$${}^m A_0 = \frac{(-1)^m}{m} \sum_{p=1}^{k-1} \frac{1}{(b-z_p)^m};$$

$${}^m B_0 = \frac{(-1)^m}{m} \sum_{p=1}^{k-1} \frac{\bar{e}_p}{(b-z_p)^m};$$

$$\delta_{1,m} = \begin{cases} 1, & m=1 \\ 0, & m>1 \end{cases}.$$

For the determination of E_n and F_n , an infinite system of equations with an infinite number of unknowns (25) was derived. It is possible to show that this system will be quasi-regular for any zone between the holes. In fact, we can consider, without violating the generality, that the radius of the holes is $\lambda = 1$. Then, $|b - z_p| > 2$ for $p = 1, 2, \dots, k-1$, $b > 1$ and $b+1 < a$. To ensure the quasi-regularity of the system it is necessary that the sum of the n moduli of the coefficients with the unknowns E_n and F_n should be limited for each value of m (beginning with a certain number for m) and should be less than unity [7].

But

$$\begin{aligned} \sum_{n=1}^{\infty} |I_{mn}| &\leq \frac{1}{x} \left\{ \sum_{n=1}^{\infty} |n^{m+1} A_{n+1}| + b \sum_{n=1}^{\infty} |n^m A_{n+1}| + |Q_{1m}| \sum_{n=1}^{\infty} |M_{on}| + \right. \\ &\quad \left. + k \sum_{s=1}^{\infty} |R_{1sm}| \sum_{n=1}^{\infty} b^{-n-1} \binom{sk-2}{n-1} \right\}; \\ \sum_{n=1}^{\infty} |J_{mn}| &\leq \frac{1}{x} \left\{ (m+1) \sum_{n=1}^{\infty} |n^{m+1} A_n| + |Q_{1m}| \sum_{n=1}^{\infty} |N_{on}| + \right. \\ &\quad \left. + k \sum_{s=1}^{\infty} |R_{2sm}| \sum_{n=1}^{\infty} b^{-n} \binom{sk-1}{n-1} \right\}; \\ \sum_{n=1}^{\infty} |M_{mn}| &\leq b \sum_{n=1}^{\infty} |I_{mn}| + \frac{m+1}{m} \sum_{n=1}^{\infty} |I_{m-1,n}| + \frac{x}{m(m+1)} \left\{ \sum_{n=1}^{\infty} |n^m A_{n+1}| + \right. \\ &\quad \left. + |Q_{2m}| \sum_{n=1}^{\infty} |M_{on}| + k \sum_{s=1}^{\infty} |R_{3sm}| \sum_{n=1}^{\infty} b^{-n-1} \binom{sk-2}{n-1} \right\}; \end{aligned} \quad (29)$$

$$\left. \begin{aligned} \sum_{n=1}^{\infty} |N_{mn}| \leq & b \sum_{n=1}^{\infty} |J_{mn}| + \frac{m-1}{m} \sum_{n=1}^{\infty} |J_{m-1,n}| + \frac{\alpha}{m(m+1)} \left\{ |Q_{2m}| \sum_{n=1}^{\infty} |N_{on}| + \right. \\ & \left. + k \sum_{s=1}^{\infty} |R_{4sm}| \sum_{n=1}^{\infty} b^{-n} \binom{sk-1}{n-1} \right\}. \end{aligned} \right\}$$

Since

$$\sum_{n=1}^{\infty} |^m A_n| \leq \sum_{p=1}^{k-1} \frac{1}{(|b-z_p|-1)^{m+1}} \xrightarrow{m \rightarrow \infty} 0;$$

$$|Q_{1m}| \leq \sum_{p=1}^{\infty} \frac{1}{|b-z_p|^{m+1}} + \sum_{s=1}^{\infty} \frac{1}{s} |R_{2sm}| \xrightarrow{m \rightarrow \infty} 0;$$

$$|Q_{2m}| \leq \sum_{s=1}^{\infty} \frac{1}{s} |R_{4sm}| \xrightarrow{m \rightarrow \infty} 0;$$

$$k \sum_{s=1}^{\infty} |R_{1sm}| \sum_{n=1}^{\infty} b^{-n-1} \binom{sk-2}{n-1} = k(b+1)^{-2} \sum_{s=1}^{\infty} |R_{1sm}| \left(\frac{b+1}{b}\right)^{sk} \xrightarrow{m \rightarrow \infty} 0$$

$$|b-z_p|-1 > 1; \quad p = 1, 2, \dots, k-1;$$

$$\frac{b(b+1)}{a^2} < 1; \quad \frac{b}{a} < 1;$$

and $\sum_{n=1}^{\infty} |M_{on}|$ and $\sum_{n=1}^{\infty} |N_{on}|$ are limited quantities, then it is clear that each of the four sums is limited for any value of m and tends to zero when m tends to infinity, which proves the quasi-regularity of system (25). Therefore, system (25) can be solved by the method of reductions [7] and it is possible to find out a solution for very close hole boundaries at any degree of accuracy. For three holes, system (25) becomes quite regular for λ/b less than the numbers (for $b/a = 0.3$, $\lambda/b < 0.16$; for $b/a = 0.4$, $\lambda/b < 0.21$; for $b/a = 0.5$, $\lambda/b < 0.23$), i.e. it can be solved by the method of successive approximations [7].

After the determination of the unknown coefficients E_n and F_n in equations (22)-(24) from system (25), C_0 , D_0 , C_n , D_n , A , B , α and, consequently, the unknown functions $\varphi(z)$ and $\chi(\bar{z})$, are derived.

The distribution of the moment M_θ on the contour of the hole L_0 is of great significance. Since $M_\rho = 0$ on L' according to the boundary conditions (15), then we can write the following expression for M_θ on the contour L_0 .

$$\frac{M_\theta}{M_0} = -\frac{8\zeta(1+i)}{M_0} \operatorname{Re} \varphi'(z) - \frac{q(1+\nu)}{4M_0} z \bar{z} \quad (30)$$

at $z = b + \zeta$,

where $\zeta = \lambda e^{i\theta}$ and M_0 is the maximum moment in the rigid plate. For a freely supported plate, $M_0 = \frac{q(3+\nu)}{16} a^2$.

Calculations were conducted for the following cases: 1) $b/a = 0.3$, $n = 1/2, 1, 2$ and 4 ; 2) $b/a = 0.5$, $n = 1/2, 1, 2$ and 4 , where n is the distance between the holes, expressed in units of the hole diameter (see Figs. 3 and 4). With the increase of the distance between the holes, M_θ/M_0 tends to a constant value $\frac{M_\theta^\infty}{M_0} = 2 - 4 \frac{1+\nu}{3+\nu} \left(\frac{b}{a}\right)^2$. With the adherence of the holes, the maximum value M_θ/M_0 moves from the point $\theta = \pi$ to the point $\theta = 2\pi/3$, i.e. the maximum twisting moment on the hole contour is located at the point of minimum distance between the holes.

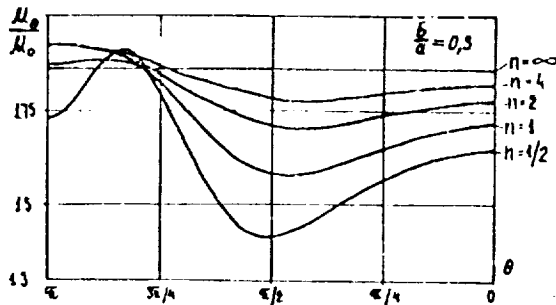


Fig. 3

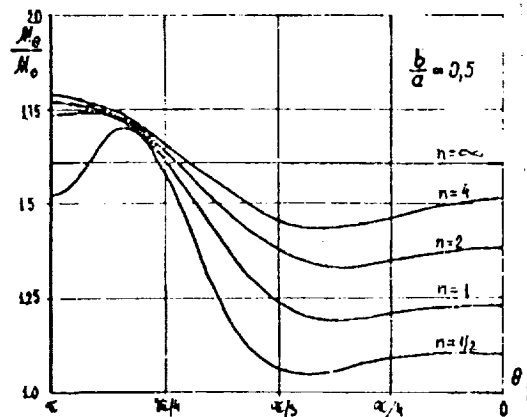


Fig. 4

Comparing the results of calculation with Kraus's results [5] it can be noted that for large distances between the holes (or small values of λ/b) the divergence will be very small, since for small values of λ/b the terms not considered by Kraus lead to an insignificant error, whereas in the case of adherence of holes (increase of λ/b) the effect of the unconsidered terms becomes significant and the divergence in the results will be significant. Therefore, for $n = 1/2$ and 1 , the values of M_θ/M_0 obtained by Kraus are 10-15% lower.

References

1. Timoshenko, S.P. and S. Voinovskii-Kriger, "Plastinki i obolochki" (Plates and shells). --- "Nauka", Moskva, 1966.
2. Savin, G.N. and N.P. Fleishman, "Plastinki i obolochki s rebrami zhestkosti" (Plates and shells with stiffening ribs). --- Naukova dumka, Kiev, 1964.
3. Muskhelishvili, N.I. "Nekotorye osnovnye zadachi matematicheskoi teorii uprugosti" (Some basic problems of the mathematical theory of elasticity). --- "Nauka", Moskva, 1966.
4. Grigolyuk, E.I and L.A. Fil'shtinskii, "Perforirovannye plastiny i obolochki" (Perforated plates and shells). --- "Nauka", Moskva, 1970.
5. Kraus, H., "Trans. ASME", Ser. E, 299(3) : 489 - 496, 1962.
6. Hawland, R.C.J., "Proc. Cambridge Philos. Soc., vol. 30 : 315 - 326, 1934.
7. Kantorovich, L.V. and V.I. Krylov, "Priblizhennyye metody vysshego analiza" (Approximate methods of high analysis). --- Fizmatgiz, Moskva, 1962.

INVESTIGATION OF THE STRESSES IN A PERFORATED DISC
SUBJECTED TO CROSS BENDING, USING AN OPTICAL METHOD

By

L.S. Zlenko, A.M. Lokoshchenko and V.P. Netrebko

Strictly speaking, the calculation of a perforated construction is based on the solution of extremely complicated boundary problems for multi-linked zones. In this case, the issue of concentration of stresses near the holes and, particularly, the mutual effect of these holes on each other, acquires a considerable significance. In the literature, there are some solutions of similar problems under very specific conditions. There are yet no solutions for plates with large numbers of circular holes of different radii and depths. The only reliable method for the investigation of such types of constructions is the optical method of determination of stresses.

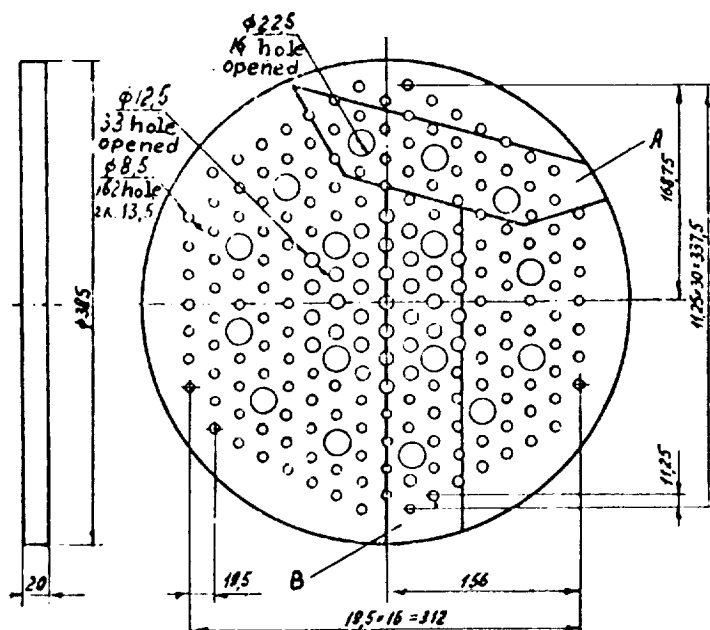


Fig. 1

A description is given below for the results of investigation of a natural disc with a concrete system of holes by this method (see Fig. 1, where the dimensions are given in mm). The disc has three types of holes of 13.5 mm depth (measured from the upper surface): through-holes, $\phi = 22.5$ mm (I) ; opened -holes, $\phi = 12.5$ mm (II), and blind-holes; $\phi = 8.5$ mm (III).

The behaviour of such a disc, which is subjected to a uniformly distributed side pressure and which is hinge-supported along its contour is considered in the elastic zone. For the determination of the stress state in the natural disc, a disc of similar dimensions was constructed. The model-disc had the same system of holes and was made of the optically sensitive polymeric material ED6-M.

The method of "freezing" of deformations was used. This method is based on the character of some optically sensitive polymeric materials. According to this property, the deformations arising in the models of these materials due to their loading under the conditions of elevated temperatures are fixed (frozen) by cooling (under load) to the room temperature. Besides the deformations, the pattern of interference strips, related to these deformations, is "frozen". After "freezing", the necessary number of plates is cut from the model and the stress state in the investigated point is measured. The plates (sections) are investigated in the same way as in the solution of plane problems.

The sequence of "freezing" of deformations for the utilized ED6-M material was as follows: heating, in the course of 3-3.5 hours, up to the "freezing" temperature (of the order of 130 - 135°C), preserving it at that temperature for about 3 hours, cooling down to the room temperature with a rate of 5-10°C/hr.

The deformations in the model of the disc with holes, which was subjected to a side load, were "frozen" in a thermostat of the type VTS-1. The rate of heating was controlled by the intensity of the current fed to the heaters. The heat in the operation chamber whose dimensions were 500x700x700 mm, was controlled by means of four thermometers, mounted at different locations in the chamber. The temperature control was provided by a contact thermometer.

For the observation and photographing of the patterns of interference strips and isoclinals in the sections, a polarization BPU set (of the type IMASh-OKB-2) and a coordinate synchronization polarimeter of the type KSP-5 were used.

The optical properties of the model material at the "freezing" temperature were determined by testing the calibration of a circular disc on its diametrical compression by two concentrated forces. The measurements were conducted by the use of a violet filter, which extracted from the mercury spectrum a wave length of $\lambda = 4358 \text{ \AA}$. The calibration showed that the optical constant of the material is $\sigma_0 = 0.408 \text{ kg/cm}$.

According to the data of the method of optical polarization, the differences in the quasi-principal stresses (i.e. the difference between the maximum and minimum stresses acting in the plane of cut) in the plates cut from the spatial model after "freezing" of deformations, as well as their angles of inclination, can be determined. For the entire determination

of the components of stresses in an arbitrary point of the spatial model, it is necessary to conduct some optical measurements in the plates, cut in three mutually perpendicular directions. It is also necessary to integrate the equations of equilibrium of the spatial theory of elasticity [1]. In the general case it is necessary to have three equally loaded similar models.

Let us consider the investigated model of the disc, perforated by a system of holes, as a spatial cylindrical body. For the full investigation of the stress state in an arbitrary point inside the disc it is necessary to have three sections passing through the given point and coinciding with the coordinate planes $zO\theta$, zOz and $zO\theta$. Since in cross bending of the disc the stress state in its plane is the major determinant factor, then it will be possible for finding out the dangerous zones to confirm ourselves to the investigation of sections parallel to the neutral plane of the disc.

The determination of the stresses on the free contours of the model is highly simplified. For example, if in the plane of the section parallel to the $zO\theta$ plane, there is a circular contour free from stresses, then on this contour $\tau_{z\theta} = 0$ and $\sigma_z = 0$, whereas

$$\sigma_\theta = \sigma_0 m/h \quad (1)$$

where h is the thickness of the model and m is the order of interference strips. The value of the circumferencial normal stress σ_θ was taken as a quantitative measure of the stress concentration on the contours of the holes.

Following such a method, the features of stress concentration near the holes of the considered disc could be studied. The model disc was supported along its contour. Using a heat-resistant paper, the model was evenly (including the area of the hole), loaded by a weight of $P = 4$ kgf, and then it was located in a thermostat of the type VTS-1. In the thermostat the disc was heated to 130°C and was kept at this temperature for 3 hours. Then it was cooled to the room temperature and unloaded. Afterwards, two specimens (A and B) (see Fig. 1) were cut from the disc. Specimen A included a part of the disc periphery, and specimen B was located in the middle part of the disc (the side edge of B passes through the disc centre). It could be considered that the investigation of the specimens A and B gives us a pattern of the stress state in the whole disc. The specimens have three large opened holes of the type I, as well as a large number of holes of the types II and III. Four plates were cut from both specimens, parallel to the neutral plane of the disc. Each of these plates had a thickness of 3 — 4 mm. The upper plates were denoted by the

subscript 1 (A_1 and B_1) and the lower ones by the subscript 4 (A_4 and B_4). The blind holes intersected the first three plates. All the eight thin plates were investigated on the polarization BPU set. The obtained results have shown that the difference of the quasi-principal stresses attains a maximum on the contours of the holes. Therefore, it is possible to confine ourselves to the determination of the stresses along the contours of the holes. The polar distribution of the dimensionless circumferential $\bar{\sigma}_\theta = \sigma_\theta h / \sigma_0$ stresses along the contours of some holes is shown in Fig. 2-4. It is clear that according to (1), the magnitude of $\bar{\sigma}_\theta$ coincides with the order m of the interference strip in the considered point.

Specimen 4 has three opened holes (I) and a large number of blind holes (III). The experiments have shown that the stresses in the two intermediate plates (A_2 and A_3), near the neutral plane, are very small, i.e. the periferal part of the disc exists under the condition of almost pure bending. Therefore, the primary interest in specimen A consists in the investigation of the stress state along the contour of the hole in the first and fourth layers.

The analysis of the experiments has shown that the mutual effect of the small holes (III) on each other is insignificant. The distribution of the $\bar{\sigma}_\theta$ stresses along the contours of large holes in A have a cyclic symmetry with a maximum of ~ 1.5 (in the direction of the neighbouring small hole) and a minimum of ~ 0.8 (in the intermediate direction between two neighbouring small holes). The similar distributions in A_4 vary insignificantly, since the blind holes (III) do not reach the lower⁴ plate A_4 . The highest $\bar{\sigma}_\theta$ stress in the whole specimen A is observed in the contour of the holes III ($\bar{\sigma}_{\theta \max} \sim 3$), and in the points located along the direction of the hole 1.

The distribution of the $\bar{\sigma}_\theta$ stress along the contours of the intermediate hole I (see Fig. 1) and the holes III adjacent to it, is, for example, shown in Fig. 2. For convenience, the distribution of $\bar{\sigma}_\theta$ stress along the contour III is excluded from the drawing. In Fig. 2-4 the direction towards the centre of the disc is indicated by an arrow, and the dotted circles indicate the scale.

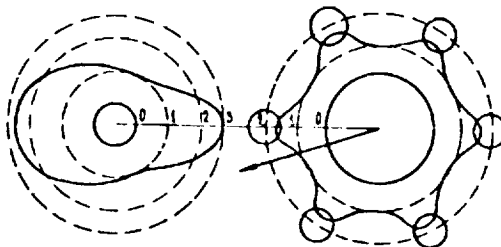


Fig. 2

Specimen B contains three large opened holes (I) and a large number of holes of the types II and III. The analysis of the photographs of the interference strips has shown that the two upper layers of specimen B (B_1 and B_2) have insignificant stresses. This can be explained by the following: Specimen B is located in the central part of the model. In this part the state of pure bending is superimposed on the all-sides tension, provided that the disc is subjected to a side load. Therefore, the two lower layers of specimen B (B_3 and B_4) are more loaded than the upper ones. Moreover, the highest stresses will arise in B_4 . Apart from those of the three holes (I), the maximum stresses will arise on the contours of the upper and intermediate holes (see Fig. 1), which are located very near to the disc centre. The distribution of $\bar{\sigma}_\theta$ in B along the contour of the intermediate hole I is shown in Fig. 3, whereas its distribution along the contour of the lower hole I is shown in Fig. 4. As in specimen A, the mutual stress concentration near the holes of the types II and III is insignificant. In the neighbourhood of the intermediate hole (I) of the large radius there are 4 holes of the type II, which lead to maximum $\bar{\sigma}_\theta$ stresses. Along the contours of the I and II holes (see Fig. 3) the stress amounts to 3.5–4.5 in the mutual direction, whereas in the rest part it amounts to 2–2.5. The variation of the stress along the contour of the lower hole (I) of the large radius (see Fig. 4) is insignificant ($\bar{\sigma}_\theta \sim 1$), since there are no holes in its vicinity.

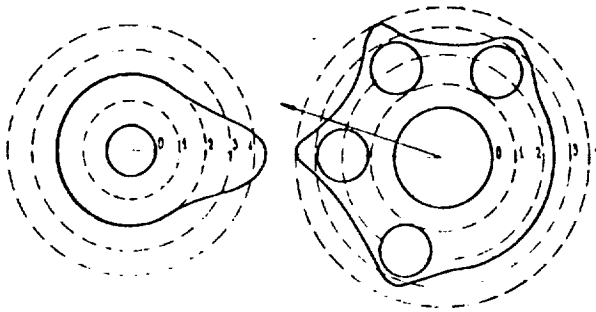


Fig. 3

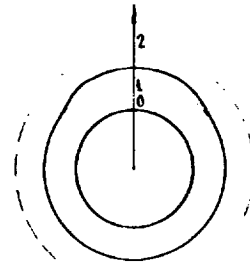


Fig. 4

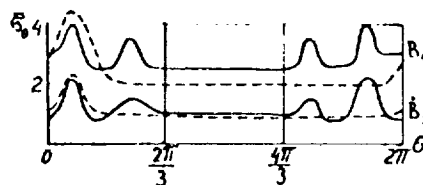


Fig. 5

The distribution of stresses in B_3 is similar to those in B_4 . But the stresses along all the corresponding holes are approximately 2 times less. Fig. 5 shows the scanning of the distribution of the $\bar{\sigma}_\theta$ stress along the contours of the intermediate hole I (solid lines) and the neighbouring hole II (dotted lines). From the analysis of the photographs of the interference strips it is possible to conclude that the maximum stress concentrations in the disc take place in these locations.

From the analysis of the interference patterns in the whole perforated disc it follows that the highest (circumferential) pressures are, according to (1), equal to :

$$\sigma_{\theta \max} = \frac{\bar{\sigma}_0 m}{h} = \frac{0.408 \times 4.5}{2} \frac{\text{kg}}{\text{cm}^2} = 0.92 \frac{\text{kg}}{\text{cm}^2}$$

Stresses arise in the solid circular disc of a radius a , which is hinge supported along its contour and subjected to an evenly distributed pressure q , with their maximum lying in its centre [2] :

$$\sigma_{\theta \max} = \frac{3(3+\nu)qa^2}{8h^2} = \frac{3(3+\nu)P}{8\pi h^2} = \frac{3 \times 3.5 \times 4}{8 \times 3.14 \times 4} = 0.42 \frac{\text{kg}}{\text{cm}^2}$$

where $\nu = 0.5$ is Poisson's coefficient of the utilized material.

Therefore, the maximum pressures in the disc are highly increased and displaced from the centre to the contours of the holes as a consequence of perforation.

After the determination of the pressures in the model it is necessary to solve the problem of transformation of the results of measurements from the model to the natural construction. The conditions of transformation can be obtained from the laws of similitude. These laws express the relationship between the basic quantities determining the flow of the processes in the model and the parent constructions.

To simulate the stress-strain states of the model and parent construction it is quite necessary to satisfy the following requirements:

- a) the model should be geometrically similar to the parent construction;
- b) the investigated processes and conditions of the parent construction and model should be described by the same equations;
- c) the initial and boundary conditions for the parent and model should coincide;
- d) the dimensionless parameters of the same notation, incoming in the differential equations, boundary and initial conditions in the model and parent construction, should be correspondingly equal.

The conditions of geometric similitude are determined by the ratio $\lambda = \ell_p / \ell_m$ of the characteristic dimensions of the parent construction (ℓ_p) to the dimensions of the model (ℓ_m), i.e. the scale of linear dimensions λ . In the case of a strict geometric similitude, the scale of variation of the linear dimensions $\lambda_1 = \Delta \ell_p / \Delta \ell_m$ should be also equal to λ , i.e. the amount of strain in the model and parent construction should be equal. However, in the method of optical polarization, the conditions of strict geometric similitude are never fulfilled, since the strains in the model usually exceed those in the parent construction. It is just required that the proportionality of the strain in the corresponding points in both the model and parent construction should be fulfilled.

The entirely closed system of equations for the determination of the stress-strain state of the body under static isothermal deformation, includes the differential equations of equilibrium boundary conditions, equations of state and equations of compatibility. The system of differential equations of equilibrium, in the case of the given processes, is valid for bodies of different materials. Consequently, this system will have the same form for both the model and the parent discs. The limiting conditions will coincide if the loads, applied to the model, are similar and proportional to the loads applied to the parent disc in the corresponding points. The equations of the state of the materials of the model and parent discs are determined in our case by Hook's law.

On the bending of elastic plates, the stress in the mean plane in the case of fulfilment of Kirchhoff's conditions can be presented in the following form :

$$\sigma = \varphi(\nu) \frac{q \ell^2}{h^2}$$

where ℓ is an arbitrary dimension in the mean plane and h is the thickness. If the model is geometrically simulated to the parent disc, and assuming that $\nu_m = \nu_p$, we get :

$$\sigma_p = \sigma_m \frac{q_p}{q_m}$$

In general, Poisson's coefficients for the model and parent materials are different. Moreover, in the method of optical polarization it is necessary to work with increased (as compared with the parent disc) strains. This leads to some unavoidable errors in the determination of the stresses in the parent disc, since they depend on the properties of model materials. The sources of errors can be determined either experimentally (by the investigation of models with materials having different values of Poisson's

coefficient) or by calculation (by the solution of analytical problems). Therefore, for the estimation of the effect of Poisson's coefficients in the problem under consideration, we should study the bending of a circular rigid plate, which is hinge-supported along its contour and which is subjected to a uniform pressure. The stress in the centre of the disc is slightly dependant on ν :

$$\sigma_{\theta \max} = \frac{3(3+\nu) q^2 a}{8h^2}$$

If it is assumed that the Poisson's coefficient of the parent disc is $\nu_p = 0.3$, whereas $\nu_m = 0.5$, then the error in the stresses will be within 6%. All the data obtained by the determination of stresses in the model-disc can be applied to a natural metallic disc almost with the same accuracy indicated above.

References

1. Krasnov, V.M. "O reshenii prostranstvennoi zadachi teorii uprugosti opticheskim metodom" (About the solution of the spatial problem of the theory of elasticity by an optical method). --- Uch. zap. MGU, 8(44), 1939.
2. Timoshenko, S.P. and S. Voinovskii-Kriger, "Plastinki i obolochki" (Plates and shells). --- Moskva, 1963.

AN APPROXIMATE METHOD FOR THE ESTIMATION OF
THE DYNAMIC TEMPERATURE FIELDS

By

S.A. Shesterikov and M.A. Yumasheva

In few practically important conditions of operation of elements of construction under elevated temperatures, cases are encountered when some of these elements undergo quick and intensive heating. In such cases, the estimation of the strength, temperature distortions and other effects converge around the necessity of determination of the arising dynamic temperature fields. Naturally, this temporary distribution of temperatures in the rigid body should be determined with an accuracy not exceeding that of the input data. Moreover, this distribution should be expressed in a form convenient for further utilization (for example, for the determination of the fields of stresses in the infinite problem of thermoelasticity or thermoplasticity). A version of the method of calculation of the dynamic temperature fields is suggested below for a class of such problems.

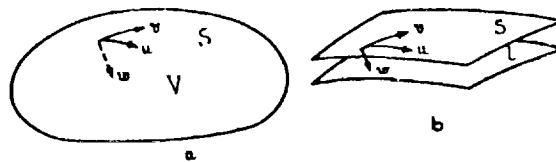


Fig. 1

Let us consider a body (see Fig. 1) of a volume V , limited by a surface S . The point P on the surface S is determined by a system of orthogonal curvilinear coordinates u and v ; the coordinate w is directed towards the normal inside the body. It may be assumed that before a certain period of time (which is taken as a reference) there was an even temperature field in the body. It may be assumed also that beginning from this moment a temperature field is created on the surface of the body, which is dependent on time according to the following relationship:

$$T = T_s(\rho, t) \quad (1)$$

Then, for the determination of the temperature field in the body as a function of the coordinates and time it is necessary to solve the following

equation :

$$\kappa \Delta T = \frac{\partial T}{\partial t} , \quad (2)$$

where κ is the coefficient of thermal conductivity. The analysis of the known exact solution of equation (2) under the boundary conditions (1) shows that although, theoretically, the temperature in any point of the body varies instantaneously with the temperature on the surface, then, in reality, some gradual change will take place in the temperature of the body beginning from the surface. This change attains real values inside the body only after a definite period of time varying with the value of the coordinates w . Therefore, it is natural to introduce a surface parameter L , which will be considered as a border separating the heated part of the body from the part where the temperature up to the moment of approach of the front can be practically considered constant. Consequently, the conditions on L will take the following form :

$$T|_{w=L} = 0 \quad \text{and} \quad \frac{\partial T}{\partial w} \Big|_{w=L} = 0 \quad (3)$$

The solution of equation (2) under the conditions (1) and (3) can take the following form :

$$T(P, w, t) = \sum A_i(P, t) \varphi_i , \quad (4)$$

where φ_i is some selected basic functions, dependent on unknown parameters (the method of their selection is indicated below). Such an approach is identical to the methods elaborated in similar problems by several authors [1,2]. The functions A_i are selected from the boundary conditions. Let us consider the particular case of selection of equation (4). If we search for a simple expression of the type (4) it is necessary, in accordance with the three boundary conditions, to assume that the value of the three terms in series (4), is minimum. Then, we will have :

$$T = A_0 + A_1 \varphi_1 + A_2 \varphi_2 \quad (5)$$

In this case it is always possible to consider that $\varphi_i(0) = 0$. Therefore, from the conditions (1) and (3) we will have :

$$T = T_1 [1 + B_1(L) \varphi_1(w) + B_2(L) \varphi_2(w)] \quad (6)$$

where

$$B_1 = - \frac{\varphi_2'}{\varphi_1 \varphi_2' - \varphi_2 \varphi_1'} \Big|_{w=\ell} , \quad B_2 = \frac{\varphi_1'}{\varphi_1 \varphi_2' - \varphi_2 \varphi_1'} \Big|_{w=\ell}$$

or

$$\tau = \tau_1(\rho, t) \varphi(\ell, w)$$

Let us change the variables by introducing the time t with respect to the reference t_1 , according to the following relationship :

$$t = (\lambda^2 / \alpha) t \quad (7)$$

where λ is some characteristic dimension. All the coordinates (u, v, w) will be considered dimensionless with respect to the same λ . Then, equation (2) can be written in the following dimensionless form :

$$\begin{aligned} & \frac{\partial}{\partial u} \left(\frac{L_v L_w}{L_u} \frac{\partial \tau}{\partial u} \right) + \frac{\partial}{\partial v} \left(\frac{L_u L_w}{L_v} \frac{\partial \tau}{\partial v} \right) + \\ & + \frac{\partial}{\partial w} \left(\frac{L_u L_v}{L_w} \frac{\partial \tau}{\partial w} \right) = L_u L_v L_w \frac{\partial \tau}{\partial t} \end{aligned} \quad (8)$$

where Lamé's coefficients are determined from the following relationships:

$$L_\kappa^2 = \left(\frac{\partial x}{\partial \kappa} \right)^2 + \left(\frac{\partial y}{\partial \kappa} \right)^2 + \left(\frac{\partial z}{\partial \kappa} \right)^2 \quad (\kappa = u, v, w)$$

The yet unknown value of the depth of the heated layer ℓ can be determined from the condition of the integral satisfaction of equation (8) in the heated zone

$$\begin{aligned} & \int_0^\ell \left\{ \int_0^\ell \left[\frac{\partial}{\partial u} \left(\frac{L_v L_w}{L_u} \frac{\partial \tau}{\partial u} \right) + \frac{\partial}{\partial v} \left(\frac{L_u L_w}{L_v} \frac{\partial \tau}{\partial v} \right) + \right. \right. \\ & \quad \left. \left. + \frac{\partial}{\partial w} \left(\frac{L_u L_v}{L_w} \frac{\partial \tau}{\partial w} \right) \right] dw \right\} du dv = \\ & = \int_0^\ell \left\{ \int_0^\ell L_u L_v L_w \frac{\partial \tau}{\partial t} dw \right\} du dv \end{aligned} \quad (9)$$

Let us assume that the heating process is, in some sense, almost regular. Then, in this case, the first two terms in the left hand side of the equation will be much less than the third term. As a result, we will have :

$$\iint_S \left\{ \int_0^l \frac{\partial}{\partial w} \left(\frac{L_u L_v}{L_w} \frac{\partial T}{\partial w} \right) dw \right\} du dv = \iint_S \left\{ \int_0^l L_u L_v L_w \frac{\partial T}{\partial t} dw \right\} du dv \quad (10)$$

Integrating the left part of the equation with respect to w , taking into consideration the boundary condition (3), and substituting T by its value in (6), we get from (10) :

$$\iint_S \left\{ \left. \frac{L_u L_v}{L_w} \right|_{w=0} T_1 \frac{\partial \varphi}{\partial w} \right|_{w=0} + \int_0^l L_u L_v L_w \frac{\partial \varphi T_1}{\partial t} dw \right\} du dv = 0 \quad (11)$$

In the case when L_u , L_v and L_w are independent of u and v , the function T can be represented in the form of a multiplication :

$$T_1 = \theta(t) \Psi(\rho) \quad , \quad (12)$$

Equation (11) can be represented in the form :

$$\left\{ \frac{\partial \varphi}{\partial w} \right|_{w=0} \theta + \int_0^l K(w) \frac{\partial \theta \varphi}{\partial t} dw \right\} \iint_S \Psi(\rho) du dv = 0 \quad (13)$$

where

$$K(w) = \frac{L_u L_v L_w}{L_u L_v / L_w |_{w=0}}$$

The second integral is a definite expression that is considered different from zero. Therefore, in the fulfillment of condition (12) the following equation is obtained :

$$\theta \left[\frac{\partial \varphi}{\partial w} \right]_{w=0} + \int_0^l K(w) \frac{\partial \theta \varphi}{\partial t} dw = 0 \quad (14)$$

Let us consider in details condition (12). In fact, this condition does not put rigid limitations on the temperature field T_1 or on the boundary S . In most problems, the temperature T_1 can be represented with any given degree of accuracy by the following relationship :

$$T_1 = \sum_{\kappa} \theta_{\kappa}(t) \psi_{\kappa}(\rho) \quad (15)$$

Due to the linearity of the problem of heat conductivity, it is now possible to find out a solution for one component and then to determine the general distribution of temperature as a sum of separate solutions. Let us return to the analysis of equation (14), and use the exponential functions as basic functions for φ_1 and φ_2 . In the simplest case we can assume :

$$\varphi_1(x) = x^{n_1}, \quad \varphi_2 = x^{n_2} \quad (16)$$

Then, from (6) it is easy to get :

$$\varphi = 1 - \alpha_2 \varphi_1 \left(\frac{w}{\ell} \right) + \alpha_1 \varphi_2 \left(\frac{w}{\ell} \right) \quad (17)$$

where

$$\alpha_i = \frac{n_i}{n_2 - n_1}$$

The preservation of the arbitrary values of the indices n_1 and n_2 in expressions (16) is justified by the fact that in the future it will be possible to improve the solution by the corresponding selection of these parameters, using, for example, the principle of least square deviation of the solution from the exact one, with respect to volume and the characteristic time. For example, we have :

$$\frac{\partial J}{\partial n_1} = 0 \quad \text{and} \quad \frac{\partial J}{\partial n_2} = 0 \quad ,$$

where

$$J(n_1, n_2) = \int_0^{\tau} \left\{ \iiint_V (\Delta T - \dot{T})^2 dv \right\} dt \quad (18)$$

In this case the characteristic time τ is selected from the condition that the whole considered time interval t was taken.

It is clear that the method can be also generalized when a large number of basic functions and unknown parameters is introduced. However, due to the sharp increase of the volume of investigation such a method begins to lose its advantage before the exact solution of the problem of heat conductivity in series and in numbers.

Let us consider the application of the mentioned method to the calculation of a concrete element. We may select, as an example, the temperature field in a cylinder whose surface temperature Θ is given. As an approximating system of the functions φ_1 , and φ_2 let us take :

$$\varphi_1 \equiv x \quad , \quad \varphi_2 \equiv x^2 \quad (19)$$

Then, from (17) we have :

$$\varphi = 1 - 2 \frac{w}{\ell} + \frac{w^2}{\ell^2} = \left(1 - \frac{w}{\ell}\right)^2 \quad (20)$$

Substituting (20) in (14), we get :

$$-\frac{2\Theta}{\ell} + \int_0^{\ell} k(w) \frac{\partial}{\partial t} (\Theta \varphi) dw = 0 \quad (21)$$

Let us introduce the cylindrical system of coordinates with the z axis coinciding with the cylinder axis. Then, if the radius of the cylinder is denoted by R , and R is taken as the characteristic dimension λ , we will have :

$$u = \varphi \quad , \quad z/R = v \quad , \quad w = 1 - r/R$$

From which we get :

$$k(w) = 1 - w$$

Substituting this expression in (21), we get :

$$-\frac{2\Theta}{\ell} + \int_0^{\ell} (1-w) \frac{\partial}{\partial t} \left[\Theta \left(1 - \frac{w}{\ell}\right)^2 \right] dw \quad (22)$$

Let us consider the steady state when $\Theta = \text{const.}$ Then, equation (22) can be rewritten in the form :

$$-\frac{2}{\ell} + \int_0^{\ell} (1-w) \cdot 2 \left(1 - \frac{w}{\ell}\right) \cdot \frac{w}{\ell^2} dw = 0 \quad (23)$$

and it is easy to get an equation of the form :

$$\frac{12}{\ell} = (2 - \ell) \dot{\ell} , \quad (24)$$

Integrating the last expression we get an equation relating ℓ with t

$$12t = \ell^2 - \frac{\ell^3}{3} \quad (25)$$

For the dynamic external field, when Θ depends on t , the equation becomes more complex. But for definite laws of the relationship $\Theta(t)$, this equation can be integrated in a closed form. For the considered case, the equation of τ , t and w can be obtained in a parametric form :

$$\begin{aligned} \tau &= \Theta \left(1 - \frac{w}{\ell}\right)^2 & \text{at } w < \ell , \\ \tau &\equiv 0 & \text{at } w > \ell \end{aligned} \quad (26)$$

where ℓ and t are related by equation (25). The obtained relationships are valid for that moment when ℓ becomes equal to 1. From (25), we get the value of t , for which $\ell = 1$. Further on, the temperature field will vary in the whole cylinder, and instead of the boundary conditions (3) we will have the following condition :

$$\left. \frac{\partial \tau}{\partial w} \right|_{w=1} = 0$$

Assuming once more that the temperature field has a parabolic relationship with w , we will get for τ the following expression :

$$\tau = \alpha (1 - w)^2 + \Theta - \alpha \quad (27)$$

In deriving the last expression the indicated condition, as well as condition (1), were used. The parameter $\alpha(t)$ can be determined from the condition of integral satisfaction of the equation of thermal conductivity (either type (10) or (11)), i.e.

$$-2\alpha + \int_0^1 (1 - w) \dot{\alpha} [(1 - w)^2 - 1] dw = 0 \quad (28)$$

Using the condition $t = t_0$, $\alpha = \Theta$, we get :

$$\alpha = \Theta e^{-\beta(t-t_0)} \quad (29)$$

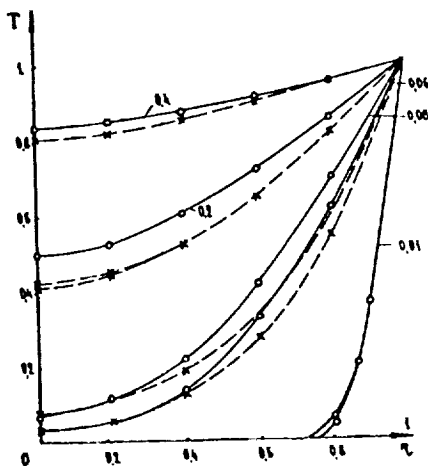


Fig. 2

Equations (24), (25) and (27), (29) represent completely the relationship between temperature and time, as well as the coordinate w . The comparison of these relationships with the exact solution [3] is represented in Fig. 2. In this figure, the solid lines represent the curves obtained from the exact solution, whereas the dotted lines represent the curves obtained according to the suggested method (the values of the dimensionless time are marked near the corresponding curves).

References

1. Barenblatt, G.I. --- *Izv. AN SSSR, Otd. tekhn. n.*, No. 9, 1954.
2. Minin, O.V. and N.A. Yaryshev. --- *IFZh*, 17(3), 1969.
3. Karslou, G. and G. Eger, "Teploprovodnost' tverdykh tel" (Thermal conductivity of solid bodies). --- *Fizmatgiz*, Moskva, 1964.

RELAXATION AND CREEP STRENGTH OF PIPES SUBJECTED
TO COMPLEX STRESS STATES

By

S.A. Shesterikov, V.D. Kurov, G.P. Mel'nikov,
E.A. Myakotin and M.A. Yumasheva

The operation of several elements of electric equipment [1] can be characterized by the combined processes of creep and relaxation flowing in different basic directions. One of the most characteristic forms of such a strain is the condition of tubular elements subjected to the simultaneous action of the internal pressure and the given axial deformation. It is clear that such a form of a complex stress state can be very easily realized in experiments. Let us consider some features of this case, and investigate the process of stress relaxation in a tube subjected to the combined action of an internal pressure q and a given axial deformation ϵ_x .

In the specimen, the following system of stresses will emerge :

$$\sigma_\theta = \frac{q a}{h} \quad , \quad \sigma_r = 0 \quad , \quad \sigma_z = \sigma_z(t) \quad , \quad (1)$$

where a is the tube radius, and h is the thickness. The axial stress σ_z can be represented as the sum of two components

$$\sigma_z = \sigma_{z_1} + \sigma_{z_2} \quad (2)$$

where σ_{z_1} is the stress caused by the pressure q , whereas σ_{z_2} is the stress arising as a result of the additional axial tension ϵ_x . The deformation ϵ_{x_0} can be simulated as a thermoexpansion or constrained deformation of tubes in a packet. It is evident that :

$$\sigma_{z_1} = \sigma_\theta/2 \quad (3)$$

The superposition of the two processes - creep in the circumferential direction and relaxation in the axial direction (the stress in the radial direction will be neglected, and it will be considered that $\sigma_r \equiv 0$), will lead to a quasi-plane stress state. For the discussion of such a stress-strain state it is necessary to select thoroughly (physically uncontradictory) the equations of the theory of creep, describing the processes of creep under multi-axial stress conditions. As a basis, let us take the equation of the flow theory [2] for a steady creep :

$$\dot{\rho}_{ij} = f S_{ij} \quad (4)$$

where \dot{P}_{ij} are the components of the tensor of creep deformations, S_{ij} are the components of the deviator of stresses, and f is the function of the invariants of the stresses tensor. It is assumed here that the creep strain satisfies the condition of incompressibility. For decreasing the transformations it could be assumed that the function f depends only on the second invariant of the stresses tensor (although it can be shown that all the data given below are valid on the selection of an another relationship for f and the use of other invariants). Therefore, the axial component of deformation in the considered case can be expressed in the following form :

$$\dot{P}_z = f(\sigma_z^2 - \sigma_z \sigma_\theta + \sigma_\theta^2)(2\sigma_z - \sigma_\theta)/3 \quad (5)$$

In equation (5), σ_θ is a constant parameter. Therefore in the case when

$$E_z \equiv P_z + (1/E)(\sigma_z - \nu \sigma_\theta) = \text{const}$$

we get from (5) an expression for σ_z

$$\dot{\sigma}_z = -E f(\sigma_z^2 - \sigma_z \sigma_\theta + \sigma_\theta^2)(2\sigma_z - \sigma_\theta)/3 \quad (6)$$

Initially, $\sigma_z(0) = \sigma_0$

Let us compare the relaxation curves described by equation (6), for the following two cases: a) on the existence of a pressure q , b) when $q = 0$. Moreover, assume that the initial stress σ_0 is the same in both cases. The equation of σ_z will then take the following forms :

$$(a) \quad \dot{\sigma}_z = -E f(\sigma_z^2) 2\sigma_z/3 \quad (\text{for } q = 0); \quad (7)$$

$$(b) \quad \dot{\sigma}_z = -E f(\sigma_z^2 - \sigma_z \sigma_\theta + \sigma_\theta^2)(2\sigma_z - \sigma_\theta)/3 \quad (\text{for } q \neq 0)$$

Since $\sigma_0 > \sigma_0/2$, then divide the whole zone of variation of σ_z to three sections :

- 1) $\sigma_z > \sigma_\theta$;
- 2) $\sigma_\theta > \sigma_z > \sigma_\theta/2$;
- 3) $\sigma_\theta/2 > \sigma_z$.

and consider that $\partial f(x)/\partial x > 0$ (i.e. the function f is steadily increasing). Then, it will be clear that in the first zone the right hand side of equation (6), for the case when q is absent (further on we will call this case "a"), is greater by its absolute value than for the case when $q \neq 0$ (this case will be denoted by case "b"). Since both relaxation processes begin from one level, then in this zone the curve of case "a" will lie below that of case "b". In the second zone it seems that the intensity of the stresses for case "b" is greater than that for "a". This may lead to the fact that the relaxation curves begin to converge, then they may intersect and, further on, curve "a" can go higher than curve "b" (see Fig. 1). But since curve "b" has a horizontal asymptote of $\sigma_z = \sigma_\theta / 2$, then if even such an intersection occurs it will imply that further on another intersection of both relaxation curves will occur and curve "a" will necessarily go below curve "b" (the asymptote of curve "a" is the time axis). All the above mentioned points are related to the case when the relaxation process begins with $\sigma_0 > \sigma_\theta$.

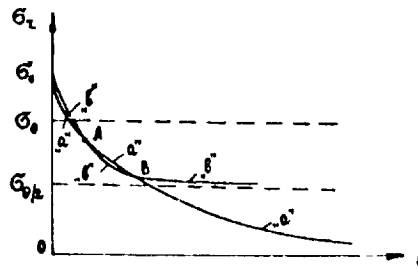


Fig. 1

When $\sigma_0 < \sigma_\theta$, two cases are possible: either curve "a" goes above "b" or vice versa. The limiting conditions will be those where both curves emerge from point σ_0 with equal inclinations. In this limiting condition, $\dot{\sigma}_z(0)$ of case "a" should coincide with $\dot{\sigma}_z(0)$ of case "b". Then, from (1.7) it follows that:

$$f(\sigma_0^2)2\sigma_0 = f(\sigma_0^2 - \sigma_0\sigma_\theta + \sigma_\theta^2)(2\sigma_0 - \sigma_\theta) \quad (8)$$

where

$$\sigma_\theta > \sigma_0 > \sigma_\theta/2$$

It is easy in certain cases to prove that equation (8) may or may not have roots in the necessary range.

For the case when the exponential relationship has the form

$$f(x) \equiv x^k \quad (9)$$

equation (8) will have roots at :

$$k \geq k_1 \equiv 2.4 \quad (10)$$

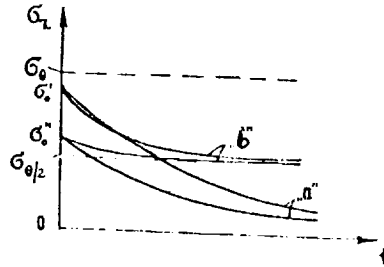


Fig. 2

Therefore, if $k < k_1$, curve "a" will always lie below curve "b". At $k > k_1$, there are two values of σ_0 (σ_0^* and σ_0') dividing the zone of the initial values of σ_0 into three zones (see Fig. 2). At $\sigma_0 < \sigma_0^*$, curve "a" will always lie below curve "b". At $\sigma_0' > \sigma_0 > \sigma_0^*$, curve "b" will lie firstly below curve "a", then both curves will intersect each other and curve "a" will diverge below curve "b". At $\sigma_0 > \sigma_0'$, the process will be either as previously described (see Fig. 1), or it may happen that both curves may not intersect each other. Let us analyse in details this latter case. Since at $\sigma_0 > \sigma_0'$ (independent of whether σ_0 is greater or smaller than σ_0) a double intersection of curves "a" and "b" (see Fig. 1) may take place, or no intersection may occur at all; then, the limiting case may be that when A and B coincide. Thus, due to the smoothness of the curves, there will be a tangency, i.e. the following condition will be fulfilled :

$$f(\bar{\sigma}_z^2) 2\bar{\sigma}_z = f(\bar{\sigma}_z^2 - \bar{\sigma}_z \sigma_\theta + \sigma_\theta^2)(2\bar{\sigma}_z - \sigma_\theta) \quad (11)$$

where $\bar{\sigma}_z$ is the value of σ_z corresponding to the moment of tangency of the curves. Moreover, the times needed for the fulfilment of this point for the compared processes will be equal, i.e. :

$$\int_{\bar{\sigma}_z}^{\sigma_0} \frac{d\sigma_z}{2f(\sigma_z^2)\sigma_z} = \int_{\bar{\sigma}_z}^{\sigma_0} \frac{d\sigma_z}{(2\sigma_z - \sigma_\theta)f(\sigma_z^2 - \sigma_z \sigma_\theta + \sigma_\theta^2)} \quad (12)$$

Since even for a relationship of the type (9) the general case of equation (12) could not be integrated in elementary functions, a detailed analysis was conducted by numerical methods on the digital computer "NAIRI". For the given σ_0 (or q) it is possible from systems (11) and (12) to determine σ_0 as a function of the parameters included in f . For equation (9), the relationship between σ_0 and K is derived. It can be noted that in this case, σ_0 enters in this relationship as a simple multiplier, i.e.

$\sigma_0 = \sigma_0 \psi(K)$. Moreover, at $K < K_1$, functions ψ do not exist, whereas at $K > K_1$, $\sigma_0 > \bar{\sigma}_0$. The calculations have shown that σ_0 increases with the increase of K . The limiting value of K is determined from the condition $\sigma_0 \rightarrow \infty$. Then, instead of (11) and (12) we have the following system :

$$2\bar{u}^{2\kappa+1} = (2\bar{u}-1)(\bar{u}^2 - \bar{u} + 1)^\kappa ; \quad (13)$$

$$\frac{1}{4\kappa\bar{u}^{2\kappa}} = \int_{\bar{u}}^{\infty} \frac{du}{(2u-1)(u^2 - u + 1)^\kappa} ;$$

where the replacement $\sigma_z = \sigma_0 u$ and $\bar{\sigma}_z = \sigma_0 \bar{u}$ was made. \bar{u} and K are determined from (13), which we denote by K_2 . The calculations have also shown that

$$K_2 \approx 2.72 \quad (14)$$

Consequently, at $K > K_2$ the case shown in Fig. 1 may take place at any $\sigma_0 > \bar{\sigma}_0$. At $K_2 > K > K_1$, σ_0^* can be always found, such that at $\sigma_0 > \sigma_0^*$, curves "a" and "b" would not intersect, whereas at $\sigma_0^* > \sigma_0 > \bar{\sigma}_0$, a double intersection of these curves may take place (as shown in Fig. 1). Therefore, σ_0^* is determined from systems (11) and (12) at the given value of K , and corresponds to the initial stress at which curve "a" is always located below curve "b". But the tangency of these curves is clear in one point.

Therefore, all the possibilities were investigated for a relationship of the type (9). A similar analysis was conducted when the maximum tensile stress was considered as a determining factor, and it was proven that all the above indicated features are valid. The conducted analysis has revealed the basic features of the shells behaviour in the case of the combined action of internal pressure and axial relaxation. It has also allowed to estimate the variation of the stress state with respect to time under such conditions of operation, and the study of the creep strength on testing the sets of the Koffin type. The experimental investigations conducted in the IVT laboratory on similar sets have proved the validity of the obtained estimates. Moreover, these investigations have highly improved the accuracy of the analysis of similar effects, studied in [1].

A series of experiments was conducted on a set of the Koffin's type for the determination of the characteristics of the creep strength under different conditions. Cyclic tests were conducted (with a base of 6 hours) on tubular specimens loaded internally by a constant pressure under the conditions of axial relaxation. Let us consider a single method for the estimation of accumulation of damage under the indicated conditions. It will be assumed that the kinetic equation for the damage parameter ω_k written for the principal directions, has the following form :

$$\dot{\omega}_k = \Psi(\sigma_i, \sigma_k) \quad (k = 1, 2, 3) , \quad (15)$$

where σ_k is the principal stresses and σ_i is the intensity.

Moreover, the relationship with σ_k can have the character of the relationship with a combination type of $\sigma_k + |\sigma_k|$.

For the uniaxial case and a constant stress, this equation leads to the law of linear summation of damage. In the conducted tests, the specimen exists under the conditions of a plane stress varying with time and from one cycle to another. For the determination of the simplest value, it was assumed that the variation from one cycle to another can be neglected. Actually, as shown by experiments, the first two-three cycles are only different. Further on, a condition prevails when the residual deformation becomes practically the same from cycle to another. Since in the specimen, only σ_θ and σ_z are actually different from zero, equation (15) can be written in the form :

$$\dot{\omega}_\theta = 2A\sigma_i^{n_1} \sigma_\theta^{n_2} , \quad \dot{\omega}_z = 2A\sigma_i^{n_1} \sigma_z^{n_2} \quad (16)$$

It is then possible to find an exact solution for equations (16). Integrating equation (6) and substituting the parameter $\sigma_i = \sigma_i(t)$, we get $\Delta\omega_\theta$ and $\Delta\omega_z$ for one cycle. It is also possible by the use of the experimental values of the parameters $\sigma_z(t)$ to get similar values for the damage increments.

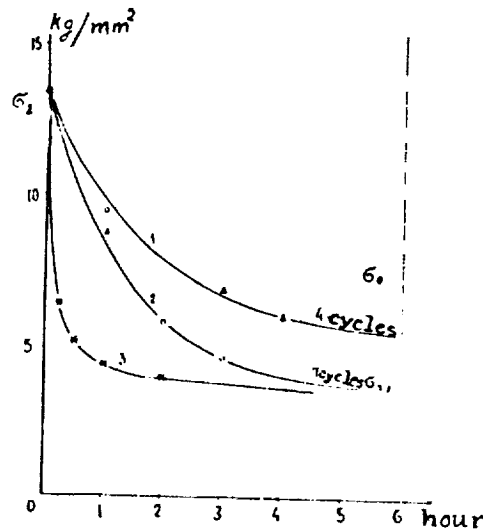


Fig. 3

Since for the first version it is necessary to know all the characteristics of creep, and since it is impossible to determine them due to the insufficiency of the experimental material, then the second version should be considered. From practice it follows that under the conditions of the conducted experiments the relaxation curve can be represented in the form shown in Fig. 3 for a steady cycle state. In the conducted series of experiments, σ_0 was varied, whereas the difference $\sigma_0 - \sigma_{0/2}$ remained constant since the same $\varepsilon_{z0}(0.9 \cdot 10^{-3})$, corresponding to the conditions of the tests ($\sigma_0 - \sigma_{0/2} = 10 \text{ kg/mm}^2$), was given; σ_0 was varied in the experiments from 6.6 to 7.7 kg/mm^2 . Due to the insignificant variation of the q curves, $\sigma_z(t)$ proved to be similar for different values of σ_0 .

The characteristic relaxation curves are represented in Fig. 3. These curves are taken for a specimen with $\sigma = 7.1 \text{ kg/mm}^2$. They indicate the gradual acceleration of the relaxation process from one cycle to another, and, consequently, the decrease of the stress intensity. Let us move to the estimation of the obtained experimental data.

If we assume that for all the cycles of the tests there is a similar relaxation process, as shown in Fig. 3, curve 3 (which is an evidence of the decrease of the intensity of pressure), then the equation of relaxation of the axial component σ_{z2} can be conditionally written in the form of a displaced branch of a hyperbola

$$\sigma_{z2} = (\tau + 0.1)^{-1} \quad \text{where } 0 \leq \tau \leq 6 \quad (\text{hour}) \quad (17)$$

Then, at

$$\tau = 0, \quad \sigma_{z2} = 10 \text{ kg/mm}^2; \quad \tau = 6, \quad \sigma_{z2} = 0.16 \text{ kg/mm}^2$$

For the approximate determination of the stress intensity, the value of the equivalent axial stress σ_z^* is introduced, which is defined as the average with respect to time

$$\sigma_z^* = \frac{1}{\tau_0} \int_0^{\tau} [\sigma_{z1} + \sigma_{z2}(\tau)] d\tau \quad (18)$$

For specimen No. 8, for which $\sigma_0 = 6.6 \text{ kg/mm}^2$, we have:

$$\begin{aligned} \sigma_{z1} &= 3.3 \text{ kg/mm}^2; \\ \sigma_z^* &= 4.2 \text{ kg/mm}^2; \\ \sigma_z^* &= 5.8 \text{ kg/mm}^2. \end{aligned}$$

For specimen No.11, for which $\sigma_0 = 7.7 \text{ kg/mm}^2$, we have :

$$\sigma_{z1} = 3.85 \text{ kg/mm}^2;$$

$$\sigma_z^* = 4.56 \text{ kg/mm}^2;$$

$$\sigma_i^* = 6.78 \text{ kg/mm}^2.$$

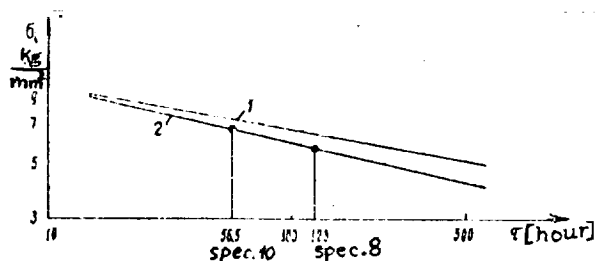


Fig. 4

Let us compare all the obtained values with the data of the creep strength determined under other conditions. In Fig. 4, a graph is plotted in the logarithmic coordinates: the intensity of pressure and log time. The straight line 1 corresponds to the tests carried out on creep strength without pause, whereas line 2 corresponds to the tests carried out with 6-hours cycles. If the experimental points are plotted on this graph, taking σ_z^* into consideration, as calculated from equation (18) and from the obtained value of σ_i^* , then the experimental points will lie above line 1. If we consider that all the values are determined only by the maximum tensile stress, i.e. in (16) $n_1 = 0$, then the experimental results will be in good agreement with the straight line 2. The last statement is in perfect coincidence with the results of the series of experimental investigations previously conducted in the IVT laboratories on the same material. Those last investigations have shown that the criterion of maximum tensile stress is determinant in the estimation of the creep strength under complex stress states.

References

1. Mel'nikov, G.I. and V.B. Gorlov, "Relaksatsiya temperaturnykh napryazhenii v usloviyakh slozhnogo napryazhennogo sostoyaniya" (Relaxation of thermal stresses under complex stress states). --- Probl. prochn., No.4, 70-73, 1971.
2. Rabotnov, Yu.N. "Polzuchest' elementov konstruktsii" (Creep of elements of construction). --- Moskva, "Nauka", 1966.

THE RELATIONSHIP BETWEEN THE LIFE OF MATERIAL
AND THE LEVEL OF CREEP STRESSES IN THE CASE
OF COMBINED LOADING

By

G.A. Tulyakov, G.I. Mel'nikov and Yu.D. Starostin

The investigation of the life of material under the conditions of combined action of thermocycling and creep, has shown that the service life of the material is determined by the sequence of application of different groups of loads, prehistory of loading (duration of the previous stages of loading) and, to a large extent, by the level of creep stress [1,2].

As a result of the study of the processes of accumulation of the damages and failure of austenitic steel (Kh18NiOT), two principally different zones varying with the level of static loading were established [3]. Under low stresses, i.e. relatively long duration of the experiment, the most intensive process of accumulation of the damages produced from thermocycling and static loading was observed. This process is "located" mainly along the grain boundaries. As a result, a significant decrease of the absolute as well as the relative life of the material occurs independent of the sequence of application of loads.

Under high stresses an intensive strain hardening takes place inside the grains due to thermocyclic deformation and the accumulation of damages inside the grains, as well as along their boundaries (due to creep). In this case no actual accumulation of damages occurs since, as shown by metallurgical researches, an intrograin failure is basically produced. As a result, a remarkable increase of the relative as well as the absolute life of the metal is observed under the conditions of initial thermocycling due to the strain-hardening processes.

Proceeding from the data of the indicated works and from the results of investigation of the mechanisms of accumulation of damages in the structural material it is possible to assume that the relationship between the life of the material in combined loading and creep stress should have extreme values corresponding to the maximum and minimum life capacity.

The correctness of the above stated assumption can be also checked on a family of curves, described by equation (1) [2] :

$$A = \tilde{N} + \tilde{\tau} = 1 \pm \sqrt{2} \alpha [1 - (\tilde{N} - \tilde{\tau})^2] \quad (1)$$

If the left hand side of equation (1) is expressed as a function of creep stress, the graph of the family of curves will acquire the shape shown in Fig. 1, independent of the sequence of application of loads and their relative magnitudes.

In the general case the family of such curves can be described by the following relationships

$$F(\sigma) = K \cdot \sigma^\alpha |\sigma - \sigma_1|^\beta \cdot |\sigma - \sigma_2|^\gamma \cdot \text{sign}\{(\sigma - \sigma_1)(\sigma - \sigma_2)\} + 1 \quad (2)$$

where σ_1 and σ_2 are the roots of equation (2), and

K, α, β and γ are constants.

In certain cases, equation (2) (of curve (a) shown in Fig. 1) can be represented in the form of a family of two equations at a relative initial creep of $\tilde{\tau} = 0.43$:

for $\sigma \leq 16$

$$F(\sigma) = 2.22 \cdot 10^{-4} \cdot \sigma^{2.305} |\sigma - 16|^{1.047} \cdot \text{sign}(\sigma - 16) + 1 \quad ; \quad (3)$$

for $\sigma > 16$

$$F(\sigma) = -1.105 \cdot 10^{-8} |\sigma - 16|^{1.19} |\sigma - 42|^5 \cdot \text{sign}\{(\sigma - 16)(\sigma - 42)\} + 1 \quad (4)$$

Curve (b) (see Fig. 1), with a preliminary relative number of $\tilde{N} = 0.57$ for the initial thermocycles, can be described by the following system: for $\sigma \leq 15$

$$F(\sigma) = 1.01 \cdot 10^{-3} \cdot \sigma^{1.56} |\sigma - 15|^{1.04} \cdot \text{sign}(\sigma - 15) + 1 \quad ; \quad (5)$$

for $\sigma > 15$

$$F(\sigma) = -1.62 \cdot 10^{-5} |\sigma - 15|^{1.035} |\sigma - 42|^{2.87} \cdot \text{sign}\{(\sigma - 15)(\sigma - 42)\} + 1 \quad (6)$$

It is therefore clear that a significant increase in the relative life of the material corresponds to a relatively high level of creep stress exceeding the yield limit of Kh18N10T steel at the given temperature (the test temperature was 600°C). This increase in the life of the material is, as stated above, due to the processes of intrograin thermocyclic strain-hardening. This is the reason why such an increase is most clearly revealed under the conditions of initial thermocycling.

For creep stresses lying in the range of 8-12 kg/mm², which is very close to the stress level of many elements operating under steady power machinery, a minimum relative life is observed, which is slightly dependent on the sequence of application of thermocyclic and static loads. The least life capacity of the material in this zone is conditioned by the processes of intensive actual accumulation of damages.

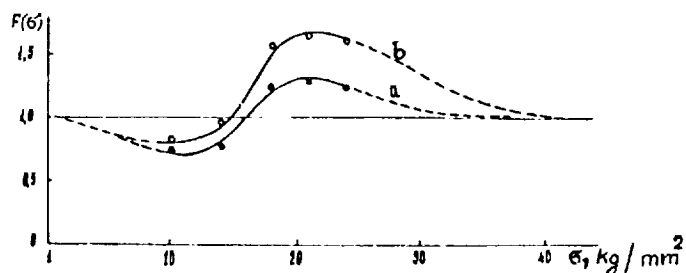


Fig. 1

Graph of the relationship between the life of the material in combined loading $F(\sigma)$ and the level of creep stresses σ : a- is the value of initial loading at a relative initial creep of $\bar{\epsilon} = 0.47$ (\bullet = experimental results); b - is the value of initial loading by thermocycling, $\bar{N} = 0.57$ (\circ = experimental results).

References

1. Tulyakov, G.A. "O soprotivlenii stali Kh18NiOT termicheskoi ustalosti" (About the resistance of Kh18NiOT steel to thermal fatigue). --- Teploenergetika, No. 6, 1972.
2. Tulyakov, G.A. Yu.D. Starostin and G.P. Mel'nikov, "Ob odnom metode otsenki dolgovechnosti pri kombinirovannom deistvii polzuchesti i termicheskoi ustalosti" (About one method of estimation of longevity in the case of the combined action of creep and thermal fatigue). --- See the present collection.
3. Tylyakov, G.A. Yu.D. Starostin, and V.A. Plekhanov, "Vliyanie predvaritel'nogo termotsiklirovaniya na kharakteristiki zharoprochnosti austenitnoi stali" (The effect of initial thermocycling on the characteristics of thermal strength of austenitic steel). --- "Probl. prochnosti," No. 1, 1972.

ABOUT ONE METHOD OF ESTIMATION OF LONGEVITY IN THE
CASE OF THE COMBINED ACTION OF CREEP AND THERMAL
FATIGUE

By

G.A. Tulyakov, Yu.D. Starostin and G.P. Mel'nikov

A method was previously suggested for the estimation of life of elements and aggregates of power machinery operating under the conditions of creep and small thermocyclic fatigue[1]. This method is based on the summation of relative lives, using the general form of linear law, expressed by the following relationship :

$$\frac{N_i}{N_{ip}} + \frac{\tau_i}{\tau_{ip}} = 1 \quad (1)$$

where N_i is the number of cycles in the experiment ;
 N_{ip} is the number of cycles leading to damages ;
 τ_i is the creep time in the experiment ;
and τ_{ip} is the failure time.

At the same time, the results of some works[2,3,4] have shown that the data obtained from the experiments on creep and small cycle thermo-mechanical fatigue are highly different from linear summation. If the right hand side of equation (1) is denoted by the parameter of life "A", the results of the above mentioned experiments can be expressed as $A > 1$, in the case of strainhardening of the material, and as $A < 1$, in the case of its softening (with respect to linear summation).

An investigation of some aspects of life in the case of combined action of static and thermocyclic loading is illustrated below.

The analysis of the experimental results [3,5] has shown that the process of development of damage is highly dependent on the amplitude level of the thermocyclic and static stresses, as well as the sequence of their application. It follows, therefore, that the graph of life performance, expressed by the relative coordinates $\tilde{N} = \frac{N_i}{N_{ip}}$ and $\tilde{\tau} = \frac{\tau_i}{\tau_{ip}}$, can be approximated in the form of a family of curves, symmetrically located on both sides of the straight line, for which (in certain cases) the law of linear summation (1) is valid.

In the general case, the equation of life for the complex action of thermal fatigue and creep can be represented as a family of parabolas :

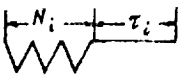
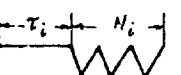

$$\tilde{N} + \tilde{\tau} = 1 \pm \alpha \sqrt{2} [1 - (\tilde{N} - \tilde{\tau})^2] \quad (2)$$

where $0 \leq |\alpha| < \frac{\sqrt{2}}{2}$ is the coefficient of summation characterizing the degree of deviation of the relative life obtained from the linear law under the conditions of strain hardening and softening of the material. The value of this coefficient depends basically on the sequence of application of different types of loads, as well as on the level of stresses and the material. At $\alpha = 0$, the family of curves converge to an equation of the type (1).

The applied relationship of life was experimentally checked on thin-walled tubular specimens ($\phi 14 \times 1$) of Kh18Ni10T steel in the case of coincidence of the lines of action of the principal stresses arising due to static and thermocyclic loading. The program of loading of the specimens was as follows :

1. Initial thermocycling, given the number of cycles in the interval (0.1 — 0.9) N_p , then static deformation up to failure.

Table

① Вид программы испытания	② Номер режима *)	③ Напряжение ползучести σ кг/мм ²	④ Деформация за цикл $\Delta \epsilon$ %	⑤ Параметр долговечности A_{cp} **)	⑥ Коэффициент суммирования α
I 	1	24	0,75	1,4	-
	2	18	1,2	1,7	-
	3	18	0,75	1,5	-
	4	14	1,2	1,27	+0,23
	5	14	0,75	1,02	0,0
	6	10	0,75	0,88	-0,12
II 	7	18	0,75	1,2	+0,17
	8	14	0,75	0,82	-0,18
	9	10	0,75	0,78	-0,20
III 	10	14	0,75	0,84	-0,14

Notes:

*) In each case, different versions of specimens (9-16 specimens) were tested for the given number of thermocycles (N_i) or creep time (τ_i)

**) This parameter was determined as the arithmetic average of all the tested specimens.

Key: 1- Form of the test program; 2- Number of case; 3- Creep stress (σ); kg/mm²; 4- Deformation for one cycle ($\Delta \epsilon$), %; 5- Life parameter (A_{av}); 6- Coefficient of summation.

2. Deformation under static loading, given the duration of application of load in the interval $(0.1 - 0.85)\theta_p$ then thermocycling up to failure.

3. Interchangeable application of thermocycling and static loading.

The conditions of testing under stresses and strains are given in the previous Table .

The static deformation was conducted under constant loading and a temperature of 600°C in the stress range of $10-24 \text{ kg/mm}^2$. The thermal fatigue was tested by heating a rigidly-fixed tubular specimen (the coefficient of rigidity is 4.6) by a current of industrial frequency and its cooling by compressed air, introduced in the internal cavity, with a zigzag cycle of temperature variation. The upper cycle temperature was constant (600°C), whereas the lower one was varied within the range of $100-300^\circ\text{C}$ to provide the failure of the specimens in the zone of the small cycle fatigue ($10^3 - 10^4$ cycles). In this case the deformation parameters of the cycle (in the calculated elastoplastic deformations) were used as principal parameters.

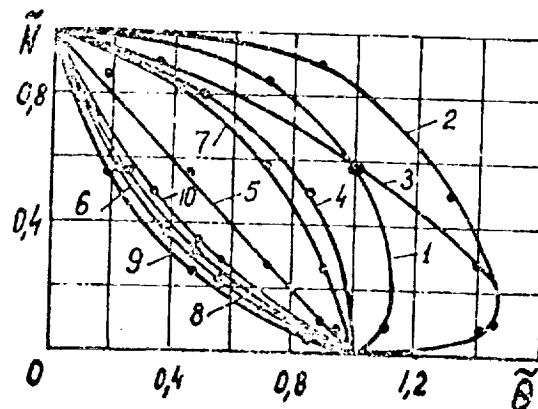


Fig. 1

The analysis of the results of the combined tests in all the three programs is shown in Fig. 1 in the form of life diagrams. These diagrams indicate that in the general case the summation of the relative lines does not follow the linear law.

The magnitude of the parameter of relative life varies widely in accordance with the test conditions (see the Table). In all the cases a drop in the relative life is observed with the decrease of the loading parameters of the tests (creep stresses and amplitudes of thermocycles). In the case of equal values of loading parameters (cases No. 5, 8 and 10) the test cases with initial creep lead most dangerously to the utmost drop of relative life. The life in the case of tests with interchangeable application of static and cyclic loading occupies an intermediate position.

The effect of the sequence of application of different loads (static and thermocyclic) is very clearly shown in the case of high values of test parameters, and less clearly pronounced with low values of these parameters.

The experimental results have shown that in the range of static loads below the thermal limit of steel yielding at 600°C, i.e. under the conditions when the creep process is actually realized, they are satisfactorily described by equation (2) with a deviation not exceeding 15%. In this case it is observed that the damages produced from creep and thermal fatigue are summed up. This process proceeds in the case of strainhardening and softening as compared with the linear law.

Under the conditions of creep of initially thermocycled specimens (the 1st program, cases No. 1, 2 and 3), for static load stresses of $\sigma \geq 18 \text{ kg/mm}^2$, the experimental results cannot be described by equation (2) due to the intensive strainhardening by thermocycling (increase of the absolute life) occurring basically inside the grains.

References

1. Tair, S. "Termicheskaya ustalost' v sochetanii s postoyannym mekhanicheskim napryazheniem" (Thermal fatigue in combination with a constant mechanical stress). --- Trudy 3-go Mezhdunarodnogo simpoziuma po konstruktsiyam i materialam, rabotayushchim pri vysokoi temperature, London, 1964.
2. Wood, D.S. The effect of creep on the high strain fatigue behaviour of a pressure vessel steel. "Weld. J.", No. 2, 1966.
3. Tulyakov, G.A., Yu. D. Starostin and V.A. Plekhanov, "Razrushenie stali Kh18NiOT pri kombinirovannom geistvii termicheskoi ustalosti i polzuchesti" (Failure of Kh18NiOT steel in the case of combined action of thermal fatigue and creep). --- "Nauchnaya publikatsiya TsNIITMASH", No. 325, 1971.
4. Langneborg, R. and R. Attermo. The effect of combined low-cycle fatigue and creep on the life of austenitic stainless steels "Met. Trans.", No. 2, No. 7, 1971.
5. Tulyakov, G.A. "Vliyanie nekotorykh ekspluatatsionnykh faktorov na soprotivlenie termicheskoi ustalosti kotel'noi stali" (The effect of some operational factors on the resistance of boiler steel to thermal fatigue). --- Trudy 10 Mezhdunarodnogo simpoziuma po zharoprochnym metallicheskim materialam ChSSR, 1971.

ABOUT THE UTILIZATION OF SAN-VENAN'S CRITERION FOR
THE ESTIMATION OF LIFE IN THE CASE OF THERMAL FATIGUE
UNDER THE CONDITIONS OF COMPLEX LOADING

By

G.A. Tulyakov and V.A. Metel'kov

In TsNIITMASH, some tests were conducted on austenitic steel (Kh18Ni10T) for the investigation of thermal fatigue under tension and compression when the deformations are given at a constant ratio of the angular and axial components. The tests were conducted on specially-prepared equipment [1]. The ratios are as follows :

$R_e = \frac{\Delta \gamma_{xy}}{\Delta \epsilon_x}$ (tension and compression), 0.7, 1.0, 1.5, 2.0, 5.0 and ∞ - (pure shear).

The failure criterion was taken as the number of cycles up to the formation of the first macrograde. In the case when the parameters are given in the range of 650 - 1500°C, the failure takes place in the range of $2 \times 10^2 - 2 \times 10^4$ cycles.

During testing the diagrams of thermocyclic deformation were recorded.

The obtained experimental data [2] on thermal fatigue at different

$R_e = \frac{\Delta \gamma_{xy}}{\Delta \epsilon_x}$ ratios have allowed to plot the relationship between the number of cycles and damage N in the form of paired functions on the variation of the axial and angular deformations for one cycle (see Fig. 1), which are approximated (in logarithmic coordinates) the straight lines and which can be described by the following equations :

$$\Delta \epsilon_x N^{K_1} = C_1, \quad (1)$$

$$\Delta \tau_{xy} N^{K_2} = C_2 \quad (2)$$

where K_1 , K_2 , C_1 and C_2 are constants.

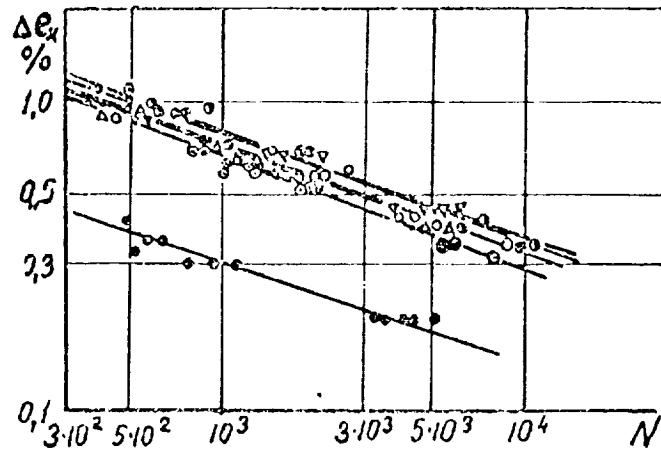


Fig. 1a

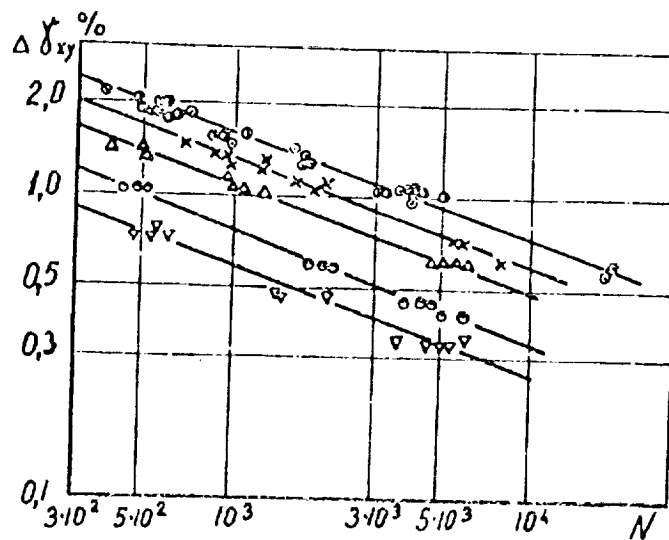


Fig. 1b

Curves of thermal fatigue

- a) with respect to axial deformation in one cycle;
 $\bullet - R_e = 0$, $\nabla - R_e = 0.7$, $\circ - R_e = 1.0$, $\nabla - R_e = 1.5$, $\circ - R_e = 2.0$, $\circ - R_e = 5.0$
- b) with respect to angular deformation in one cycle;
 $\circ - R_e = \infty$, $\circ - R_e = 5.0$, $\times - R_e = 2.0$, $\Delta - R_e = 1.5$, $\circ - R_e = 1.0$, $\nabla - R_e = 0.7$

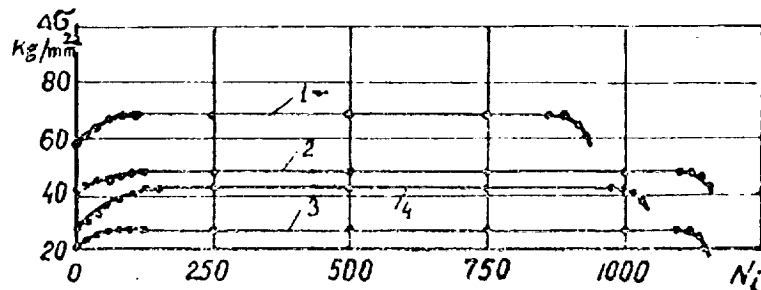


Fig. 2

Curves of the variation of stresses in one cycle with respect to the number of thermocycles.

- 1- tension (compression), $R_e = 0$; 2- torsion, $R_e = 5.0$;
3- tension (compression), $R_e = 5.0$; 4- pure shear, $R_e = \infty$.

Fig. 2 shows the variation of normal and tangential stresses in one cycle at different values of R_e . It is clear that after the lapse of a certain number of cycles (3-10% of that corresponding to failure) the stresses are stabilized and remain practically constant up to damage, whereas the values of the observed cyclic strainhardening along the tangential and normal directions are of the same order of magnitude ($\sim 9-16\%$).

Consequently, if we pay attention to the fact that the curves in Fig. 1 are practically parallel, it can be considered that the mechanism of plastic deformation is similar for the investigated cases and that in the course of the experiment the ratio $\Delta\tau_{xy} / \Delta\sigma_x$ (taken for the extreme points) will remain constant. This will permit to plot a generalized curve for the thermal fatigue using as a criterion for strength any parameter of the stress-strain state in accordance with the adopted hypothesis.

Since the failure in thermal fatigue is a process of accumulation and development of plastic deformations, then it is natural to assume that the most convenient criteria are the generalized conditions of San-Venan and Mises.

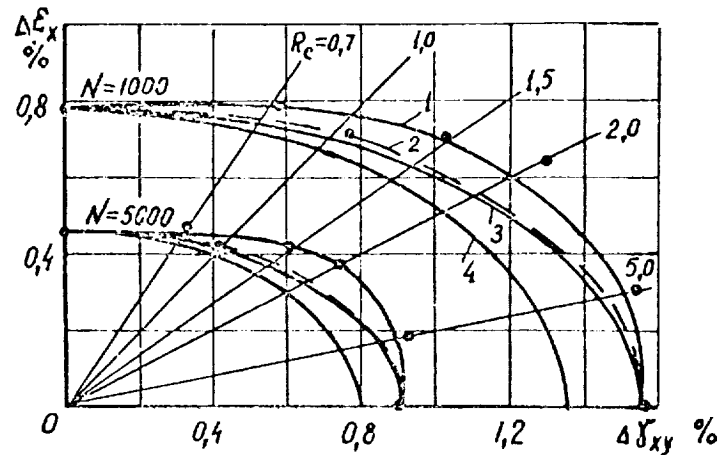


Fig. 3

Diagram of the limiting amplitudes of thermocyclic deformations; ● - experimental points, 1- curve calculated according to the equation $\Delta e_{eq}^2 = D^2 \Delta e_x^2 + \frac{1}{4} \Delta \gamma_{xy}^2$, 2- curve calculated according to Odling; 3 - curve calculated according to San-Venan; 4- curve calculated according to Mises.

Fig. 3 shows the diagrams of the limiting amplitudes of deformations for the 1000 and 5000 cycles before failure. It is clear that the experimental data are near to an ellipse corresponding to San-Venan's condition. This confirms the known proposition [3,4] that in the case of developed plastic deformations San-Venan's condition describes the experiment better than Mises's condition.

However, by examination of Fig. 3 it can be noted that there is no full correspondance of San-Venan's condition to the experiment for the determined values of the coefficient of deformation. This is apparently explained, first of all by the fact that in the process of thermocyclic deformation the initial properties of the material will vary, i.e. in each N_k cycle we have a material whose physicomachanical properties differ from the properties of the material in the N_{k-1} cycle. A metallographic research work was conducted for illucidation of the possibility of activation of the new processes in the case of variation of the type of the stress state in the structure of the material. The results of this work have proved the absence of any processes different from those observed in the case of a linear uniaxial stress state.

Apparently, such factors as: the anisotropy of material in microvolumes (it was not observed in macrovolumes), the locality of flow of

the processes of plastic deformation, and the noncoincidence of the principal axes of stresses and principal deformations, have an influence on the character of flow of the process of plastic deformation under the conditions of complex stresses and thermal fatigue, as well as on the experimental results.

Consequently, for a more precise estimate of the criteria of thermal-fatigue failure in the case of a plane stress state, a parameter taking into consideration the behaviour of the material in the process of thermocyclic deformation should be included.

In his time, Odling [5] suggested to correct San-Venan's condition by the corresponding coefficients for the consideration of structural factors and the nonhomogeneity of distribution of stresses related with them. These coefficients take into consideration the different effects produced by the action of the tangential stresses.

The utilization of Odling's theory, transformed in deformation, did not produce the required effect (see Fig. 3). The observed deviation is apparently due to the nonhomogeneity of the flow of plastic deformation, as well as to the strainhardening of the material in the process of "complete deformation".

Taking into consideration the last factor, the condition of strength can be written in the following form :

$$\Delta e_{eq.}^2 = D^2 \Delta e_x^2 + \frac{1}{4} \Delta \gamma_{xy}^2, \quad (3)$$

where

$$D = \frac{\Delta \gamma_{oxy}}{2 \Delta e_{ox}} \frac{1}{(1+\eta)}$$

$\Delta \gamma_{oxy}$ and Δe_{ox} are deformations in the case of limited (by the number of cycles) ranges of fatigue, corresponding to the case of pure shear as well as to tension and compression; η is the relative value of strain-hardening (in our case $\eta \approx 0.12$).

As shown in Fig. 3, the corrected curve obtained by calculation, coincides quite well with the experiment. This allows to utilize the suggested criterion for the calculation of the life of material in the case of thermal fatigue under the conditions of complex stresses according to the following equation :

$$\Delta e_{eq.} \times N^{K_3} = C_3, \quad (4)$$

where $\Delta e_{eq.}$ is determined from equation (3), and K_3 and C_3 are constants .

It was shown experimentally that for Kh18NiOT steel, in the case of a maximum cycle temperature of 650°C, the values of the constants in equation (4) are $K_3 = 0.34$ and $C_3 = 8.7$.

References

1. Tulyakov, G.A., V.A. Plekhanov and V.A. Metel'kov, "Problemy prochnosti" (Problems of strength). --- No. 6, 1972.
2. Tulyakov, G.A. and V.A. Metel'kov, "Problemy prochnosti" (Problems of strength). --- No. 7, 1972.
3. Ratner, S.I. "Prochnost' i plastichnost' metallov" (Strength and plasticity of metals). --- Moskva, Gosoborongiz, 1949.
4. Mitrokhin, N.M. and Yu. I. Yagn. --- Dokl AN SSSR, 135 (4), 1965.
5. Oding, I.A. "Dopuskaemye napryazheniya v mashinostroenii i tsiklicheskaya prochnost' metallov" (Permissible stresses in machinery, and cyclic strength of metals). --- Moskva, Mashgiz, 1944.

ABOUT ONE POSSIBILITY FOR THE DESCRIPTION OF THE
LAWS OF CREEP

By
I. I. Trunin

It was previously shown [1-3] that, from the mathematical point of view, many relationships obtained in the analysis of various physical models of development of plastic deformations and failure under the conditions of creep [4-6], are particular cases of one equation, which for the minimum creep rate and failure time can be correspondingly represented in the following form :

$$\dot{\epsilon} = B T^{-2} \sigma_0^n \exp \left[- \frac{u_0 - \gamma \sigma_0}{RT} \right] , \quad (1)$$

$$\tau_k = A T^2 \sigma_0^{-m} \exp \left[\frac{H_0 - \mu \sigma_0}{RT} \right] , \quad (2)$$

where $\dot{\epsilon}$ is the minimum or average creep rate; τ_k is the time of failure; T is the absolute temperature; R is the gas constant; σ_0 is the nominal stress; $A, B, m, n, \gamma, \mu, H_0$ and u_0 are parameters characterizing the individual features of the material.

Usually, the creep tests, particularly on complex heat-resistant alloys and steel, are conducted under a constant load. Consequently, in utilization of σ_0 in equations (1) and (2) it is necessary to take into consideration the variation of the cross sectional area F_0 due to creep deformation.

The even plastic strain ϵ leads to the decrease of F_0 and, consequently, to the increase of σ_0 by e^ϵ times.

$$\sigma = \sigma_0 e^\epsilon \quad (3)$$

The effect of plastic strain on the rate of creep is not limited by the increase of nominal stresses: the plastic deformation leads to strainhardening as well as to softening, and stimulates the development of failure.

The resultant value of plastic deformation consists of an active component arising in the specimen with the application of load, (ϵ_e) and a passive component induced in the process of creep (ϵ_p)

$$\epsilon = \epsilon_e + \epsilon_p$$

Each of the components of plastic deformation can influence the development of creep [4] in many ways, i.e. it is convenient to express the role of each part in terms of independent parameters.

The resultant influence of the factors of softening and the development of damages can be represented by the introduction of a constant parameter " ω " in equation (3).

$$\sigma = \sigma_0 e^{\omega \varepsilon} \quad (4)$$

In reference [4] it was shown that the effect of the strainhardening factors can be very precisely represented by the introduction of a term of the form $\varepsilon^{-\alpha}$ in the equation of creep rate.

Therefore, the equation of the type (1), in which the creep rate in the yield point of the curve (see Fig. 1) is introduced instead of the minimum rate, can be represented in the following form :

$$\begin{aligned} \dot{\varepsilon} = & B T^{-2} \sigma_0^n (\varepsilon_0 + \varepsilon_p)^{-\alpha} \exp[n(\varepsilon_0 + \omega \varepsilon_p)] \cdot \\ & \cdot \exp\left[-\frac{u_0}{RT}\right] \cdot \exp\left[\frac{T \sigma_0}{RT} \exp(\varepsilon_0 + \omega \varepsilon_p)\right] \end{aligned} \quad (5)$$

Equation (5) is one of the possible forms of the equation of state [4]. The parameters of this equation reflect the influence of the basic factors determining the physical laws of the process:

u_0 represents the effective activation energy of creep occurring in the macrovolumes of the material, B is the parameter representing the effect of interatomic distance, period of thermal vibrations of atoms and entropy of state [7, 8, 9, 10], γ is the activation volume of the creep process in the macrovolumes of the material, α is a parameter representing the resultant effect of strainhardening factors, ω is a parameter representing the resultant influence of the softening factors and the development of microdamages.

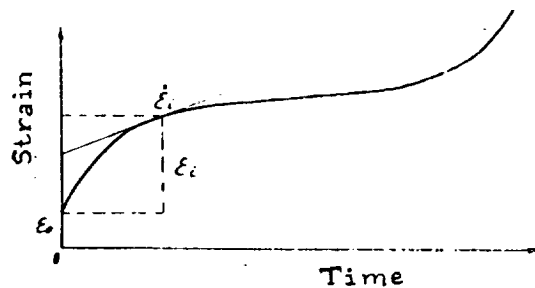


Fig. 1

Initial creep curve at $T = \text{const}$ and $\sigma_0 = \text{const}$.

The results of the creep tests (each point is determined by T , σ_0 , $\dot{\epsilon}$, ϵ_0 and ϵ_p) were mathematically treated in some range of temperatures and stresses. Therefore, the optimum values of the six parameters of equation (5) were obtained. This equation characterizes the structural condition, and represents statistically the role of the basic micromechanisms in the development of plastic deformation and damages in the macrovolumes of the material.

The experimental data providing the determination of the values of coefficients were treated by the method of least squares using a digital computer.

By getting the value of the six parameters of equation (5) it will be possible to describe the creep process in all its stages. Integrating equation (5) at $T = \text{const}$, $\sigma_0 = \text{const}$ and $\epsilon_0 = \text{const}$, we get an expression for the determination of time, in the course of which the creep deformation attains a value of ϵ

$$\tau_c = B^{-1} T^2 \sigma_0^{-n} \exp \left[\frac{U_0}{RT} - n \epsilon_0 - \frac{T \sigma_0}{RT} \exp(\epsilon_0) \right] \times$$

$$\times \int_0^{\epsilon} (\epsilon_0 + \epsilon_p)^{\alpha} \exp \left\{ - \left[\frac{T \sigma_0}{RT} \exp(\omega \epsilon_p) - n \omega \epsilon_p \right] \right\} d\epsilon \quad (6)$$

It is possible to conduct the necessary calculations for plotting the initial creep curves by the method of numerical integration using the digital computer.

Processing and analysing the results of testing perlitic as well as austenitic steels has shown that the values of the parameters of equation (5), determined according to the elaborated program, represent, to a sufficient degree of accuracy, the laws of creep.

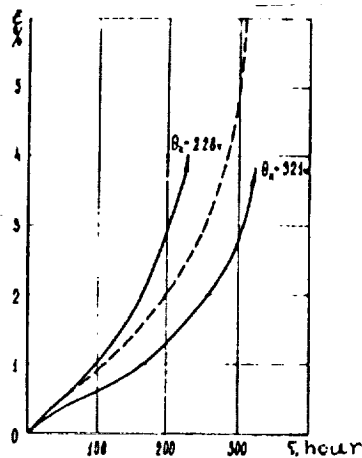


Fig. 2

Initial creep curves: 15KhIMF steel, $t_{\text{test}} = 540^\circ\text{C}$ and $\sigma_0 = 32 \text{ kg/mm}^2$,
— experimental curves, --- calculated curve.

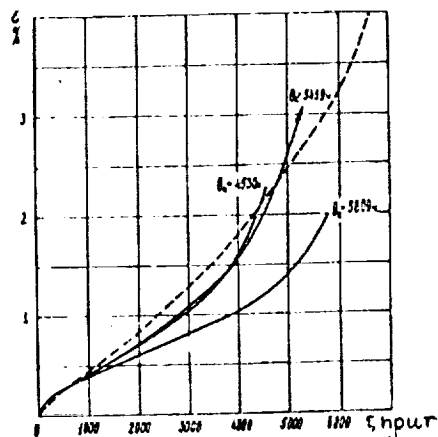


Fig. 3

Initial creep curves: 15KhIMF steel, $t_{\text{test}} = 565^{\circ}\text{C}$ and $\sigma_0 = 20 \text{ kg/mm}^2$,
— experimental curves, --- calculated curve.

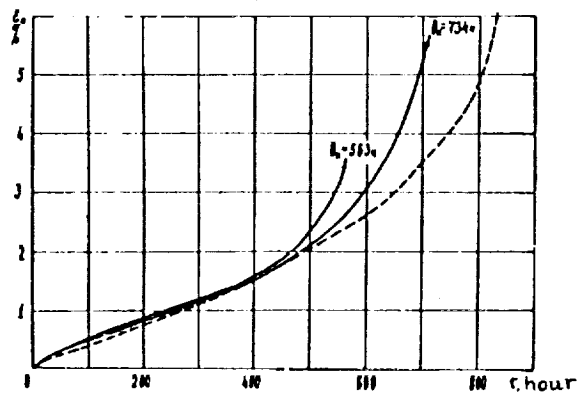


Fig. 4

Initial creep curves: 15KhIMF steel, $t_{\text{test}} = 585^{\circ}\text{C}$ and $\sigma_0 = 24 \text{ kg/mm}^2$,
— experimental curves, --- calculated curve.

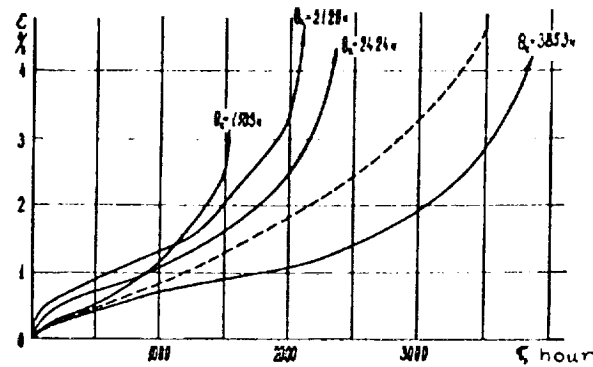


Fig. 5

Initial creep curves: 15KhIMIF steel, $t_{\text{test}} = 585^{\circ}\text{C}$ and $\sigma_0 = 20 \text{ kg/mm}^2$,
 — experimental curves, --- calculated curve.

For example, the experimental creep curves of steel of the perlitic type (mark 15KhIMIF) are shown in Fig. 2-5. The tests were conducted at three levels of temperature, and 3-4 specimens were tested in each case (at $T = \text{const}$ and $\sigma_0 = \text{const}$).

The parameters of equation (5) were determined from the results of the tests at the following four temperatures: 540, 565, 585 and 610°C . In Fig. 2-5, the solid lines represent the experimental creep curves, whereas the dotted lines represent the corresponding calculated curves, plotted according to the following equation

$$\dot{\epsilon} = \exp(12,92) T^{-2} \sigma_0^{6,35} (\epsilon_0 + \epsilon_p)^{2,4} \exp[6,35(\epsilon_0 + 7,5 \epsilon_p)] \cdot \\ \cdot \exp\left(\frac{29312}{T}\right) \exp\left[\frac{7260}{T} \exp(\epsilon_0 + 7,5 \epsilon_p)\right].$$

The data in Fig. 2-5 allow to note that in all the cases the calculated curves represent, to a sufficient degree of accuracy, the development of fatigue in all the stages of the process.

Consequently, it is possible, in a certain range of temperatures and stresses to utilize the constant values of the parameters of equation (5) for the description of the creep process.

If the parameters of equation (5) are separately determined for different stages of creep, it will be possible to obtain additional information about the accumulation of damages and activation energy in the different stages of creep.

Assuming in equation (6) that $\epsilon = \epsilon_k$ (the creep deformation prior to failure), it will be possible to determine the corresponding life (τ_k). In utilization of equation (2) it is implicitly assumed that the value of plastic deformation in failure is constant. The deviation of the individual values of ϵ_p from the mean values is often insignificant. Therefore, by the aid of equations (1) and (2), it is possible to obtain quite reliable estimates. In those cases, when the indicated condition is not fulfilled (for example, the value of ϵ_k decreases with the increase of service life and decrease of σ_0), equation (2) can give a low estimate of the mean life, i.e. the factor of safety is increased.

References

1. Trunin, I.I. "Problemy prochnosti" (Problems of strength). --- No. 6 : 3-8, 1969.
2. Trunin, I.I. --- "Energomashinostroyeniye", No. 9 : 28 - 31 , 1970 .
3. Trunin, I.I. and E.A. Loginov . --- "Mashinostroyeniye", No. 2 : 66 - 74 , 1971 .
4. Rabotnov, Yu.N. "Polzuchest' elementov konstruktsii" (Creep of elements of construction). --- "Nauka", Moskva , 1966.
5. Garofalo, F., "Zakony polzuchesti i dlitel'noi prochnosti metallov i spalovov" (Creep laws and creep strength of metals and alloys). --- Metallurgia, 1968.
6. Sbornik: pod red. Dorna "Mekhanicheskie svoystva materialov pri novyshennykh temperaturakh" (Mechanical properties of materials at elevated temperatures)... "Metallurgiya" , 1965 .
7. Pines, B.Ya., "Ocherki po metallofizike" (Essays on the physics of metals). --- Kar'kov Kar'kovsk. gos. un-T, 1961 .
8. Geguzin, Ya.E., "Mikroskopicheskie defekty v metallakh" (Macroscopic defects in metals). --- Metallurgizdat, Moskva , 1962.
9. Gurevich, L.E. and V.I. Vladimirov. --- "Fiz. tverdogo tela", II (8), 1960.
10. Pranka, T. and V. Foldyna . The creep properties of low-alloy Cr-Mo-v steels with low carbon content. "The Iron and Steel Institute Publication 97 High - temperature properties of steel", 1967.

THE EFFECT OF THE STRUCTURE OF MATERIAL ON CREEP STRENGTH

By

V.D. Kurov, G.P. Mel'nikov and A.A. Sokolov

One of the possible methods of description of life under the conditions of creep consists in the introduction of the parameters of state when a certain relationship is drawn between temperature, initial grain size in the structure of the material, level of stresses and failure time

$$\tau = f(\sigma, t, d) \quad (1)$$

In the TsNII TMASH, investigations were conducted for the determination of the creep strength of Kh18N12T steel under steady state conditions and different grain sizes in the temperature range of 600-650°C [1]. The average experimental results are given in Table 1.

For the estimation of the material and solution of the optimization problem, let us utilize the method of statistical planning of the experiments. The use of progressive analysis in the treatment of the results allows to determine the extreme values of the parameters of the process model. For establishing the plane, the curves of creep strength, extrapolated from the data included in Table 1, were used.

Moreover, the results of the creep strength experiments were introduced. These experiments were conducted under variable temperature-loading conditions on tubular specimens of Kh18N10T steel with different initial structure.

The factorial experiment 2^3 [2] lies in the foundation of the utilized method of statistical planning, i.e., three parameters are varied on 2 levels of each.

temperature : $t = 600$ and 650°C ,
stress : $\sigma = 20$ and 24 kg/mm^2
grain size according to GOST No. : $d = 7-6$ and $3-2$.

In the factorial space, the variables are replaced in the following form :

$$x_j = \frac{z_j - z_{j0}}{\Delta_j}, \quad (2)$$

where x_j is the coordinates of the experimental points in the new system;

z_j is the initial coordinates corresponding to the natural values of the parameters;

z_{j0} is the basic level of the factor;

Δ_j is the interval of variation.

Table 1

① Тем-ра испытан. $t^{\circ}C$	② Напряжение σ кг/мм ²	③ Величина зерна, d, балл ГОСТ	④ Время разруше- ния τ , час
600	24	7 - 6	178 208 124
		4 - 5	796 1001
		3 - 2	679 712
	26	7 - 6	158 158
		4 - 5	743 654
		3 - 2	1258 1300
	28	7 - 6	45 74
		4 - 5	340 461
		3 - 2	351 536
650	16	7 - 6	679 503
		4 - 5	673 925
		3 - 2	460 1100
	18	7 - 6	181 242
		4 - 5	504 569
		3 - 2	479 618
	20	7 - 6	70 98
		4 - 5	127 225
		3 - 2	182 207

Key: 1- Test temperature, $t^{\circ}C$; 2- Stress, σ kg/mm²; 3- Grain size, d, according to GOST No; 4- Time of failure τ , hours.

As a result, we have :
for the temperature

$$x_1 = \frac{t - 625}{25} ; \quad (3)$$

for the stress

$$x_2 = \frac{\sigma - 22}{2} \quad (4)$$

for the grain size

$$x_3 = \frac{d - 5}{2} \quad (5)$$

The obtained values of the new variables have the property of orthogonality, and are represented in a matrix form in Table 2.

If the symbols of the new parameters indicate the transformed values of the initial parameters, the following regression equation will be obtained :

$$Y = b_0 + b_1 x_1 + b_2 x_2 + b_3 x_3 + b_4 x_4 + b_5 x_5 + b_6 x_6 + b_7 x_7 \quad (6)$$

where the values of the coefficients of equation (6) are determined from the following equation :

$$b_i = \frac{\sum_{j=1}^m x_j Y_j}{\sum_{j=1}^m x_j^2} , \quad (7)$$

where m is the number of experimental points;

j is the number of variables in the regression equation.

From the solution of equation(7) and transformation of equation(6) , the regression equation can be converted to the following final form:

$$Y_{cal.} = \tau_{scan} = 788 - 687x_1 - 533x_2 + 457x_3 + 491x_1x_2 - 321x_2x_3 - 417x_3x_1 + 304x_1x_2x_3. \quad (8)$$

For the investigation of the surface of equation (8) it is necessary to solve the system of nonhomogeneous equations :

$$\left. \begin{aligned} 491x_2 - 417x_3 + 304x_2x_3 &= 687 \\ 491x_1 - 321x_3 + 304x_1x_3 &= 533 \\ -321x_2 - 417x_3 + 304x_1x_2 &= 457 \end{aligned} \right\} \quad (9)$$

Table 2

№ № точек (1)	X_0	X_1	X_2	X_3	X_4 X_1X_2	X_5 X_2X_3	X_6 X_3X_1	X_7 $X_1X_2X_3$	② \bar{Y} эксп. по 2-м точк.	③ \bar{Y} расч.	④ % расхожд.
1	1	1	1	1	1	1	1	1	80	82	2,5
2	1	1	-1	1	-1	-1	1	-1	200	197	1,5
3	1	-1	1	1	-1	1	-1	-1	700	700	0
4	1	-1	-1	1	1	-1	-1	1	4000	3998	0
5	1	1	1	-1	1	-1	-1	-1	35	36	3
6	1	1	-1	-1	-1	1	-1	1	85	88	2,5
7	1	-1	1	-1	-1	-1	1	1	200	202	1,0
8	1	-1	-1	-1	1	1	1	-1	1000	1000	0
8	0	0	0	0	0	0	0	0	6300	6313	
8	8	8	8	8	8	8	8				

Key: 1- Number of points; 2- Average of $\bar{Y}_{\text{exper.}}$ for two points; 3- $\bar{Y}_{\text{calc.}}$; 4- Percentage deviation.

The solution of system (9) gives the values of the unknowns corresponding to the least life :

$$x_1 = 0.62 ; \quad x_2 = 1.5 ; \quad x_3 = -1.74 ;$$

which denotes that $t = 640.5^\circ\text{C}$; $\sigma = 25 \text{ kg/mm}^2$; $d = 8.5$ on the GOST scale.

For checking the influence of the structural state of the material of construction on creep strength under the conditions of varying the duty of the type "starting-stoppage" [3], tests were conducted on tubular specimens (36 x 1.0), made of Kh18N10T steel, under an internal pressure and a temperature of 750°C . The tests were conducted on specimens with an initial structural material corresponding to the 6-7 state of delivery on the GOST scale and heat-treated in vacuum (10 mm mercury column) at a temperature of 1100°C in the course of 2 hours, which corresponded, as a result, to a structure with a grain size of 4.

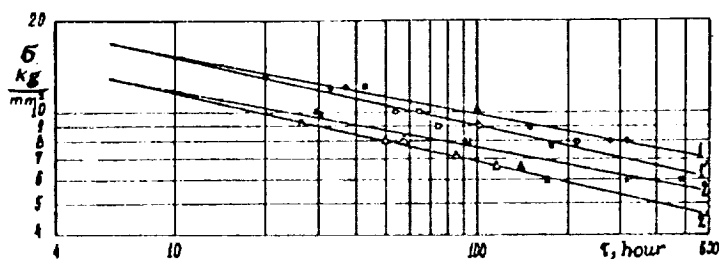


Fig. 1

Creep strength curves: 1- steady duty, heat-treated specimens; 1'- variable duty in the course of 6 hours; 2- steady duty, untreated specimens; 2'- variable duty in the course of 6 hours.

For each pair of the obtained curves (see Fig. 1) it is possible to derive a relationship for life in the case of a variable duty

$$\tau_{\text{var}} = \tau_{\text{const}} \left(\frac{\sigma}{\sigma_0} \right)^{n_1 - n_2} \quad (10)$$

where σ_0 is the level of stress corresponding to the point of intersection of the curves of steady and variable cases of loading.
 n_1 and n_2 are constants characterizing the inclination of the curves of creep strength.

The comparison of the experimental results have shown that the life of specimens with large-grain structure significantly increases. A condition of the type "starting-stoppage", decreases the service life of the material as compared with the steady duty case. The angle of deviation of the curves of creep strength for specimens with an initial structure of the material (6-7 on the GOST scale) is larger than for the heat-treated specimens. This shows the low performance capacity of the construction material with a small grain size. This is clear from the graph and the following relationships :

$$\begin{aligned}\tau_{var} &= \tau_{const} \times \left(\frac{\sigma}{\sigma_{01}}\right)^{0.05} \\ \tau_{var} &= \tau_{const} \times \left(\frac{\sigma}{\sigma_{02}}\right)^{0.78}\end{aligned}\quad (11)$$

where the first equation corresponds to curve 1', whereas the second one corresponds to curve 2'.

References

1. Tykochinskaya, T.V. "Vliyanie razmera zerna na kharakteristiki zharoprochnosti stali Kh18N12T pri razlichnoi temperature" (The effect of grain size on the character of heat resistivity of Kh18N12T steel at different temperatures). --- Tr. TsNIIITMASh. Issledovanie zharoprochnykh materialov dlya teploenergetiki, Moskva, 87-88, 1969.
2. Ruzinov, L.P. "Regressionnyi analiz i statisticheskoe planirovanie eksperimentov" (Regressive analysis and statistical planning of experiments). --- Moskva, Giredmet, 1966.
3. Mel'nikov, G.P. "Nekotorye osobennosti raboty tonkostennykh trub iz stali Kh18N10T v usloviyakh vysokotemperaturnoi polzuchesti" (Some aspects of operation of thin-walled tubes of Kh18N10T steel under the conditions of creep at elevated temperatures). --- Moskva, Atomizdat, 1968.

THE EFFECT OF HYDROSTATIC COMPRESSION ON POROUS MATERIALS

By

A.M. Lokoshchenko and E.A. Myakotin

The analysis of the process of packing of different media has been the subject of the study in many works [1-3]. In these works, experimental investigations were basically conducted, where the specimens were loaded in a closed space by a moving piston, or in an elastic shell by hydrostatic compression. The last method has proved to be extremely effective, in particular, for the increase of the strength of cement stone [4], namely, in the case when its initial porosity is very high.

Different empirical formulae were suggested for the description of the relationship between the density of pressing ρ and the magnitude of pressure. The following are the most reliable formulae :

$$\rho = \rho_{max} - B e^{-a p} [2] \quad \text{or} \quad \rho = \rho_0 \frac{1 + a p}{1 + b p} [3] \quad (1)$$

A theoretical model of the process of packing of a porous material (the initial porosity may be tens of hundredths) is described below. This model allows to draw the relationship between a certain density parameter of the system and the external hydrostatic pressure. It is convenient to use the relative density v (i.e. the ratio of the volume of the solid phase to the overall volume) as the density parameter.

The model is based on the assumption of correct packing of equal isotropic incompressible balls of very small radii, and of the independence of the density of packing of the form of the boundary surface. The simple cubic and pyramidal forms are considered. These forms, which are known systems of regular packing of equal balls, are supposed to have limiting values of density [5]; their relative density is $v_{cr} = \pi/6 \approx 0.52$ and $v_{pr} = \pi/3\sqrt{2} \approx 0.74$, respectively. If on the surface, limiting the system of balls, a hydrostatic pressure p is applied, then contact forces N will be exerted between the balls. From the condition of symmetry, these forces should be equal to each other and should be directed along the lines of centres. Contact areas are formed around the initial points of contact as a result of these forces. In addition, these areas are located in planes perpendicular to the centres lines, and represent circles with radii a . As in [6] it will be considered that apart from the contact areas the surface of the spheres will maintain its spherical form. Therefore, as a result of deformation, each ball with an initial radius R_0 will acquire a spherical form of a radius $R > R_0$, with a number of n "cut" spherical segments equal to the number of contacts (for cubic

packing, $n = 6$, and for pyramidal packing, $n = 12$). Figs. 1 and 2 show the elementary cells cut from the corresponding cubic and pyramidal packages.

From the condition of incompressibility of the balls material it is possible to draw the relationship between the current ball radius and the dimensions of the contact areas. Denoting the volume of the ball segment by V , the condition of incompressibility can be expressed in the following form :

$$\frac{4}{3}\pi R^3 - nV = \frac{4}{3}\pi R_0^3. \quad (2)$$

By analysing the elementary cells it is possible to calculate the relative density after deformation. Taking into consideration the condition of incompressibility (2), it is possible to determine the relationship between the relative density of the system and the degree of deformability of each ball element. Let us denote the degree of deformability by $A = a/R$ (a = the radius of the contact area and R = the radius of the ball element). Accordingly, we get :

$$\frac{v}{v_{cr}} = \frac{4.5}{1-A^2} - \frac{2}{(1-A^2)^{3/2}} - 1.5, \quad (3')$$

$$\frac{v}{v_{pr}} = \frac{9}{1-A^2} - \frac{5}{(1-A^2)^{3/2}} - 3 \quad (3'')$$

there and further on, the case of cubic packing will be denoted by ('), whereas that of pyramidal packing will be denoted by (').

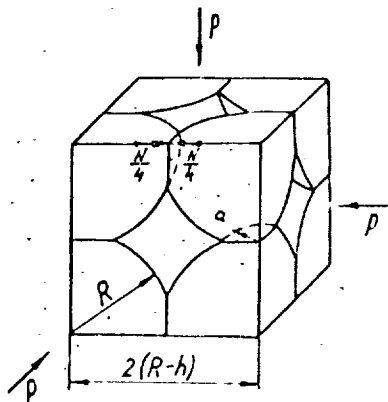


Fig. 1

Elementary cell of cubic packing in the process of deformation by hydrostatic compression.

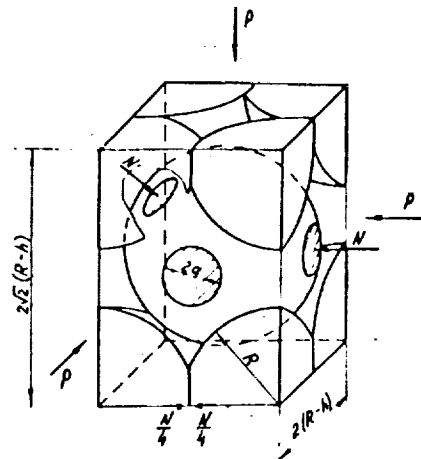


Fig. 2

Elementary cell of pyramidal packing in the process of deformation by hydrostatic compression.

The relationship between the hydrostatic pressure p , the contact force N and the parameter A is derived from the condition of equilibrium of elementary cells

$$N = 4pR^2(1-A^2) , \quad (4')$$

$$N = \sqrt{2}pR^2(1-A^2) . \quad (4'')$$

Each of the systems (3') - (4') and (3'') - (4'') will be closed if it is supplemented by the relationship between the contact force N and the geometric parameter A . This relationship is determined by the type of the stress-strain diagram of the balls material. Let us assume that the diagram has the form of an "elastic-ideal plasticity". Moreover, we may neglect the elastic deformations in the plastic zone.

For the zone of elastic deformation we may assume, as a first approximation, that for each contact area the relationship between its radius a and the contact force N follows the relationship of Herz [7]

$$a^3 = \Theta NR , \quad \Theta = \frac{3(1-\nu^2)}{4E} , \quad (5)$$

where Θ is a property characteristic of the material, determined by Young modulus (E) and Poisson's coefficient (ν) (since it is assumed that the balls material is incompressible, then $\nu = 0.5$).

Let us introduce the dimensionless pressure parameter $q = p\Theta$ and determine the relative density φ as a function of q . For this purpose, we get from equation (5) :

$$N = \frac{R^2 A^3}{\Theta} \quad (6)$$

Solving equation (6) together with equations (4') and (4'') we get :

$$q = \frac{1}{4} \frac{A^3}{1-A^2} \quad (7')$$

$$q = \frac{1}{\sqrt{2}} \frac{A^3}{1-A^2} \quad (7'')$$

The pairs of equations (3') - (7') and (3'') - (7'') transform the relationship between the relative density φ and the dimensionless pressure q , for the cubic and pyramidal packages in the case of ideally elastic balls, into a parametric form.

For an ideally plastic material it is assumed that the contact force is proportional to the contact area

$$N = \kappa \pi a^2 , \quad (8)$$

where K is a constant characterizing the resistance of the ball material to plastic deformation. Such a hypothesis is based, to a certain extent, on the solution of Prandtl's problem [8] about the pressing of a flat stamp into a plastic medium, where K (the yield limit) = $(2 + \frac{1}{2})K$. Moreover, the elastoplastic contact of spherical elements was analysed in reference [9]. It was stated that in the case of very high contact stresses, when almost the whole contact area is occupied by the zone of plastic flow, the magnitude of deformation is proportional to the contact force which is similar to (8). In [10], the results of the experimental investigation of large local elastoplastic deformations are given for the case of axial compression of a bar with a spherical end by a rigid plate. The relationship between the value of deformation h and the compressive force N determined in the statistical tests, is approximated by the equation $h = \kappa N^n$. For duraluminium specimens a value of $n = 1.15$ was obtained, i.e. a value very close to unity, which is also in accordance with (8).

Let us introduce a dimensionless parameter characteristic of the material

$$D = \frac{1}{9\pi K \theta} \quad (9)$$

Taking (9) into consideration, equation (8) will acquire the following form :

$$N = \frac{1}{D \theta} a^2 \quad (10)$$

In accordance with the previously mentioned assumptions, the relationship between A and q was obtained for ideally plastic materials by solving equation (10) together with each of the equations (4') and (4'').

$$\frac{A^2}{1 - A^2} = 4 D q \quad (11')$$

$$\frac{A^2}{1 - A^2} = \sqrt{2} D q \quad (11'')$$

The pairs of the equations (11'), (3') and (11''), (3'') transform the relationship between v and q , for the cubic and pyramidal packages in the case of ideally plastic balls, into a parametric form. However, we have in this case, as distinguished from the case of elastic balls, the possibility of deriving this relationship in a clear form. Excluding A , we get :

$$v/v_{cr} = 4.5(1 + 4 D q) - 2(1 + 4 D q)^{3/2} - 1.5, \quad (12')$$

$$v/v_{pr} = 9(1 + \sqrt{2} D q) - 5(1 + \sqrt{2} D q)^{3/2} - 3. \quad (12'')$$

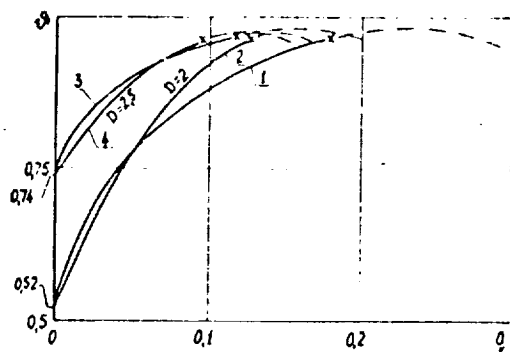


Fig. 3

Theoretical curves showing the relationship between the relative density v and the dimensionless hydrostatic pressure q . For cubic packing : 1- balls of an ideally elastic material, 2- balls of an ideally plastic material; for pyramidal packing : 3- balls of an ideally elastic material, 4- balls of an ideally plastic material.

The results of calculation of the process of packing of cubic and pyramidal forms are graphically represented in Fig. 3. Curve 1 denotes cubic packing of ideally elastic spheres, and curve 2 denotes the same but for ideally plastic spheres (for the parameter $D = 2$). It is clear that for ideally elastoplastic spheres the initial part of the actual curve will practically coincide with curve 1, whereas in the zone of high densities, it will coincide with curve 2 at the corresponding value of the parameter D . For the case of pyramidal packing the corresponding curves are denoted by the following numbers : 3- ideally elastic balls; 4- ideally plastic balls (for $D = 2.5$). The asterisks on the curves denote the points corresponding to the moment when the neighbouring contact areas on one ball coincide with each other. Beyond these points, the curves are devoid of any physical meaning, since the initial relationships are violated. It would have been possible to take into consideration the change of the form of the contact area and extend the obtained curves in the zone of higher densities. But since the obtained limiting points correspond to $v \approx 0.96$, this will denote practically the attainment of a zero porosity; therefore, there will be no need for any further analysis.

The effect of hydrostatic compression on a porous material was experimentally investigated on a test rig, in the operating chamber of which it is possible to create and maintain a hydraulic pressure of up to 1000 kg/cm^2 [11]. The scheme of the operation chamber of the rig is shown in Fig. 4.

For the preparation of porous specimens, portland cement of the marks 200 and 400 was taken without the addition of sand and coarse aggregates. The addition of water was conducted at maximum water-cement ratios, near to the water maintaining capacity of the taken cements. The specimens were extracted from the moulds after 24 hours and kept in the air at room conditions up to the moment of conducting the tests. These specimens had the form of cylinders of 4 cm diameter and 8 cm height. Before compression each specimen was isolated from the compressing liquid by a rubber sheath. Three types of specimens were subjected to testing :

- I- cement mark 200, squeezed 3 years after manufacture;
- II- cement mark 200, squeezed 72 hours after manufacture;
- III- cement mark 400, squeezed 72 hours after manufacture.

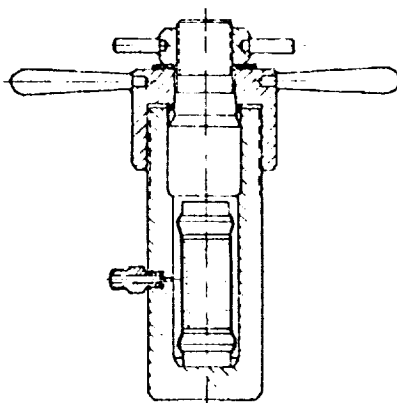


Fig. 4

Operating chamber for testing the specimens by hydrostatic compression.

Up to the moment of testing, all the specimens had a relative density of 0.44 - 0.56. The relative density was determined by the method of water-suspension in vacuum. The squeezing of all the specimens lasted for 20 minutes. The compression in the chamber was given in the range of 50 to 1000 kg/cm².

Equation (12') was used to describe the relationship between the relative density ν of cement stone subjected to hydrostatic compression and the magnitude of the dimensionless pressure q applied in that case. This equation was obtained for cubic packing of ideally plastic balls.

As a result of testing the three types of specimens the following initial values of relative density (ν_1), compressive strength (R_c), modulus of elasticity (E_c), pressure at the beginning of plastic deformation (q_n) and the dimensionless parameter characteristic of material (D), were determined from equation (9):

① № серия	I	II	III
ν_1	0,53	0,44	0,56
R_0 кг/см ² ②	84	43	160
E_0 кг/см ² ②	$4,3 \cdot 10^4$	$0,87 \cdot 10^4$	$7 \cdot 10^4$
q_n	$2 \cdot 10^{-3}$	0	$1,2 \cdot 10^{-3}$
D	5,6	2	24

Key: 1- Type of specimen; 2- kg/cm².

Actually, for the specimens of the second type (II) the value of q_n should be different from zero. But since the value of their initial strength was only ~ 40 kg/cm², it was found that $q_n < 10^{-3}$. In the given case, this quantity can be neglected.

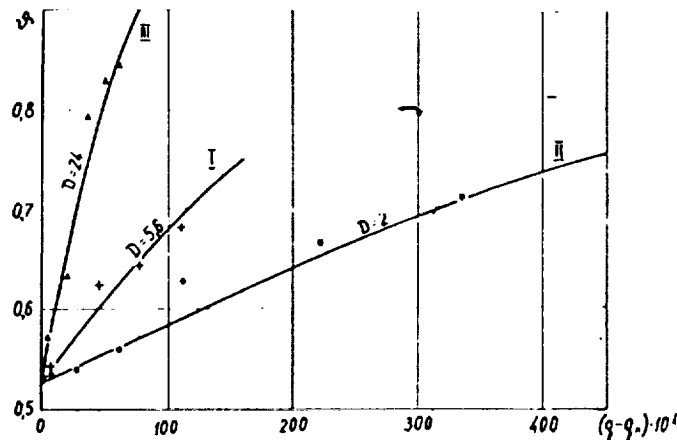


Fig. 5

Variation of the relative density of cement stone specimens as a result of hydrostatic compression: I (+) - specimens of cement, mark 200, three years curing period; II (•) - specimens of cement, mark 200, 72 hours curing period; III (▲) - specimens of cement, mark 400, 72 hours curing period. The solid lines represent the theoretical curves.

In Fig. 5 the theoretical curves of $\nu \sim (q - q_n)$ are compared with the experimental results of the three types of specimens (denoted by the corresponding Roman numbers). The calculated data are in good agreement with the obtained experimental results.

References

1. Bal'shin, M. Yu. "Poroshkovaya metallurgiya" (Powder metallurgy). --- Moskva, 1948.
2. Kunin, M. F. and B. D. Yurchenko, "O ratsional'nom uravnenii pressovaniya metallicheskih poroshkov" (About a rational equation for compression of metallic powders). --- "Poroshkovaya metallurgiya", No. 2: 3 - 10, 1964 .
3. Ioselevich, V. A. "O zakonakh deformirovaniya neskal'nykh gruntov" (About the rules of deformation of nonrocky soils). --- "Osnovaniya fundamenty i mekh. gruntov", No. 4 , 1967 .
4. Myakotin, E. A. "O vliyaniy gidrostaticheskogo szhatiya na prochnost' tsementnogo kamnya" (About the influence of hydrostatic compression on the strength of cement stone). --- "Beton i zhelezobeton", No. 8 : 13-14, 1969.
5. Tot, L. F. "Raspolozheniya na ploskosti, na sfere i v prostranstve" (Location in a plane, sphere and space). --- Moskva, 1958.
6. Pelzel, E. Über das Verhalten kugelförmiger Metallpulver beim Pressen und Sintern. "Metallkunde", 46(II): 813 - 817, 1955 .
7. Shtaerman, I. Ya. "Kontaktная задача теории упругости" (Contact problem of the theory of elasticity). --- Moskva-Leningrad, 1949.
8. Kachanov, L. M. "Osnovy teorii plastichnosti" (Principles of the theory of plasticity). --- Moskva, 192-193, 1969.
9. Bagreev, V. V. "Issledovanie udara tverdykh tel." (Investigation of the impact of a solid body). --- Dokt. diss. MIIT, Moskva , 1969.
10. Betuev, G. S., A. A. Fedosev and A. K. Efremov, "Soudarenie massivnykh tel pri uprugoplasticheskikh deformatsiyakh v zone kontakta" (Failure of massive bodies in the case of elastoplastic deformations in the contact zone). --- Sb. "Raschety na prochnost'", vol. 10, 1964.

11. Lantsevitskaya, S.L., and E.A. Myakotin, "Ustanovka dlya ispytaniy gornykh porod i tsementnogo kamnya na polzuchest' pri slozhnom napryazhennom sostoyanii i povyshennoi temperature" (A rig for testing the creep of rocks and cement stone under complex stress states and elevated temperatures). -- Informats. nauch.-tekhn. sb. VNIIOENG, Seriya "Burenie", vol. 5 : 5 - 8 , 1967 .